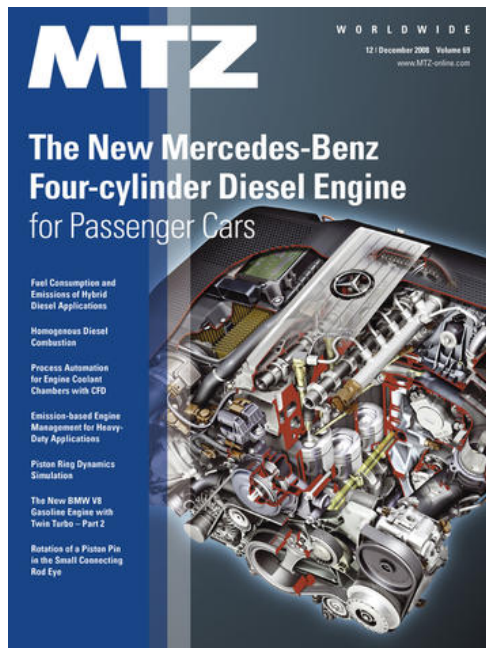


personal buildup for

## Force Motors Ltd.



MTZ worldwide 12/2008 released on n.a.

### copyright

The PDF download of contributions is a service for our subscribers. This compilation was created individually for Force Motors Ltd..  
Any duplication, renting, leasing, distribution and public reproduction of the material supplied by the publisher, as well as making it publicly available, is prohibited without his permission.

## The New Mercedes-Benz Four-cylinder Diesel Engine for Passenger Cars

**Fuel Consumption and  
Emissions of Hybrid  
Diesel Applications**

**Homogenous Diesel  
Combustion**

**Process Automation  
for Engine Coolant  
Chambers with CFD**

**Emission-based Engine  
Management for Heavy-  
Duty Applications**

**Piston Ring Dynamics  
Simulation**

**The New BMW V8  
Gasoline Engine with  
Twin Turbo – Part 2**

**Rotation of a Piston Pin  
in the Small Connecting  
Rod Eye**



For more information visit:  
[www.MTZ-online.com](http://www.MTZ-online.com)

## COVER STORY

# The New Mercedes-Benz Four-cylinder Diesel Engine for Passenger Cars



4

Following a successful optimisation programme lasting several years for the previous **Four-cylinder Diesel Engine** whose basic dimensions are still based on the OM 601 prechamber natural aspirated engine of the year 1983, Mercedes-Benz has developed a completely new engine, bearing the internal designation OM 651, to production maturity.

## COVER STORY

**Diesel Engines:**

- 4 **The New Mercedes-Benz Four-cylinder Diesel Engine for Passenger Cars**

Joachim Schommers, Johannes Leweux, Thomas Betz, Jürgen Huter, Bernhard Jutz, Peter Knauel, Gregor Renner, Heiko Sass

## DEVELOPMENT

**Alternative Drives:**

- 12 **Fuel Consumption and Emissions of Hybrid Diesel Applications**

Andrea Emilio Catania, Ezio Spessa, Vanessa Paladini, Alberto Vassallo

**Combustion:**

- 20 **Homogenous Diesel Combustion – Challenge for System, Components and Fuels**

Roderich Otte, Thorsten Raatz, Thomas Wintrich

**Fluid Dynamics:**

- 26 **Process Automation for Engine Coolant Chambers with CFD**

Matthias Heinz

**Controlling:**

- 30 **Emission-based Engine Management for Heavy-Duty Applications**

Eckhard Stöling, Jörn Seebode, Ralf Gratzke, Kai Behnk

**Piston:**

- 36 **Piston Ring Dynamics Simulation Based on FEA Software**

Timo Ortjohann, A. P. J. Voncken, Stefan Pischinger

**Gasoline Engines:**

- 42 **The New BMW V8 Gasoline Engine with Twin Turbo Part 2 – Functional Characteristics**

Christian Bock, Klaus Hirschfelder, Bernd Ofner, Christian Schwarz

## RESEARCH

- 50 **Research News**

**Crankshaft Drive:**

- 52 **Rotation of a Piston Pin in the Small Connecting Rod Eye During Engine Operation**

Georg Wachtmeister, Andreas Hubert

## RUBRICS

- 3 **Editorial**

- 3 | 41 **Imprint**

# Just Be Courageous

Dear Reader,

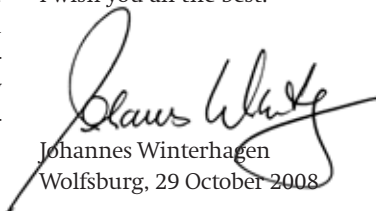
It became clearly apparent to me in numerous conversations at managerial level – for example recently at the International Suppliers Fair in Wolfsburg – that 2009 will be a challenging year for many suppliers. On the one hand, they have to invest in new technologies to support car makers and engine manufacturers in meeting fleet emissions targets (CO<sub>2</sub>) and complying with even stricter emissions standards (EU6). On the other hand, work on finalising the budget for 2009 seems more like an esoteric activity than serious business management, as it is virtually impossible to reliably predict how the market might development.

But every crisis is also an opportunity, as it separates the wheat from the chaff. Every supplier who is able to raise funds in a difficult economic climate in order to invest in future technologies will emerge stronger than ever before when the market eventually turns around. The focus should now be on accepting a temporary drop in operating profit and not on ‘massaging the figures’ in a private equity manner while saving money on R&D, employee training and communication. Such short-sightedness simply means that you’ll no longer be competitive tomorrow.

Communication is an issue that directly concerns us as a magazine. As is the case with recruiting or company acquisitions, it is those who act anti-cyclically who will achieve the highest rewards. Those who continue to communicate openly will find an attentive audience – in contrast to those who scale down their communication activities on the basis of misguided austerity measures. In times of limited budgets in particular, it is vital to keep a sense of proportion. So don’t choose an ‘all or nothing’ approach but concentrate on specialist magazines like MTZ, on important congresses, on online business portals (with their huge reach for little investment) and on recruiting fairs like careers4engineers. In other words, instead of grand gestures, choose investment opportunities that go right to the heart of the target group.

Therefore, I suggest the following motto for the next twelve months: don’t be downhearted, but don’t be reckless either. Just be courageous.

I wish you all the best.



Johannes Winterhagen  
Wolfsburg, 29 October 2008



Johannes Winterhagen  
Editor-in-Chief

personal buildup for Force Motors Ltd.

**MTZ** WORLDWIDE  
12|2008

Founded 1939 by  
Prof. Dr.-Ing. E. h. Heinrich Buschmann and  
Dr.-Ing. E. h. Prosper L'Orange

Organ of the Fachverband Motoren und  
Systeme im VDMA, Verband Deutscher  
Maschinen- und Anlagenbau e. V.,  
Frankfurt/Main, for the areas combustion  
engines and gas turbines

Organ of the Forschungsvereinigung  
Verbrennungskraftmaschinen e. V. (FVV)

Organ of the Wissenschaftliche  
Gesellschaft für Kraftfahrzeug- und  
Motorentechnik e. V. (WKM)

Organ of the Österreichischer  
Verein für Kraftfahrzeugtechnik (ÖVK)

Cooperation with the STG,  
Schiffbautechnische Gesellschaft e. V.,  
Hamburg, in the area of ship drives  
by combustion engines

#### EDITORS-IN-CHARGE

Dr.-Ing. E. h. Richard van Basshuysen  
Wolfgang Siebenpfeiffer

#### SCIENTIFIC ADVISORY BOARD

Prof. Dr.-Ing. Michael Bargende  
Universität Stuttgart

Dipl.-Ing. Wolfgang Dürheimer  
Dr. Ing. h. c. F. Porsche AG

Dr. Klaus Egger

Dipl.-Ing. Dietmar Goericke  
Forschungsvereinigung  
Verbrennungskraftmaschinen e. V.

Prof. Dr.-Ing. Uwe-Dieter Grebe  
GM Powertrain

Dipl.-Ing. Thorsten Herdan  
VDMA-Fachverband Motoren und Systeme

Prof. Dr.-Ing. habil. Günter Hohenberg  
TU Darmstadt

Prof. Dr.-Ing. Heinz K. Junker  
Mahle GmbH

Prof. Dr. Hans Peter Lenz  
ÖVK

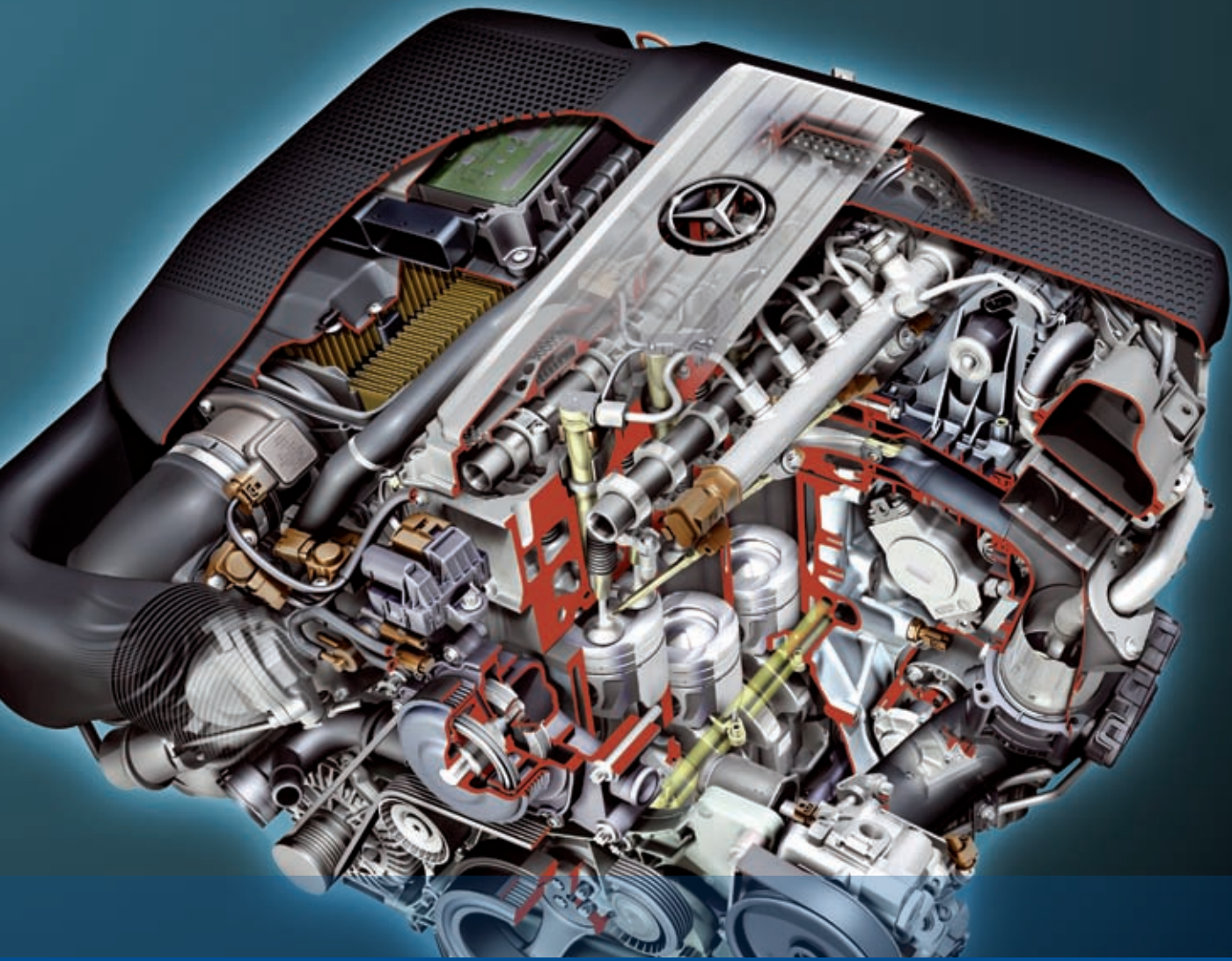
Prof. Dr. h. c. Helmut List  
AVL List GmbH

Prof. Dr.-Ing. Stefan Pischinger  
FEV Motorentechnik GmbH

Prof. Dr.-Ing. Ulrich Seiffert  
TU Braunschweig

Prof. Dr.-Ing. Ulrich Spicher  
WKM

Dr.-Ing. Gerd-Michael Wolters  
MTU Friedrichshafen



# The New Mercedes-Benz Four-cylinder Diesel Engine for Passenger Cars

Following a successful optimisation programme lasting several years for the previous four-cylinder diesel engine whose basic dimensions are still based on the OM 601 prechamber natural aspirated engine of the year 1983, Mercedes-Benz has developed a completely new engine, bearing the internal designation OM 651, to production maturity. The potential of this engine in terms of consumption, emissions and performance was achieved through the systematic advancement of familiar technologies and the use of important new engine-related innovations.

## 1 Introduction and Objective

The four-cylinder diesel engine is traditionally of high importance to Daimler AG, not only due to its market share in the E-Class and C-Class, but also in commercial vehicles with traction weights up to 7.5 t and in transversely installed drive units, which account for similarly high unit figures.

With regard to the need to reduce CO<sub>2</sub> emissions, the key objective was not only to develop a four-cylinder engine capable of setting the class benchmark in terms of consumption, but also to offer it as an alternative to a six-cylinder entry-level engine with similar torque and output potential.

Based on these requirements, the following development objectives were derived:

- significantly improved fuel consumption compared with the previous engine with better driving performance at the same time
- maximum torque to be increased by 25 % from 400 Nm to 500 Nm
- maximum output to be increased by 20 % from 125 kW to 150 kW
- the agility of a larger-displacement six-cylinder engine
- the EU5 emissions level including test bench approvals for commercial vehicle applications without active NO<sub>x</sub> aftertreatment, and the scope for additional significant untreated emissions potential with regard to EU6
- a common engine design for in-line and transverse installations and for commercial vehicle applications

- optimise and standardise of modules and assembly processes with the aim of boosting quality while at the same time improving the cost situation.

## 2 Engine Design

Given the planned scope of applications of the OM 651, the designers had to rise to the challenge of designing a basic engine that was as compact as possible and uniform across all applications. An engine that they could expand to meet the packaging or specification requirements of individual vehicles by integrating the relevant additional modules to create an overall system, **Figure 1**.

The key packaging challenges for passenger car applications arose, for example, in connection with longitudinal installations and the need for upward sloping engine hoods that meet pedestrian protection requirements. These factors affected the engine height, while the engine length was an issue that arose in connection with transverse installations. Since the camshaft drive is one of the determining parameters that affects the engine height, it is located on the transmission side of the engine. In order to achieve a simultaneous reduction in the engine's length, the camshaft drive features a combined gear and short chain drive, **Figure 2**.

### 2.1 Crankcase and Oil System

The crankcase has an apron design and is made of cast iron. The deep connection of the cylinder head bolts enabled the

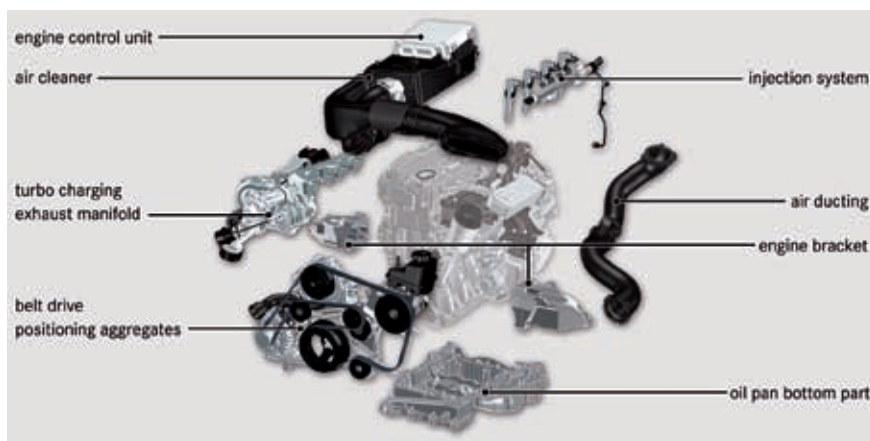


**Figure 1:** Component sharing principle: basic engine with additional modules

## The Authors



**Dr.-Ing. Joachim Schommers** is Director Development Passenger Car Diesel Engines at the Daimler AG in Stuttgart (Germany).



**Dipl.-Ing. Johannes Leweux** is Senior Manager Development OM 651 at the Daimler AG in Stuttgart (Germany).



**Dipl.-Ing. Thomas Betz** is Manager in the Combustion Department Development Passenger Car Diesel Engines at the Daimler AG in Stuttgart (Germany).



**Dipl.-Ing. Jürgen Huter** is Manager Design Charge Exchange at the Daimler AG in Stuttgart (Germany).



**Dipl.-Ing. Bernhard Jutz** is Manager Design Base Engine at the Daimler AG in Stuttgart (Germany).



**Dipl.-Ing. Peter Knauel** is Manager Turbocharging Diesel Engines at the Daimler AG in Stuttgart (Germany).



**Dr.-Ing. Gregor Renner** is Manager CR-System Development at the Daimler AG in Stuttgart (Germany).



**Dipl.-Ing. Heiko Sass** is Manager Mechanical Development at the Daimler AG in Stuttgart (Germany).

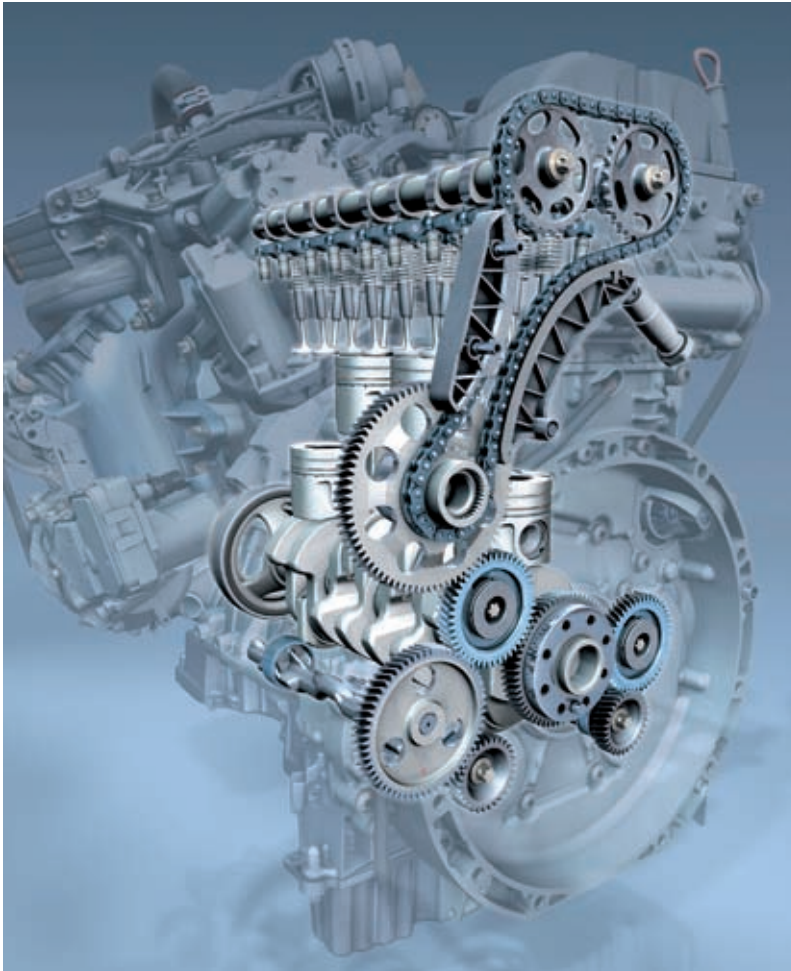


**Figure 2:** Camshaft drive as a combination of a gear and a chain drive

cylinder shape of the barrels to be significantly improved compared with the predecessor engine. A corresponding reduction in the tangential forces in the ring assembly leads to lower friction in the piston assembly. This is accompanied by outstanding oil consumption and blow-by values. The honing of the barrels is finer than in the predecessor and also contributes to the reduction in friction losses.

Another main focus of the economy-driven configuration of the OM 651 was the design of the oil system, **Figure 3**. The controlled variable for the delivery volume of the pump is the oil pressure in the main oil duct of the crankcase. This arrangement offers the benefit of a requirement-driven control system that is independent of the load condition of the oil filter and works perfectly together with the switchable piston cooling. For this purpose, a separate oil duct that sup-

plies the oil injection nozzles is located in the crankcase. The oil supply to this oil duct is controlled by an electric valve. In addition to the consumption potential due to the lower oil delivery volume, the resulting capability to switch the piston

cooling on or off based on the performance map features a HC emissions module due to the higher piston temperatures during the warm-up phase.

The oil pump in the Mercedes-Benz OM 651 is a closed-loop vane cell pump that provides for automatic and adaptive control of the delivery volume.

## 2.2 Main Dimensions

The basic dimensions of the new OM 651 four-cylinder diesel engine were derived from the following considerations:

- the optimum design in terms of starting torque, emissions and the most compact dimensions proved to be a uniform displacement of 2.15 l
- a peak power model with 150 kW. This equates to a specific output of 70 kW/l
- combined with a compression ratio of 16.2 suited to cold idling, this resulted in an optimum thermodynamic maximum peak pressure of 200 bar and an absolute degree of turbocharging rate in the intake manifold of just under 3 bar
- in the interest of high peak pressure, a long-stroke concept with a bore of 83 mm and a stroke of 99 mm was chosen.

The high thermodynamic requirements that apply at 70 kW/l demand bridge dimensions that provide for effective cooling while at the same time ensuring that the mechanical limits are adhered to. The chosen bridge width of 11 mm results in a cylinder clearance of 94  $\mu$ m. The valve angle of 6° enables extremely effective cooling of the combustion chamber roof, **Figure 4**. In order to minimise the thermal

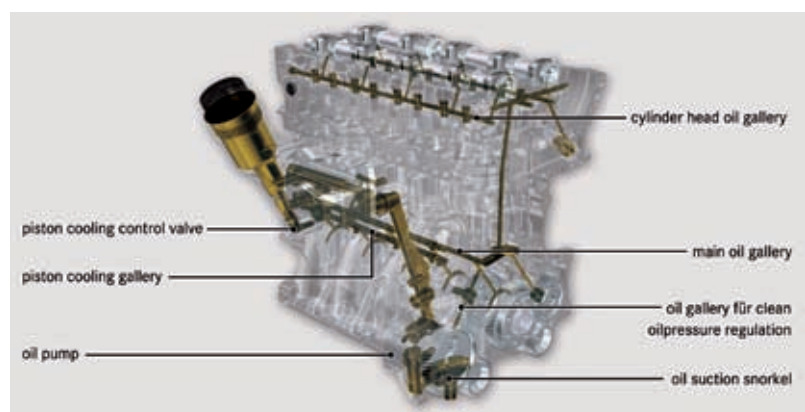


**Figure 3:** Oil circulation OM 651

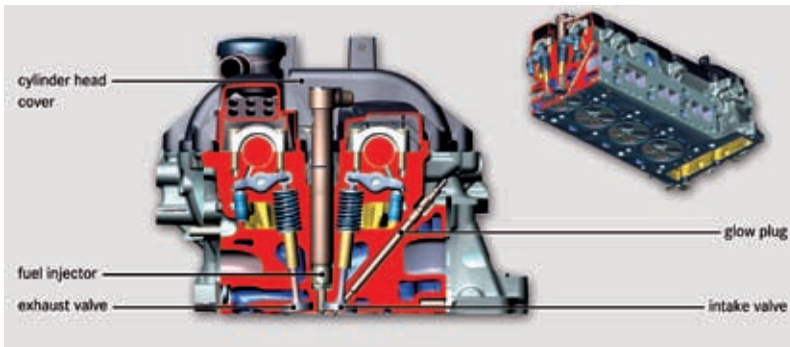


**Figure 4:** Section cylinder head/valve angle

**Table:** Main characteristics of OM 651 in comparison with its predecessor

Engine		OM 646 evo	OM 651
Cylinders			R4
Valve / cylinder			4
Capacity	cm <sup>3</sup>	2149	2143
Cylinder spacing	mm	97	94
Bore	mm	88	83
Stroke	mm	88.3	99
Stroke / bore ratio		1.004	1.193
Length of connecting-rod	mm	147	143.55
Nominal performance	kW	125	150
at rpm	min <sup>-1</sup>	3800	4200
Nominal torque	Nm	400	500
at rpm	min <sup>-1</sup>	2000	1600 – 1800
Compression		17.5	16.2
Maximum mean pressure	bar	23,4	29.33
Emission standard		EU4	EU5

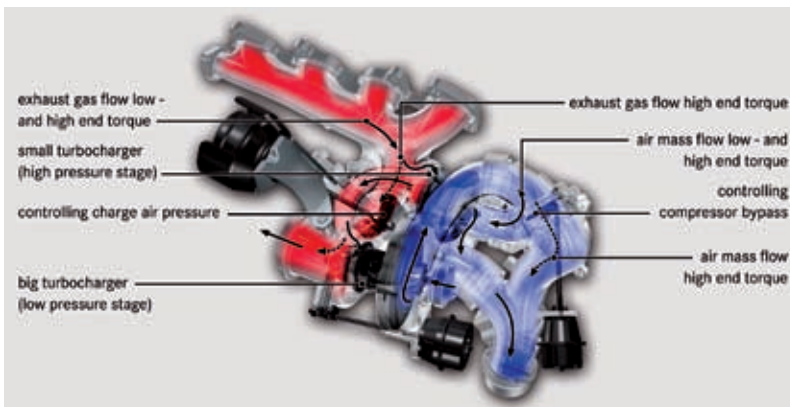


**Figure 5:** Packaging of the two-stage turbocharger

load on the combustion chamber plate, the water jacket in the cylinder head has a two-piece design. The **Table** summarises the key data for the OM 651.

### 2.3 Turbocharging and Air Ducting

This engine uses two different charging concepts depending on the engine output. For engine outputs up to 120 kW in pas-

senger car applications, the engine is fitted with a single-stage exhaust gas turbocharger featuring variable turbine geometry. Higher engine outputs are achieved using two-stage turbocharging with two different exhaust gas turbochargers and wastegate turbines. This system is described in more detail below.

The two-stage turbocharging system first used by Daimler in the predecessor engine OM 646 and installed in the “Sprinter” commercial vehicle was advanced and optimised for this engine. This engine uses a KP39 turbocharger as a “high-pressure turbo” and a K04 turbocharger as a “low-pressure turbo” equipped with project-specific compressors and turbines.

The engine features a compressor bypass with an active switchable flap that can open a parallel air path in the engine’s high-output range. This has the effect of reducing pressure losses and preventing the KP39 turbo from becoming overloaded, **Figure 5**. As a result of the high supercharging rate in combination with increased exhaust gas recirculation rate – when compared with the predecessor engine – an optimized combustion efficiency can be achieved on the one hand. On the other hand longer transmission ratios are possible. Referred to as “downspeeding”, this concept contributes significantly to lower consumption. **Figure 6** illustrates which turbocharging systems are used at Mercedes-Benz and the performance and torque figures generated as a result.

### 2.4 Air Ducting

The raw air line, damper filter (engine-mounted) and clean air line make up the air intake and their design is matched such that uniform loading of the damper filter cartridge results in an even inflow to the hot-film air-mass meter (HFM) and compressor. To achieve the high specific output, the engine uses a large air-to-air intercooler that provides 20 % more cooling power than the predecessor engine. The rest of the air ducting, consisting of the air manifold, intake air throttle, charge air manifold with EGR introduction, charge air distribution line with inlet port shut-off, is made of plastic.

### 2.5 Exhaust Gas Recirculation and Cooling

The EGR precooling system, electric EGR valve (rotary disk valve), EGR-cooler by-

pass flap, EGR cooler (“u-turn cooler“) and the EGR introduction in the charge air manifold form the exhaust gas recirculation tract and are arranged above the charge air distribution line. The newly developed EGR valve is based on the rotary flap principle. The EGR valve is common to all applications.

The exhaust gas is precooled via the precooler and, depending on the engine operating point, introduced into the air ducting via the main cooler, either cooled or uncooled (bypass).

## 2.6 Common Rail Injection System

The injection system was designed with reference to the different requirements of the engine line-up.

- The key features of this system are
- maximum injection pressure of 2000 bar
  - optional use of solenoid or direct driven piezo injectors
  - up to five injection events per combustion cycle
  - double-stamped high pressure pump with volume regulation on the intake side
  - fuel-quantity drift compensation by means of structure borne noise sensor control.

In order to minimize the entry of heat into the fuel system, an inlet-metered high-pressure pump is used. Consequently, there is no need for a fuel cooling system.

### 2.6.1 Solenoid Servo Injector

The solenoid injector is a further development from the predecessor engine. It uses a compact design with a balanced pressure servo valve in close proximity to the nozzle. The injector is characterized by an extremely low dead space in the hydraulic circuit and significantly reduced leakage volumes. Thanks to a volume optimisation in the injector's high-pressure range, controllability in the pilot quantity range at high rail pressures and the shot/shot variations have been further improved.

### 2.6.2 Direct Driven Piezo Injector

The more powerful variants of the OM 651 use a new injector concept that was jointly developed with Delphi. Compared with conventional CR injectors in which the nozzle needle is servohydraulically

activated, this injector concept features direct control of the nozzle needle. In this design, the needle directly follows the stroke specified by the piezo stack and enlarged by a travel transmitter.

The maximum achievable rail pressure was increased to 2000 bar. This additional injection pressure potential represents a key building block for increasing the engine output to its current figure of 150 kW and of the torque to 500 Nm while at the same time achieving significantly improved untreated emissions behaviour, as well as improved fuel consumption.

The injector is displayed in **Figure 7**. The central component is the piezo stack, which is located directly inside the high pressure chamber. Compared with a servo injector, this generates a fuel volume that is greater by a factor of 2.3. The configuration as a ring volume also allows for significantly higher damping of the pressure wave triggered by the injection procedure

than is the case with a high-pressure bore in the servo injector [1]. This delivers clear benefits in relation to controllability in the case of multiple injections and reduced shot/shot variations. Contingent on its activation concept, the injector is capable of completely leak-free operation.

The concept of direct nozzle needle control continues to offer the possibility of realising an injection rate that is independent of the rail pressure. This injection pressure can be varied by a control logic specially developed for this purpose. The injector exhibits a steeper injection rate, particularly at low rail pressures, which has a positive impact on the emissions performance [1].

This injector concept, which is the first of its kind to be used in a diesel engine world-wide, opens up significant potential with regard to maximized flexibility and stability of the injection procedures, maximum achievable injection pressure and complete freedom from leaks.

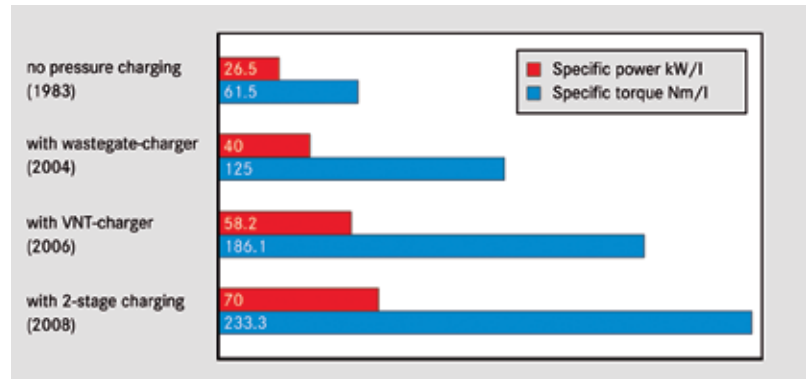


Figure 6: Comparison of turbocharging systems

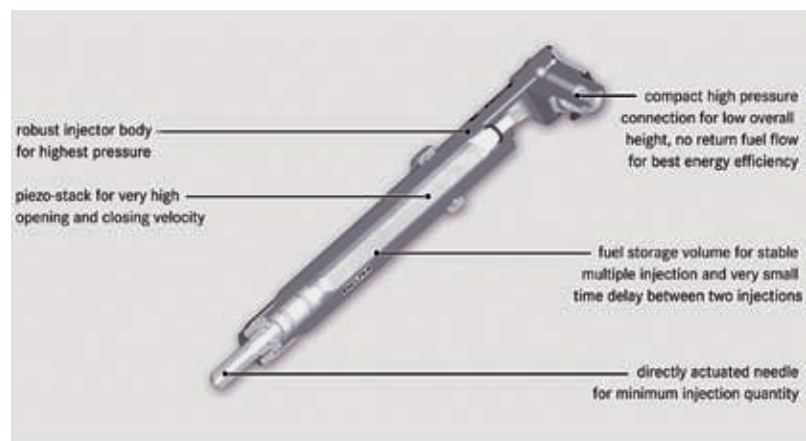


Figure 7: Direct driven Piezo injector

### 3 Thermal Management in the OM 651

The thermal management used in the OM 651 is a key prerequisite for achieving the demanding objectives of the overall system comprising the engine and the vehicle. Along with achieving reductions in consumption, these include achieving a further reduction of untreated emissions, thermal protection for all components, preventing sooting and oil dilution as well ensuring effective climate control for the passenger compartment.

#### 3.1 Component Development Based on the Example of the Switchable Coolant Pump

The main criteria during the development of the switchable coolant pump were as follows

- ensuring zero delivery
- reducing the drive output at zero delivery
- low additional weight compared with conventional coolant pumps
- low installation space requirement
- low additional costs for switchability
- no restriction on drivability in the event of failure (fail-safe principle)
- durability and resistance to residual contamination.

A new switchable water pump jointly developed with GPM is used, **Figure 8**. The pump actuator is operated by vacuum. If zero delivery is requested, the regulating valve moves across the impeller and completely blocks the coolant exit. This position prevents the flow through the impeller and, therefore, the increase in pressure. The drive output falls significantly [1]. The primary objective of preventing all movement of coolant is to reduce the untreated emissions of HC and CO by ensuring that the combustion chamber warms up as quickly as possible.

#### 3.2 Regulating the Coolant Temperature

Another important parameter that influences consumption, emissions and service life is the coolant temperature. To accommodate the high dynamics of the unit, it is important not only to adhere to the maximum permissible temperatures, but to reduce the changes in temperature as well as the collective temperatures.

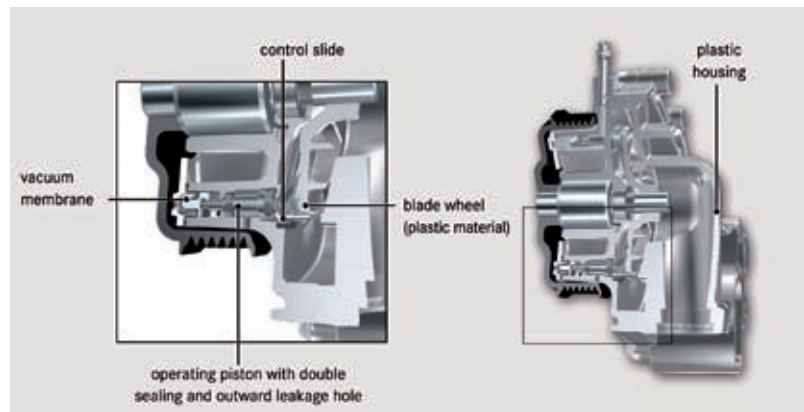


**Figure 8:** Sectional view of a switchable water pump

The base temperature is defined as 100 °C in order to achieve good efficiency rates. Depending on the load, engine speed and the type of driver, the coolant temperature is lowered to 80 °C under heavy load conditions. Furthermore, the target value is further reduced – as far as 70 °C – if the conditions of warm environment and high load apply as they pose a challenge in terms of NO<sub>x</sub> emissions. The arrangement of the EGR cooler on the coolant inflow side and the provision of a separate coolant supply to the cylinder head, with no prewarming through the crankcase results in a reduced combustion process temperature along with lower NO<sub>x</sub> emissions. On the other hand, systematically increasing the coolant temperature in conditions where sooting is likely to occur safeguards the stability and effectiveness of the EGR tract.

#### 3.3 Switchable Piston Cooling

The switchable piston cooling system achieves the following objectives

- reduced consumption
- reduced untreated emissions
- increased exhaust gas enthalpy in cold engines in order to accelerate activation of the oxidation catalytic converter.

The reduction in consumption is realized by switching off the piston cooling in various operating conditions. Both the reduction of friction in the piston assembly resulting from higher component temperatures as well as the significantly reduced oil delivery volume in conjunction with the vane cell oil pump for regulating the pure oil make a contribution

in this context. At normal operating temperature, load and engine speed are the decisive parameters used to activate the switching valve in the switchable piston cooling system. In addition, the range in which piston cooling is deactivated is expanded during the warm-up phase. This has a clear impact on the combustion chamber temperature. Untreated emissions of HC and CO can be significantly reduced in this way, particularly during the critical emissions phase before good conversion rates have been reached in the oxidation catalytic converter. Apart from this, avoiding the need to dissipate heat leads to an increase in exhaust gas enthalpy, which in turn causes the catalytic converter to warm up more quickly. Under higher loads, piston cooling may be switched on in advance of the component protection request in order to use the effectively cooled combustion chamber to reduce the formation of NO<sub>x</sub>.

### 4 Combustion

The main areas of focus when it came to designing the combustion process of the OM 651 were as follows

- minimum fuel consumption
- compliance with EU5 in the passenger car/SUV without active NO<sub>x</sub> after-treatment
- optimizing the response of the exhaust gas turbocharging
- increasing the maximum torque and output
- designing a modular engine concept to reduce the number of application variants.

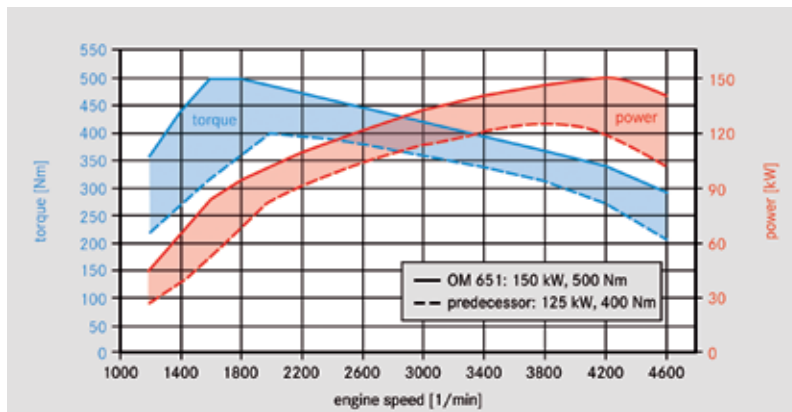


Figure 9: Torque/power

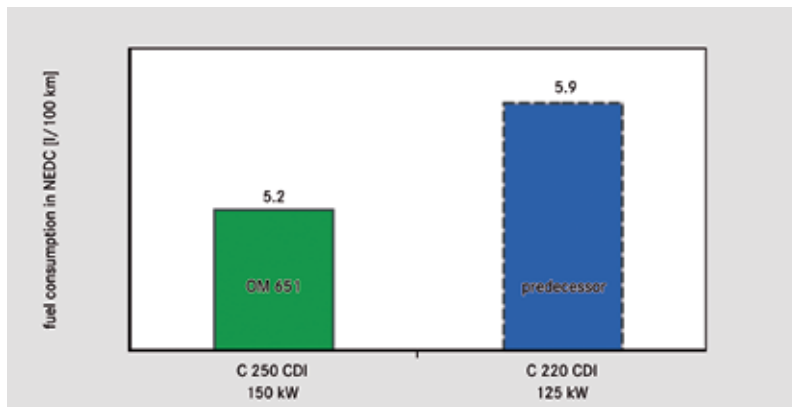


Figure 10: Fuel consumption

For this purpose, all engine components were systematically designed. Familiar technologies were developed in an evolutionary manner, and new technologies were to tap and fully exploit additional potential through the use of comprehensive functional and application optimisations.

Compared with the predecessor engine OM646, the torque of the new OM 651 has been raised by 25 % to 500 Nm, **Figure 9**, which represents by far the best performance in its competitive segment. This equates to an effective mean pressure of 29.3 bar, a new dimension in the area of diesel engines for passenger cars. It is also extremely important that this torque is available at engine speeds between 1600 to 1800 rpm. Together with the excellent response of the new two-stage turbocharger, this permits the use of longer transmission ratios and, consequently, allows the engine to operate in specifically more favourable areas of the performance map (downspeeding).

The output of the OM 651 of 150 kW at 4200 rpm is 20 % higher than that of its predecessor, which developed its peak output at 3800 rpm. Due to a gentle speed regulation breakaway and the early availability of maximum torque, the useable engine speed range has increased considerably in comparison with the OM 646. As a result of the stationary full load course described, the OM 651 sets new benchmarks for turbocharged diesel engines in the passenger car segment.

#### 4.1 Emissions

The OM 651 already complies with the EU5 emissions standard that will apply to all new registrations from September 2009 onwards. These limits will be met in vehicles up to the size of the new GLK without the use of an active NO<sub>x</sub> after-treatment. The excellent emission/consumption-trade-off [1] of this engine was achieved through the described design of the injection-, turbocharging- and

EGR-systems as well as the design of the combustion chamber.

#### 4.2 Fuel Consumption

Particularly in terms of fuel consumption, the OM 651 represents a clear step forward compared with its predecessor. With a 12 % improvement in fuel consumption, **Figure 10**, in the NEDC, the conflict of objectives between emissions and consumption was systematically exhausted. Even though the EU5 emission standards were reached, the specific consumption values in the performance map could have been significantly decreased and are now considerably below the level of usual EU4-engines.

#### 5 Summary

The engine bearing the internal designation OM 651 is a completely new four-cylinder diesel engine that offers a much greater number of possible applications than all previous units. The engineers at Daimler AG have created an engine with a high degree of commonality, which can be installed longitudinally or transversely, is suitable with the relevant applications for all-wheel drive and can be used in commercial vehicles.

In addition, the new engine meets the most technically demanding targets with regard to emissions, consumption, output, torque, response and NVH. These were achieved through the systematic evolution of familiar modules and through the use of new technologies.

With its thermodynamic configuration, the OM 651 achieves a benchmark position especially with regard to its fuel efficiency and achievable performance. The measurement results provide impressive evidence of its performance in all areas.

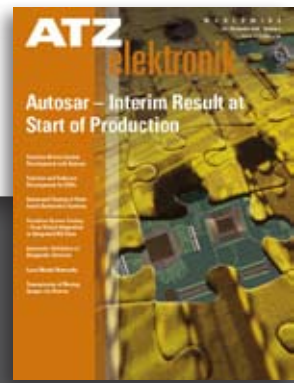
#### Reference

- [1] Schommers, J.; Leweux, J.; Betz, Th.; Huter, J.; Jutz, B.; Knauel, P.; Renner, G.; Sass, H.: Der neue 4-Zylinder Pkw-Dieselmotor von Mercedes-Benz für weltweiten Einsatz. 17th Aachen Congress 2008



personal buildup for Force Motors Ltd.

# Imagine that electronics was orange ...

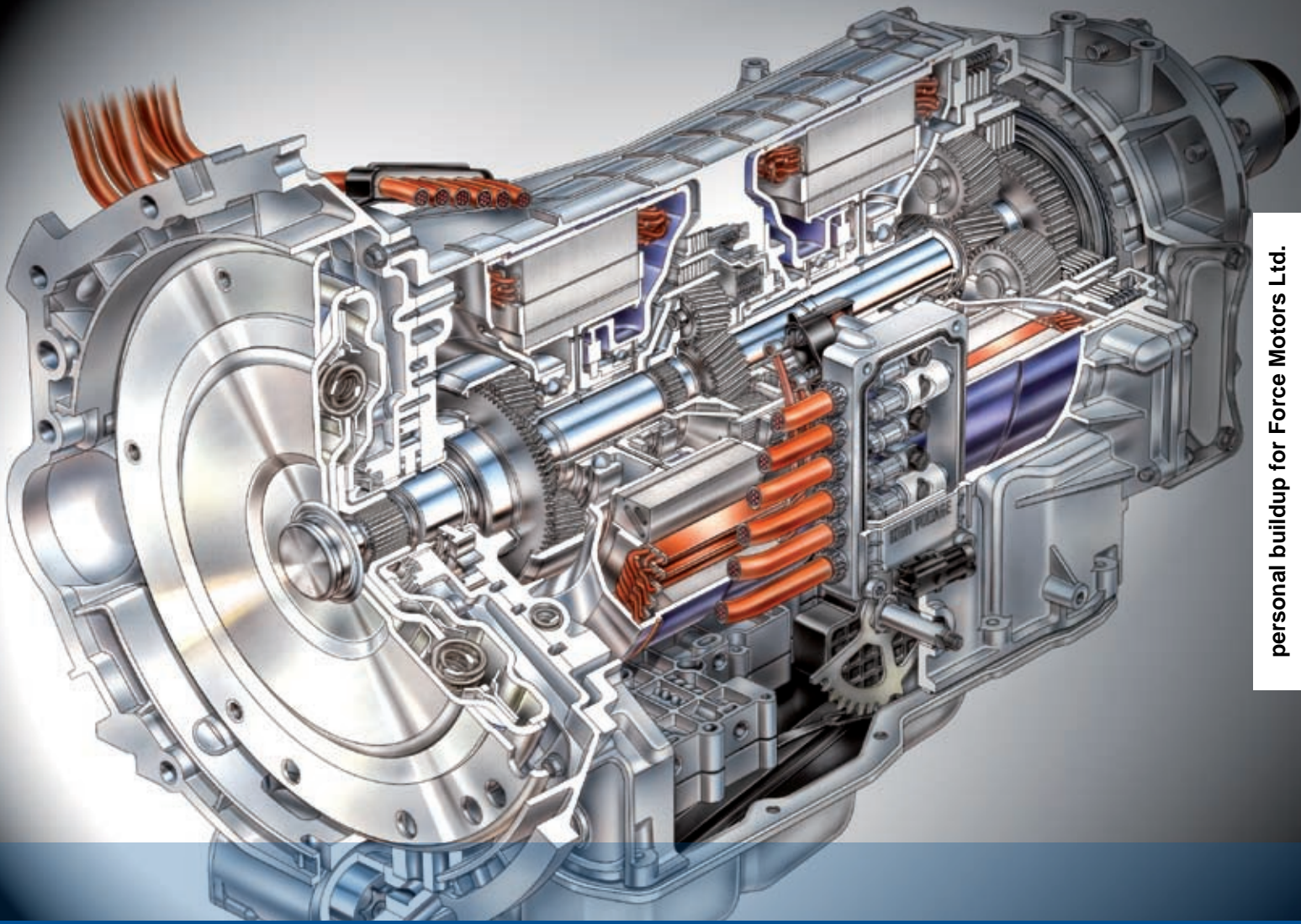


The colour orange stands for creativity and dynamic energy. And because there is hardly any other sector in which development is as active and dynamic as automotive electronics, there is now a specialist e-Magazine in orange: **ATZelektronik**.

ATZelektronik reviews the latest trends and developments in electronics and software across the global automotive industry 6 times per year. On an academic level. With a unique profundness of information.

Find out everything you need to know about the latest developments, methods and electronic components. Read how future driver-assistance systems will change our mobile society. Monitor the progress of on-board electrical systems and energy management. ATZelektronik is an essential source of information on these and many other industry topics.

Furthermore, as a subscriber to ATZelektronik, you will benefit from our online archive of articles; an indispensable research tool that offers free downloads of the articles. Want to stay ahead of the pack? Order your free electronic sample edition today at [www.ATZonline.com](http://www.ATZonline.com).



personal buildup for Force Motors Ltd.

# Fuel Consumption and Emissions of Hybrid Diesel Applications

GM Powertrain Europe and the Politecnico di Torino have experimentally assessed the potentialities in terms of fuel consumption reduction and the challenges in terms of pollutant emissions of micro-, mild- and strong-hybrid diesel applications for light-duty vehicles based on GM 1.9 l four-cylinder in-line diesel engine.

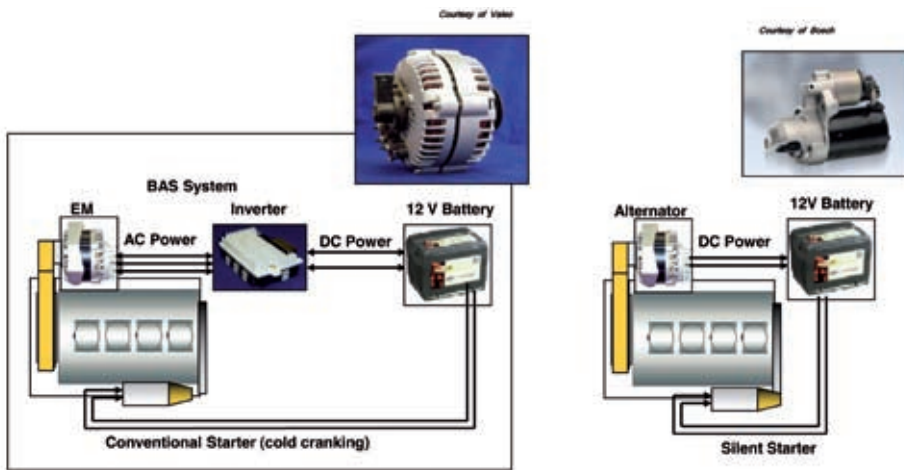


Figure 1: BAS (left) and Starter (right) based micro-hybrid architectures

## 1 Introduction

The coming years will see a very strong demand for CO<sub>2</sub> emission reduction from transportation, in particular for the private mobility. European and US manufacturers will be forced to significantly decrease fleet-average CO<sub>2</sub> emissions for new vehicles, in the framework of European and CAFE mandatory regulations, respectively. Taking into consideration European regulation, currently it is not imposing a limit to CO<sub>2</sub> emissions, but there is in place an voluntary agreement between ACEA and the EU Commission (signed in 1998) to meet a corporate average CO<sub>2</sub> emission level of 140 g/km by 2008, a reduction by 25 % over the 1995 level of 186 g/km. However, the latest estimates show that this target will not be achieved by far, since in 2007 the average new cars CO<sub>2</sub> emission level was slightly lower than 160 g/km. EU Commission is therefore undergoing a process that will likely lead to a specific CO<sub>2</sub> emission regulation kick-off in 2009, in a way very similar to that adopted for pollutant emissions in the early 1990s [1-4].

The most recent estimate for the CO<sub>2</sub> target to be enforced is 130 g/km by 2012, including credits of 10 g/km due to biofuel use, tire pressure monitoring, gear shift indication and other active measures that enable the driver to optimize fuel economy. Given this tough target, OEM manufacturers are starting sound actions in order to decrease fuel consumption both from powertrain and vehicle side.

Powertrain enhancements will include, among others, adoption of longer gear ratios and/or final drives, engine downsizing, wider employment of low-friction components and low-viscosity lubricants and active water/oil pumps management. In addition to them, Stop/Start engine operation is forecasted to be one of the biggest contributors to CO<sub>2</sub> reduction. In a second step, once even stricter CO<sub>2</sub> targets will be enforced likely around 2015 (contemporarily to EU6 regulation), new measures will be needed to stretch further fuel consumption, including further electrification of the powertrain through hybridization.

Currently there are, strictly speaking, two major hybrid architectures, in addition to the so called micro-hybrid one, this latter being based on systems able to perform engine Stop/Start (and optionally very limited regenerative braking):

- Mild-hybrid: system including a medium/high voltage (40 to 120V) AC/DC electric motor able to provide substantial torque boost and electric braking for vehicle kinetic energy recovery. No or very limited vehicle electric-only operation is allowed, due to its mechanical architecture and to the limited accumulator capacity. BAS (Belt Alternator Starter) and FAS (Flywheel Alternator Starter) are the most common configurations currently being developed and commercially employed.
- Strong-hybrid: system including one or more high voltage (>150V) AC electric motors, able to perform like mild-

hybrid, but also to move the vehicle in electric mode only with acceptable performance and range provided by accumulators. GM Two-mode and Toyota THS systems are the first applications for this concept.

Currently hybridization is generally associated with the gasoline engine, since this latter best fits the coupling with an electric motor able to increase powertrain full-load and transient output torque and to shift engine operation to more favourable bmp levels. In addition, port-fuelled gasoline engines fea-

## The Authors



Prof.-Dr. Andrea Emilio Catania is Full Professor of Mechanical Engineering and ICE Advanced Laboratory Director at Dipartimento di Energetica of Politecnico di Torino (Italy).



Prof.-Dr. Ezio Spessa is Associate Professor of Mechanical Engineering at Dipartimento di Energetica of Politecnico di Torino (Italy).



Dr.-Ing. Vanessa Paladini is Technology Senior System Engineer – Hybrids at GM Powertrain Europe, Advanced Engineering in Torino (Italy).



Dr.-Ing. Alberto Vassallo is Technology Senior System Engineer – Diesel Combustion at GM Powertrain Europe, Advanced Engineering in Torino (Italy).

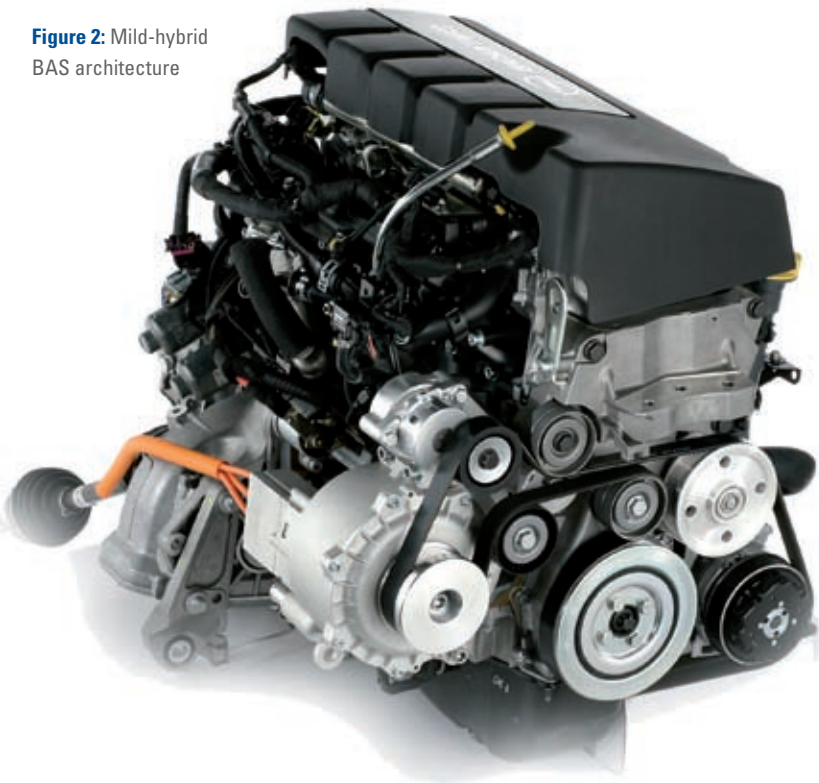
**Table:** Main specifications of the reference engine

Engine type	1.9 l Euro 4
Displacement	1.910 l
Bore x stroke	82.0 mm x 90.4 mm
Stroke-to-bore ratio	1.10
Compression ratio	17.5 : 1
Valves per cylinder	4
Turbocharger	Single-stage with VGT
Injection system	Common Rail 2nd Gen. CRI 2.2 1600 bar – injector with 7 holes
Maximum power and torque	110 kW at 4000 rpm, 320 Nm at 2000 rpm
Specific power / torque	57.6 kW / 167 Nm/l

ture low production costs that make hybridization more feasible in a challenging economic environment like the present one.

However, for the second step of CO<sub>2</sub> legislation, it is expected that also Diesel engines will require to further significantly decrease their fuel consumption, therefore hybridization, at least in the form of mild hybrid, is being considered also for this powertrain. This has recent-

ly triggered significant R&D activities to study Diesel hybridization, so to better define the differences of this technique applied to Diesel instead of gasoline engines, mainly in terms of fuel consumption reduction potential and emission impact. The results obtained in the assessment of the micro-, mild- and strong-hybrid architectures on 1.9 l four-cylinder in-line GM Diesel engine are shown hereafter.

**Figure 2:** Mild-hybrid BAS architecture

## 2 Engine and Hybrid Systems Description

The experimental investigations were carried out for assessing three different hybrid systems (micro-, mild- and strong-hybrid) based on GM Powertrain 1.9 l four-cylinder in-line 16-valves EU4 engine, whose main features are listed in the **Table** [5].

The micro-hybrid powertrain considered can be composed either by an enhanced engine starter or by a belt-driven 12 V system, both able to improve engine starting behaviour and providing the necessary durability required by the application in which cranking events are significantly increased with respect to a conventional one, **Figure 1**.

The system is therefore able to perform stop of the engine during idling and to restart it once a vehicle speed demand is detected, for example in the form of clutch pedal press or brake pedal release with stopped vehicle. Main advantage of belt driven systems are quicker cranking and better comfort during the event, because of lower noise and speed oscillations.

The mild-hybrid system considered is of the BAS type (and can be seen as an evolution of the BAS Stop/Start system previously described), thus capable of torque boost and energy recovery during deceleration phases, **Figure 2**.

In addition, during steady-state low-load operation, engine working points can be shifted up by enabling battery recharge through the electric motor. Engine load optimization is indeed the major source of improvement in powertrain efficiency for micro-hybrid architecture.

The strong-hybrid powertrain considered is a full-hybrid power split as the GM Two-mode hybrid system. This is basically composed by an electrically variable transmission, which uses electric motors to operate at nearly any speed ratio through the transmission [6]. The electric motors in the transmission also allow hybrid functions: electric vehicle operation, electric boost, and regenerative braking, as well as engine starting.

The Two-mode hybrid transmission is also an automatic transmission, without a torque converter but with conventional hydraulically-applied wet-plate clutches to

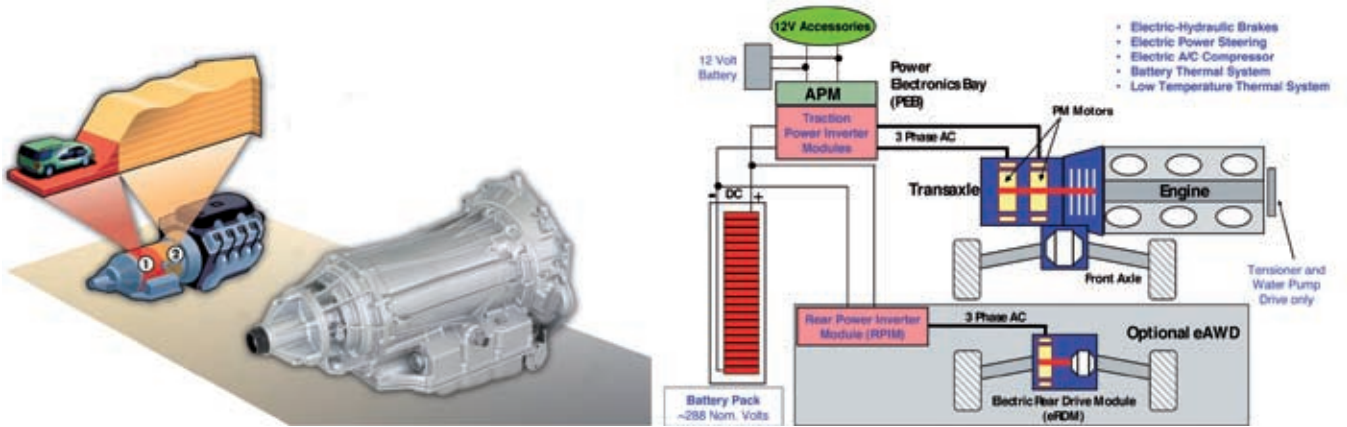


Figure 3: Packaging and complete system of GM Two-Mode Hybrid architecture

allow automatic shifting among two continuously variable modes and four fixed gears, a total of six mechanical configurations. This combination is fully integrated into a package very much like a conventional automatic transmission, with added wires leading to electronic controls and a high-voltage battery, Figure 3.

### 3 Testing Methodologies

For achieving a fair comparison, all the hybrid systems were operated so that at the beginning and at the end of the reference NEDC cycle the same charge level was reached in the battery pack, so that no artificial fuel economy boost derived from net electrical energy consumption (stemming from the energy stored in the batteries at the beginning) or no questionable electrical energy to diesel fuel conversion occurred.

The typical hybrid operation strategies were implemented on GM proprietary powertrain simulation tools with the scope of evaluating the energy flows and therefore the instantaneous mechanical output of the engine under the various operating modes. In this way, it was possible to get the engine instantaneous speed-torque trace that was imposed as a target for the dynamic test bench, allowing to test the different engine operating modes without employing the various mechanical and electrical hardware (electric motors, converters, batteries, transmissions) that would be required under a conventional approach. The operation of

the systems over the engine map is represented in Figure 4.

The symbols represent diesel engine operation points at different time steps over the NEDC cycle; each symbol type refers to a different powertrain. In addition the base engine full load curve is also represented (red solid line). It is interesting to notice the shift of engine load produced by mild-hybrid during electric boost/battery regeneration phases and the even bigger shift of load and speed caused by strong-hybrid operation. The shift in engine operating points is the biggest contributor to the improvement of hybrid powertrain efficiency, reducing the relative weight of idling and low load operation and increasing the operation at high efficiency.

Stop/Start device operation over the NEDC cycle was experimentally reproduced by considering engine stopping at

the beginning of every idling phase and engine re-starting 3 s before the following speed ramp begins. As a final consideration valid for all hybrid systems, it is important to remark that engine Stop/Start can be enabled at different phases of the NEDC cycle, mainly depending on the strategy chosen for aftertreatment management.

The reference vehicle for all the considered systems was a D-class vehicle featuring 1700 kg inertial weight and drag resistance of 14 kW at 100 km/h. In addition to the representation given in Figure 4, engine speed and load time-histories during ECE-1 and ECE-2, Figure 5, allow deeper considerations about the selected operation strategies.

The main techniques enabled by hybridization are highlighted on speed, Figure 5 (left), and load, Figure 5 (right), traces. Concerning Figure 5 (left), the red

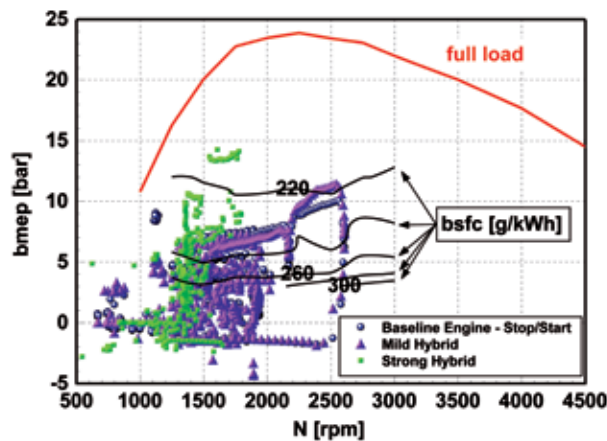


Figure 4: Engine speed and bmep time-histories during NEDC cycles for conventional, micro-, mild- and strong-hybrid operations

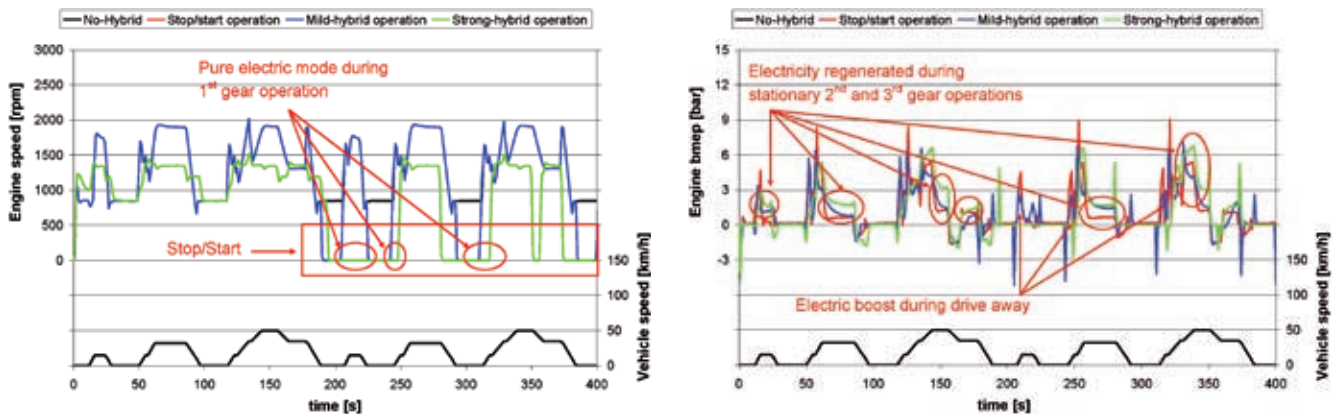


Figure 5: Engine speed (left) and bmep (right) time-histories during ECE-1 and ECE-2 for conventional, micro-, mild- and strong-hybrid operations

box corresponds to Stop/Start release from ECE-2, which is currently thought to be the most promising concept, while the red ovals highlight the pure electric mode during 1<sup>st</sup> gear operation selected

for strong-hybrid powertrain. Figure 5 illustrates other interesting hybrid potentialities, i.e. electricity regeneration during low-speed stationary operation in 2<sup>nd</sup> and 3<sup>rd</sup> gears or braking (the amount of electricity regeneration is quite different between mild- and strong-hybrid as well as electric boost during drive-away phases that effectively smooth engine noise peaks).

#### 4 Experimental Test Bed

The previously described tests were carried out on a new AVL high-dynamic test bed, Figure 6, at IC Engines Advanced Laboratory (ICEAL) of Politecnico di Torino [5]. The engine operation was directly managed by the test bench controller: vehicle control mode was employed for conventional and Stop/Start operation, while speed-load control mode was used for mild- and strong-hybrid. Checks were performed to assure that the net energy produced to propel the vehicle kept constant, since any dispersion in this quantity directly impacted the fuel economy measurements and therefore the accuracy of the comparison among powertrains.

Finally, emissions were measured by 'Pierburg AVL AMA 4000' raw gas analyzer both upstream and downstream from DOC, in order to record the transient effects related to engine dynamic operation and aftertreatment warm-up. The pollutant concentrations were then used to calculate the corresponding mass fractions to be multiplied by the instantaneous exhaust flow rate and finally inte-

grated over time, in order to get the total mass emissions over the cycle.

#### 5 Engine Map Recalibration for Strong-hybrid Operations

A preliminary analysis of strong-hybrid emission levels showed a significant deterioration in raw NO<sub>x</sub> with respect to No-Hybrid operations in the order of 75%. In order to keep the same emission certification level of baseline engine, a specific engine recalibration in low-end torque area is required. The main parameters to be optimized were EGR and boost levels as well as the injection schedule. More specifically, EGR valve opening was enabled above conventional NEDC area, which made charge and EGR temperature control critical due to maximum operating temperature of intake manifold and EGR cooler module. Boost map was increased only to a small extent, because compressor working points were already very close to actual surge line. In order to get rid of NO<sub>x</sub> production, however, the achieved boost level proved to be correct with acceptable soot, CO, HC and bsfc deteriorations. Figure 7 reports the EGR rate variations with reference to the baseline calibration, Figure 7 (left), and the exhaust gas temperature at EGR cooler inlet, Figure 7 (right).

With the specific strong-hybrid calibration, lambda levels have been decreased up to the minimum value ( $\lambda \approx 1.20$ ) that produces acceptable worsening of bsfc map, in consequence of deterioration of turbocharger and combustion efficiencies as well as of pumping-loss increases.

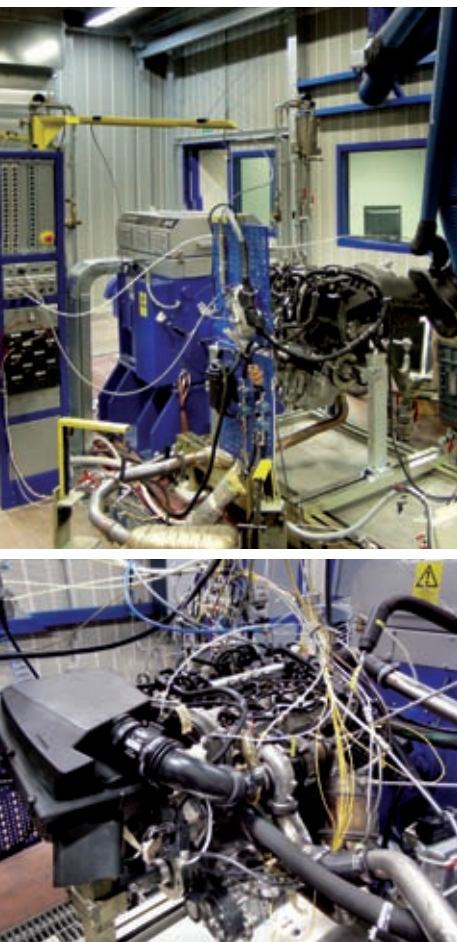
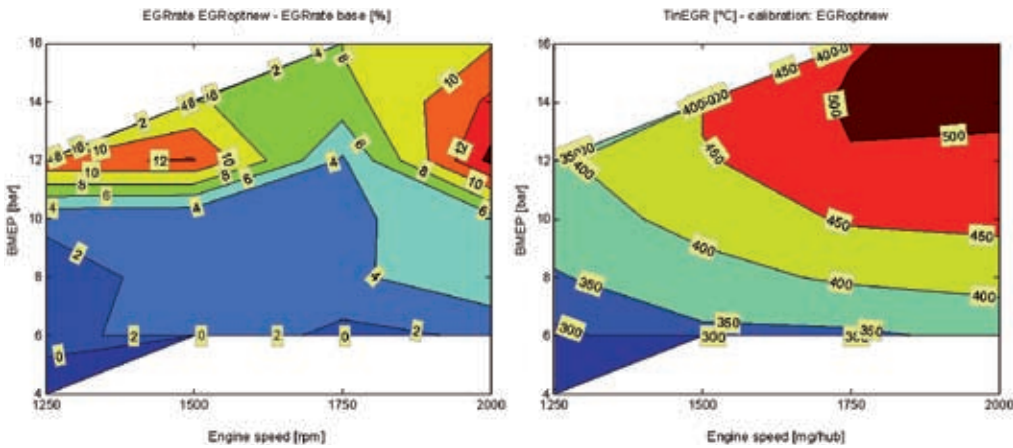


Figure 6: High-dynamic test bed (top) and detail of engine instrumentation (bottom)



**Figure 7:** Variation of EGR rate (left) with respect to baseline calibration and exhaust gas temperature at EGR cooler inlet (right) with optimized calibration as functions of engine speed and bmepp

## 6 Results and Discussion

In addition to the base engine hardware described in the Table, two modified engine configurations with lower compression ratios (CR) were also tested. More specifically, two sets of pistons were subsequently fitted to the base engine, featuring different bowl volume and shape, whose CR were 16.5 and 15.0, respectively. Anyway, the baseline engine calibration employed was optimized for each CR tested.

Regarding micro- and mild-hybrid configurations, experimental investigations were performed with baseline calibration, whereas for strong-hybrid operations both baseline and hybrid-optimized engine maps were used. Mild- and strong-hybrid operation strategies feature Stop/Start release from ECE-2, which is currently thought to be the most promising concept. The advantages

obtained with the different hybrid architectures proved to be virtually independent from engine CR. Therefore, only the results with CR=16.5 are reported. However, it is well known that lower CR can lead to appreciable variations of the absolute values of fuel consumption (FC) and pollutant emissions.

**Figure 8** shows the FC measured during a hot NEDC cycle with conventional engine operations (No-Hybrid) as well as with the application of Stop/Start (STST 1234, STST 234 and STST 34), mild- and strong-hybrid strategies, with the same engine hardware featuring the baseline calibration, Figure. 8 (left) and the strong-hybrid optimized one, Figure 8 (right). The numbers following STST indicate the ECE portion in which Stop/Start strategy is enabled. The bars in the figure are organized in different groups, which refer either to different parts of the driving cycle (ECE-1, ECE-2,

ECE-3, ECE-4 and EUDC portions) or to the whole NEDC cycle. The results are reported as percentages with respect to the FC measured under No-Hybrid operations.

Micro-hybrid strategies are capable of reducing FC of 2 to 4 % over NEDC, depending on the ECE cycle in which the Stop/Start is enabled, whereas the implemented mild- and strong-hybrid reduced FC of 10 % and 14 % over NEDC, respectively. Within strong-hybrid strategy, fuel economy is mainly achieved by operating the vehicle in pure electric mode during the 1<sup>st</sup> gear ramp of the ECE-2, 3 and 4 cycles and by shifting engine operating points towards higher-load and higher-efficiency areas of the engine map (yellow symbols in Figure 4). Extrapolations of mild- and strong-hybrid operations including also Start/Stop (and 1<sup>st</sup> gear in pure electric mode for strong-hybrid) during ECE-1 suggest

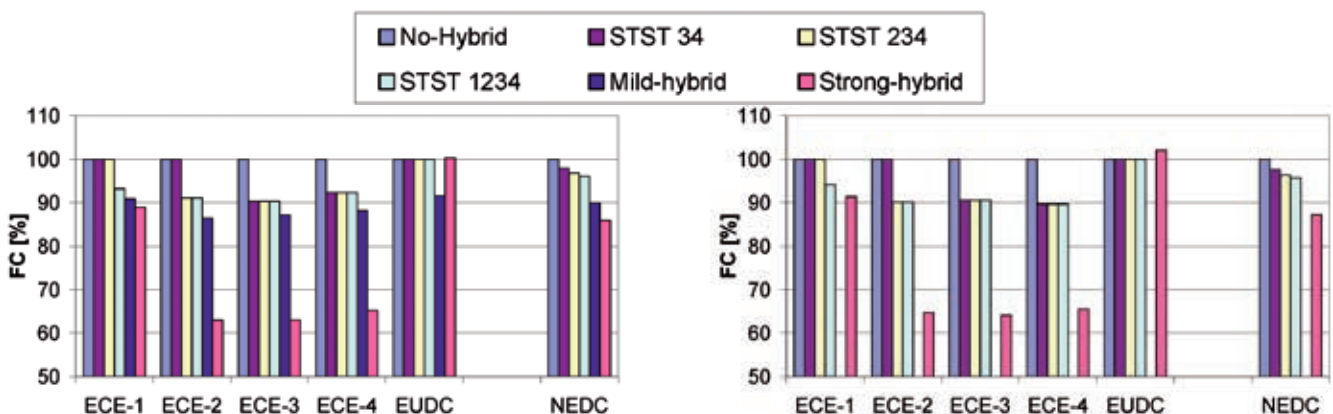


**Figure 8:** Normalized FC percentage reduction obtained with different hybridization strategies and ICE featuring baseline (left) and strong-hybrid optimized (right) calibrations during hot NEDC driving cycle

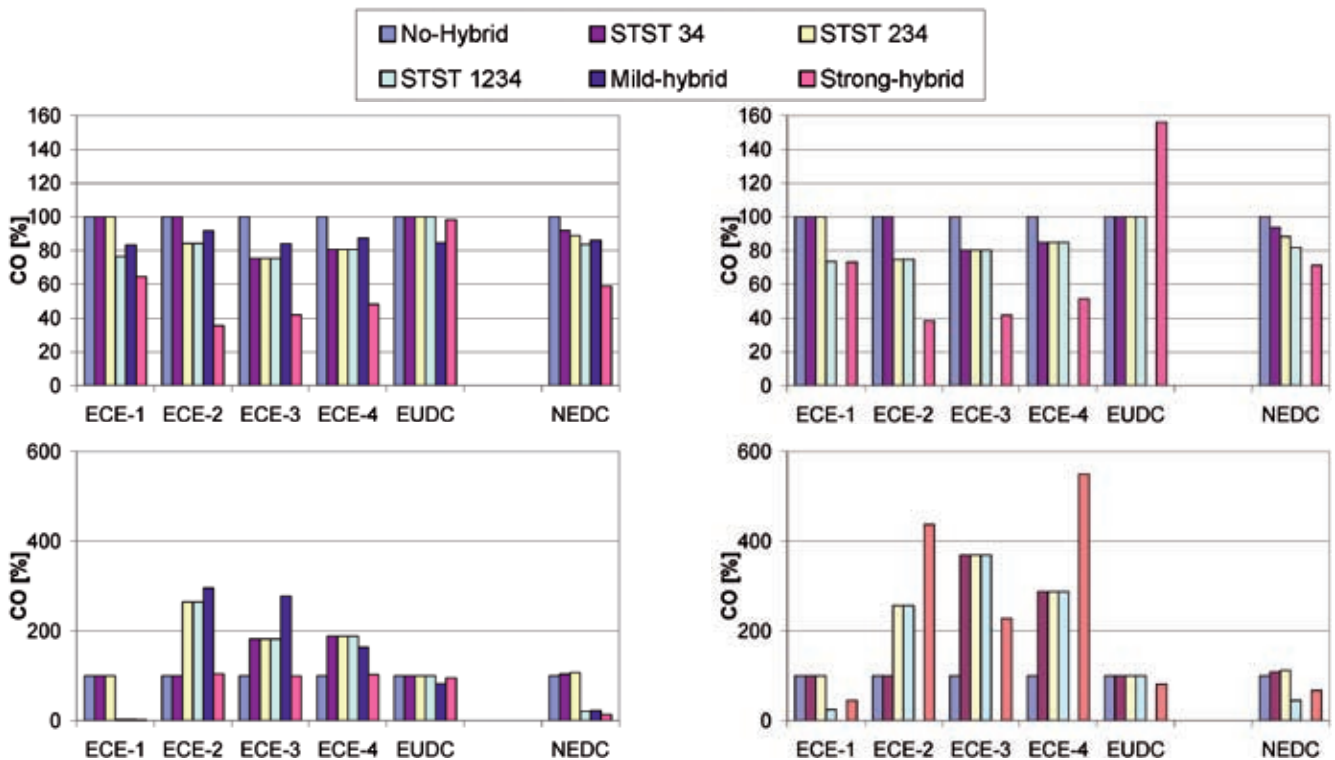


Figure 9: Normalized precat (top left and right) and postcat (bottom left and right) CO percentage reduction obtained with different hybridization strategies and ICE featuring baseline (top and bottom left) and strong-hybrid optimized (top and bottom right) calibrations during hot NEDC driving cycle

potential for further FC reductions (0.5 % and 2.5 %, respectively). FC benefits enabled by strong-hybrid are very promising, since have been obtained by comparison to a very efficient manual transmission rather than an automatic one, which instead provides the driving behaviour smoothness equivalent to strong-hybrid.

Figure 9 shows the CO emissions upstream of, Figure 9 (top left and right),

and downstream from DOC, Figure 9 (bottom left and right), measured during the same tests discussed in Figure 8.

As previously detailed, the values are normalized with respect to the reference values measured under No-Hybrid operations and expressed as percentages. Both engine-out and tailpipe CO levels are lower when Stop/Start strategies are enabled. This suggests that with hybrid operation not only CO production

during idling can be avoided, Figure 9 (top left and right), but also that a quicker DOC light-off can be achieved because of higher average temperature of exhaust gases obtained by suppressing idling. The same outcomes were also obtained under cold NEDC cycle.

Concerning THC emissions, similar considerations to those previously reported for CO levels can be done. Furthermore, a dramatic reduction (higher

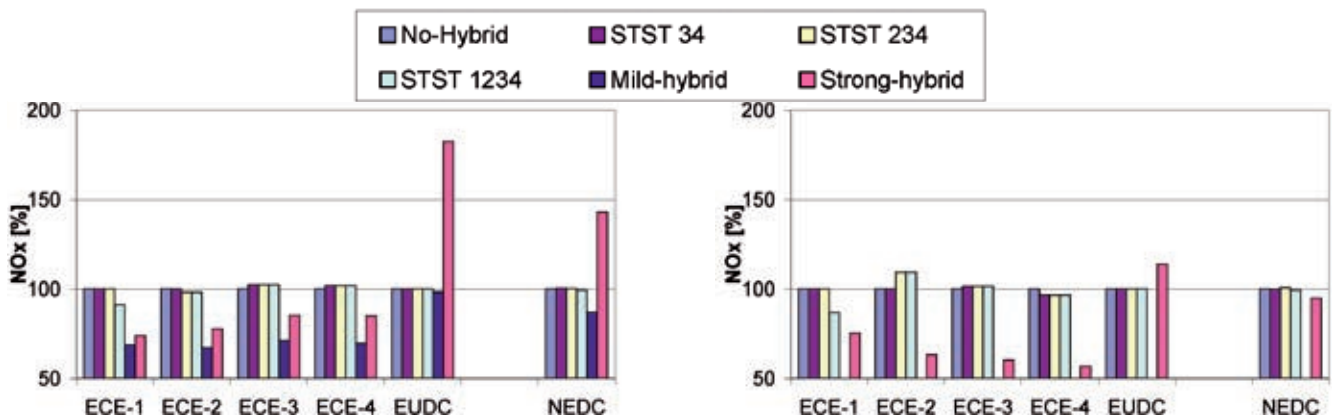


Figure 10: Normalized engine-out NOx percentage reduction obtained with different hybridization strategies and ICEs featuring baseline (left) and strong-hybrid optimized (right) calibrations during hot NEDC driving cycle.

than 50 %) of engine-out and tailpipe THC is obtained with strong-hybrid for both engine calibrations.

Micro hybrid strategies show virtually no effects on  $\text{NO}_x$  emissions, **Figure 10**, whereas the application of BAS system allows one to achieve a significant reduction in  $\text{NO}_x$  levels.

It can be speculated that  $\text{NO}_x$  reduction during electrical assisted drive away overcomes the slight  $\text{NO}_x$  deterioration during stationary 2<sup>nd</sup> and 3<sup>rd</sup> gear operations with electricity regenerations. Regarding strong-hybrid, the reduction of  $\text{NO}_x$  emissions over NEDC cycle in **Figure 10** (right) was obtained by means of the specific recalibration of the engine maps detailed in the section “Engine map recalibration for strong-hybrid operations”. A significant deterioration of  $\text{NO}_x$  emissions is measured when such a strategy is enabled without a specific recalibration of engine maps, **Figure 10** (left).

PM is almost unaffected by the application of micro and mild hybrid strategies, since PM production shows dispersion in line with measuring accuracy. On the other hand, strong-hybrid shows a higher PM production in the NEDC cycle, which can be ascribed to the EUDC phase. Even though in this case the measured PM increase is manageable by DPF application, deterioration of PM- $\text{NO}_x$  tradeoff might limit the possibility of achieving very low  $\text{NO}_x$  levels by means of engine recalibration, in particular in view of stricter emission certifications. As anticipated in the abstract, this could require the development of engine combustion system components (for example EGR cooler and turbocharger) specifically designed for strong-hybrid operation, in terms both of performance and durability.

## 7 Conclusions

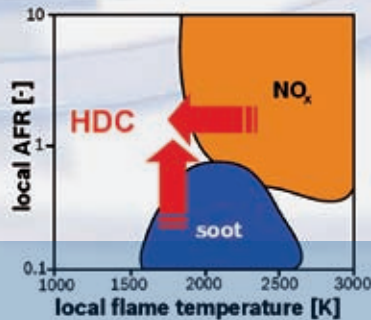
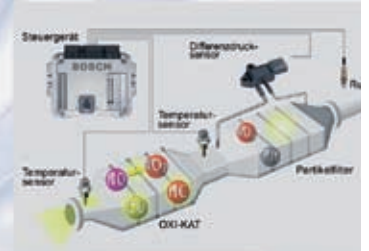
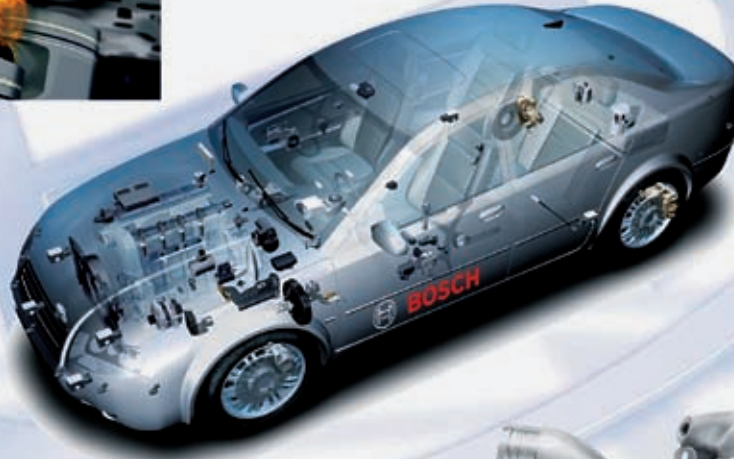
The performed experimental activity provided a first assessment of the potentialities and the challenges of micro-, mild- and strong-hybrid diesel applications for light-duty vehicles based on GM 1.9 l four-cylinder in-line diesel engine. By a proper integration with GM-proprietary powertrain simulation tools, engine operation at the dynamic test bench was controlled in order to reproduce accurately the hybrid power-

trains and their optimized schedules while avoiding to employ the complex mechanical/electric/electronic hardware of hybrid powertrains. This simplification was possible because the focus of the project was to study the effects of hybridization on diesel engine operation in terms of fuel consumption, pollutant emission production and calibration variations. Major results showed that micro-hybridization (i.e. Stop/Start system) reduced fuel consumption by roughly 4 %, mild-hybridization (i.e. Belt Alternator Starter) by roughly 10 %, whereas strong-hybridization (i.e. Full-Hybrid Power Split) by roughly 14 %. The achievements obtained by strong-hybrid are particularly promising, since they have been obtained by comparison to a very efficient reference manual transmission rather than an automatic one as it is usually done. This latter could provide a driving smoothness equivalent to strong-hybrid powertrain, but at the expenses of additional fuel penalties. Tailpipe emissions showed distinct behaviours with regards to the pollutant species and the system considered. In particular, HC and CO exhibited a general improvements due to the decrease of engine idling time, whereas, only for strong-hybrid,  $\text{NO}_x$  and PM showed increases that required a specific engine recalibration for meeting the same emission certification of the base engine. Even though in this case the PM increase was manageable by DPF application, as a general case the deterioration of PM- $\text{NO}_x$  tradeoff might limit the possibility of achieving very low  $\text{NO}_x$  levels by means of engine recalibration only, in particular in view of stricter emission certifications. This could therefore require the development of engine combustion system components (for example EGR cooler and turbocharger) specifically designed for strong-hybrid operation, in terms both of performance and durability.

## References

- [1] Cipolla, G.; Cisternino, M.; Paladini, V.: Hybrid Propulsion System - GM March to Zero Emissions. Eröffnungsvortrag der PCIM China, Shanghai, 2007
- [2] Cisternino, M.: From Micro to Full, exploiting the benefits of different degrees of hybridization in a flexible hybrid architecture. 19<sup>th</sup> International AVL Conference ‘Engine and Environment’, 2007

- [3] Louis, J.J.J.: Well-To-Wheel Energy Use and Greenhouse Gas Emissions for Various Vehicle Technologies. SAE Paper 2001-01-1343, 2001
- [4] www.dieselnet.org
- [5] Cipolla G.; Vassallo A.; Catania A.E.; Spessa E.; Stan C.; Drischmann L.: Combined Application of CFD Modeling and Pressure-Based Combustion Diagnostics for the Development of a Low Compression Ratio High-Performance Diesel Engine. SAE Transactions, Paper No. 2007-24-0034, 2007
- [6] Grewe, T.M.; Conlon B.M.; Holmes, A.G.: Defining the General Motors 2-Mode Hybrid Transmission, SAE paper 2007-01-0273, 2007
- [7] Sakata I.; Nagae M.; Omae K.; Ito H.: A New Combustion Concept for Passenger Car Diesel Engines Based on a Low Compression Ratio, XV Aachener Kolloquium Fahrzeug- und Motorentechnik, 2006



# Homogenous Diesel Combustion Challenge for System, Components and Fuels

Modern Diesel engines allow prominent road performances and low fuel consumption, resulting in a rising Diesel car fraction throughout Europe. At the same time stringent future emission legislation means a big challenge for Diesel engines. In Europe, for example, the expected 2014 nitrogen oxide threshold (Euro 6) will be approximately 30 % of the actual Euro 4 value. The Corporate Research of Bosch has been investigated the potential of Homogenous Diesel Combustion (HDC) to minimize  $\text{NO}_x$  emissions under vehicle-compliant conditions.

## 1 Introduction

The potential of the HDC could have been scientifically proven comprehensively [1, 2], whereas utilisation for vehicles in practise still is a big challenge. Dynamic operation, combustion noise and HC/CO emissions here represent the main issues. Within this investigation a EU4 series 2.0 l engine equipped with Bosch Common Rail System and Diesel particulate filter (DPF) has been enhanced for dynamic NEDC operation. Basic knowledge was first of all generated with a single-cylinder engine [3, 4].

Considering the actual CO<sub>2</sub>/climate discussion and the limited fossil resources worldwide activities to develop alternative fuels for combustion engines are being intensified at present. Sustainable combustion concept research has to account for this. Hence the influence of different fuels on combustion behaviour and emissions of the Bosch HDC engine was analysed.

## 2 Combustion Concept

Regarding the typical low load area relevant for the main pollutant emission, EGR values up to 45 % are state of the art. Combined with a relatively late injection timing close to top dead centre (TDC) this results in a retarded combustion phasing, **Figure 1** (red), with low noise and NO<sub>x</sub> levels.

To reach maximal homogeneity of fuel, air and exhaust gas with a DI-Diesel engine the injection event has to occur very early during the intake stroke. HDC theory describes that the following self ignition of each fuel molecule in the combustion chamber takes place at the same time – corresponding to the very efficient constant-volume combustion process. In practise, to avoid lubricant dilution by fuel on the one hand and allow enough time for mixture formation on the other, injection has to be initiated about 30 to 10° CA BTDC, **Figure 1**, blue lines. Homogenisation then is still ensured by EGR rates beyond 50 %.

The temperature rise during the compression stroke only depends on the compression ratio (CR). Single-cylinder experiments show that combustion phasing during HDC operation with block injec-

tion can be influenced by start of injection (SOI) with CR = 15, **Figure 1**. Together with cooled external EGR, combustion behaviour is controllable cycle-by-cycle even when only using a conventional cam-driven valve train. A pilot injection would shorten the ignition delay and is obsolete as a matter of HDC principle.

The piston bowl design for the HDC concept was optimized with the help of CFD simulation – starting from a CR = 18 series piston shape. Calculations were performed at the Robert Bosch Research and Technology Centre (RTC) in Palo Alto, USA.

Regarding a medium-sized vehicle (1800 kg) single-cylinder results allowed to predict a NO<sub>x</sub> potential of 80 % against the baseline EU4 engine – coming with tripled HC/CO values. The following chapter describes the operation strategy to enable HDC for vehicle use.

## 3 Operation Strategy

The energy released during combustion increases with the engine load and thus more and more heats up the combustion chamber and the intake system. Exceeding a certain engine load limit the HDC process can no longer be controlled by SOI.

The degree of homogeneity decreases with rising engine speed because the total duration of mixture formation becomes shorter. This cannot be compensated by the higher turbulence level. That is why the HDC concept is limited to a certain area of the engine load/speed

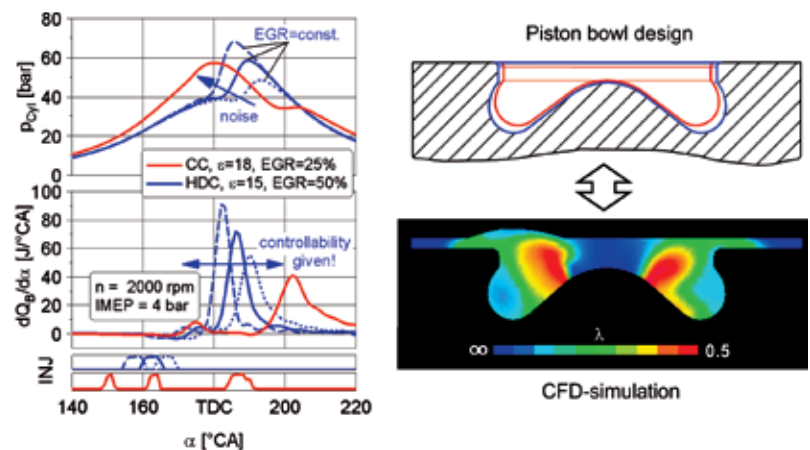


**Figure 1:** HDC concept for EU6 – combustion and piston design

## The Authors



Dr.-Ing. Roderich Otte is Project Manager “New Diesel Combustion Concepts” at Corporate Research, Robert Bosch GmbH in Stuttgart (Germany).



Dr.-Ing. Thorsten Raatz manages the project and competence-network “New Fuels” at Corporate Research, Robert Bosch GmbH in Stuttgart (Germany).



Dr.-Ing. Thomas Wintrich is Head of department “Advanced Engineering Engine” at Corporate Research, Robert Bosch GmbH in Stuttgart (Germany).

map, **Figure 2**. Vehicle operation needs a smooth change between HDC and CC modes in both directions – without changes in engine torque or noise recognizable by the driver.

To ensure compliance with noise and emission requests during HDC operation a cylinder-individual control strategy was developed together with the research department for “Software Intensive Systems”. The combustion pressure of each cylinder has to be measured to calculate and control the pressure gradient ( $dp/d\alpha$ ) and the indicated mean effective pressure (IMEP). EGR and boost pressure values are read from “steady-state” maps and accurately adjusted with the help of the Bosch Air System Modelling (ASMod) and its MBC/MCC functionality (Model based Boost/Charge Control), designed by the Bosch Diesel-Systems department.

To perform a combustion mode change, both, fuel injection parameters and EGR rate will be guided automatically to the direction of the target combustion concept. The frequency of this mode change within the NEDC or FTP test procedure can be minimised by designing an adequate air system. With a powerful charging and EGR system it is possible to use HDC even for upper engine loads.

**4 Air System**

Research engines with external boosting and pressure-flaps in the exhaust system, e.g. the Bosch single-cylinder engine, allow arbitrary combinations of boost pressure and EGR rate. In real vehicle operation these two parameters are coupled:

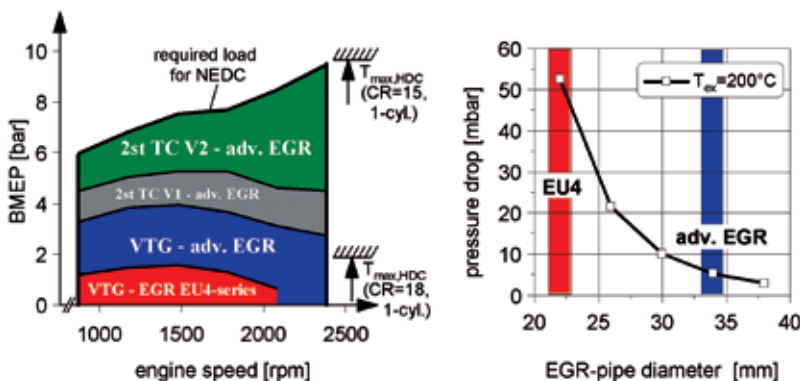


**Figure 3:** Hardware evolution from EU4 to HDC system

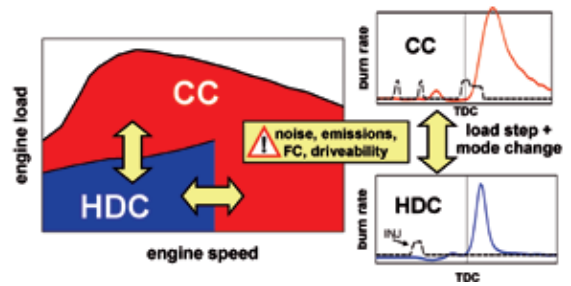


**Figure 2:** Mode change between CC and HDC

increasing EGR lowers the possible boost level and the driving pressure difference between exhaust and intake at the same time which additionally limits the possible EGR level. To cover the NEDC map with HDC the air system has to run through extensive changes, **Figure 3**.

A first step is to detrottle the EGR system by widening the effective cross sections (compare diagram on the right) and the integration of a powerful, variable EGR cooling unit. This already helps to extend the HDC map significantly, **Figure 3** (left). The application of a two-stage turbo system V1 from a light-duty truck with two non-variable chargers was a second step to the right direction. Finally 1D flow simulation leads to the appropriate charging system V2 to reach the wanted HDC map.

The conversion behaviour of a typical downstream Diesel oxidation catalyst (DOC) is strongly influenced by the thermally effective mass and the efficiency of the charging system. The exhaust temperature at DOC inlet decreases with V2, compared to the standard VTG system. Together with the higher HC/CO level this leads to a severe exhaust aftertreatment issue.

**5 Exhaust Aftertreatment**

Reactive CFD calculations (rCFD) were performed to detect the HC/CO sources [5]. As the main cause the inhomogeneity of the cylinder charge could be identified. CO emissions pre-dominantly derive from rich areas within the mixture, HC emission from the lean.

To reach EU6  $\text{NO}_x$  limits without a  $\text{DeNO}_x$  system there is no alternative to the (partly-)homogenous Diesel combustion. Two-stage charging and low exhaust gas flows lead to very low gas temperatures at DOC inlet and thus obstruct the post-oxidation. An additional catalyst between cylinder head and charging system can be a possible solution for this problem [6]. The effect of the so called Pre-Turbo Catalyst (PTC) on pollutant conversion and inlet temperature at the DOC with HDC operation is shown in **Figure 4**.

If the combustion mode at low load changes from CC to HDC and only the series DOC is used, **Figure 4** (on the left), the DOC-in temperature decreases because the charging system pulls out the same heat quantity from a lower exhaust mass flow. In the beginning the higher HC/CO mass-flow is converted by the DOC, represented by the “DOC out” value. But about 150 s later this oxidation stops and HC breaks through the aftertreatment system.

If a small PTC with a volume of  $100 \text{ cm}^3$  is added to the system, **Figure 4** (on the right), the conversion rate adds up to nearly 100 % throughout the entire experiment. The reason is a 30 % conversion along the PTC resulting in a 30 K temperature rise at DOC inlet. Already this simple experiment under hot running conditions shows that the PTC is indispensable to bring HDC concepts into a vehicle. To avoid undesirable pres-

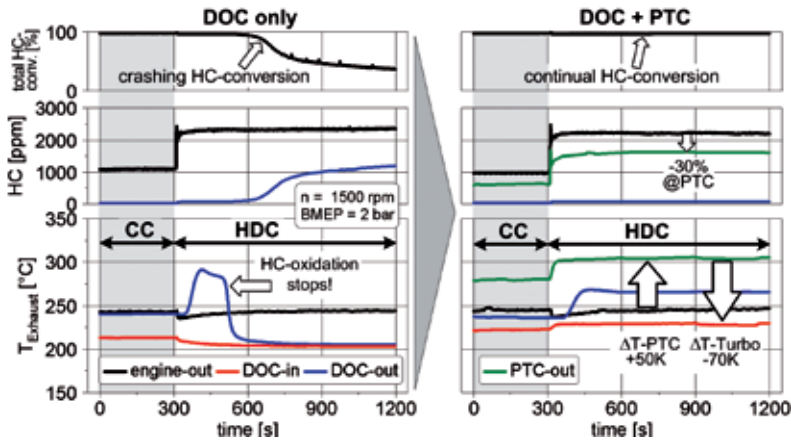


Figure 4: Effect of additional pre-turbo-catalyst (PTC) on HC-conversion at HDC

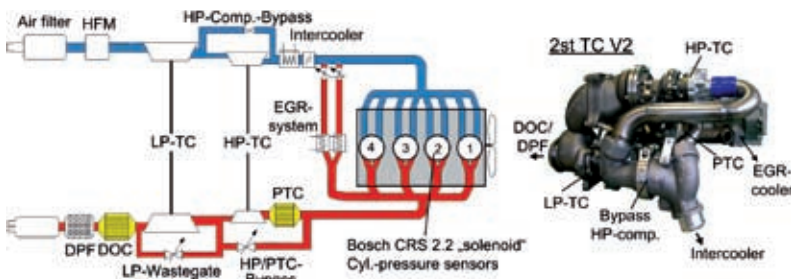


Figure 5: HDC target system

sure drops along the PTC and thus losses in power output at full load, a special arrangement of the exhaust components was developed.

### 6 Target System

The corresponding HDC target system, **Figure 5**, can be derived from the investigation so far. Air filter, HFM, intercooler, DOC/DPF and injection system (CRS 2.2, 1600 bar) are taken from the baseline production engine. The first stage of the new charging system consists of a very small high pressure turbo-charger. To minimise the mass flow trade-off between the two chargers the low pressure stage is just big enough to assure the baseline engine full load performance. The HP compressor is automatically bypassed when a certain pressure value is reached. According to 1D simulation a cooler between the two charging stages is obsolete.

On the exhaust side the burned gas reaches the HP turbine via PTC - provided that the by-pass flap is closed. At

full load and high engine speed this flap has to be opened to bypass the PTC and the narrow HP turbine. As a side-effect catalyst aging is minimised for the small PTC. The bypass flap is continuously variable between these two positions. This positioning of the PTC is ideal because both, HP turbine and PTC, have to be passed through at the same time - during HDC operation. Dynamic

boost behaviour is generally unaffected by the PTC. The volume ratio between the metallic PTC and the ceramic DOC is 1 : 25, resulting in a very small absolute precious metal requirement despite a high specific loading. The PTC could reduce the precious metal demand of the DOC because now this catalyst has to convert fewer pollutant molecules on a higher temperature level.

The EGR system consists of two parallel electrical valves and liquid/gas coolers. Combustion analysis and control is assured by Kistler 6043 pressure sensors, 1D simulation can be validated with comprehensive low pressure measurements in the intake/exhaust manifolds.

## 7 Experiments

### 7.1 Dynamic Operation at NEDC

The huge emission potential of HDC predicted with single-cylinder results were verified by very fine steady-state mapping with the full-size engine [7]. Reliable statements concerning combustion noise, tailpipe-out emissions and performance of combustion controls need dynamic experiments. Now the main results with dynamic HDC operation during NEDC are discussed. The test started with a warm engine, glow functionality and combustion mode change was not needed. Dynamic soot emission was measured by AVL Micro Soot Sensor.

**Figure 6** shows the air/fuel ratio and the EGR rate controlled by ASMod for the last city part and the subsequent extra-urban phase. The diagram emphasises

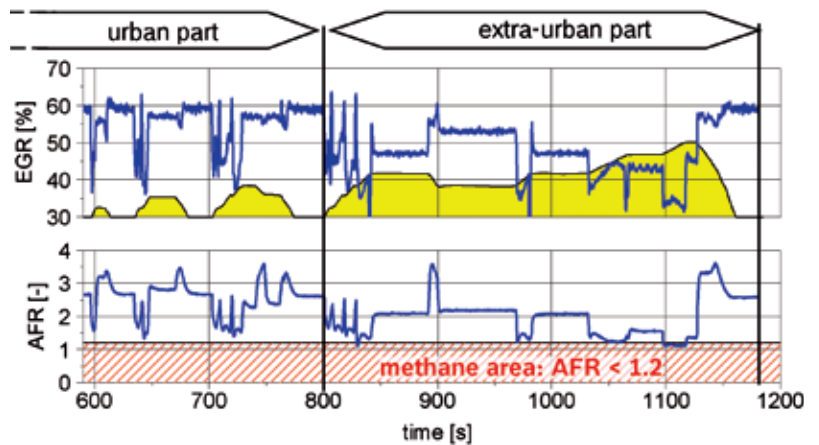


Figure 6: HDC during NEDC – EGR and air/fuel ratio

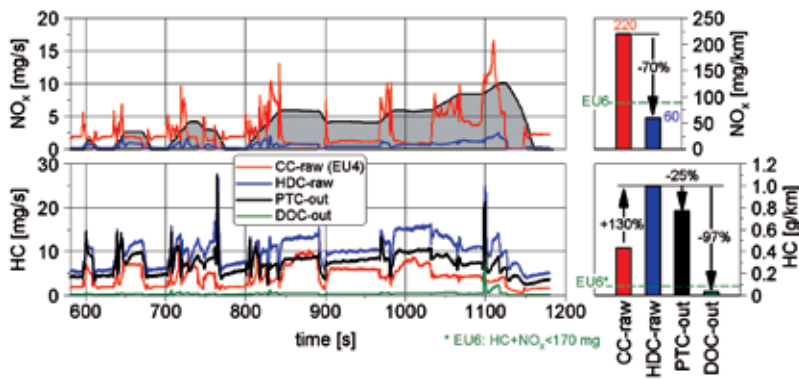


Figure 7: HDC during NEDC – NO<sub>x</sub>/HC emission

the importance of dynamic operation for alternative Diesel combustion development: Only constant vehicle speed leads to typical HDC with EGR > 50 % during the city cycle.

The extra-urban part leads to lower EGR/AFR levels due to higher loads. Acceleration and gearshifting events cause veritable crashes of the two parameters. Here combustion control is very important, because charge composition and gas temperature change instantly. To avoid methane emission during HDC operation AFR > 1.2 have to be assured [5]. During this NEDC test the critical AFR zone is avoided for 98 % of the runtime.

Figure 7 illustrates the huge potential of the introduced HDC concept to beat future emission limits. A NO<sub>x</sub> reduction by 70 % from EU4 baseline engine suffices to reach the EU6 target window. At the same time HC raw emissions are twice as high. The PTC reaches a HC conversion of 25 % (CO: -30 %, not depicted), downstream the DOC a HC value of about 40 mg/km can be detected. The NO<sub>x</sub>+HC

value is 40 % lower than the EU6 limit (170 mg/km). Without PTC and with unloaded DOC at the beginning of the test a HC breakthrough can be observed after 400 s runtime (not depicted).

The combustion control unit adjusts the cylinder-individual pressure gradients to reach acceptable values, defined with earlier steady-state experiments. Pressure gradients or calculated noise levels are not shown at this point, because different time resolution or calculation algorithms lead to highly diverging results. On the engine test bed a subjectively acceptable combustion noise could be noticed.

Fuel consumption does not differ from the baseline values because the high energy losses through HC/CO emissions could be compensated by the much higher thermodynamic efficiency of the HDC concept, Figure 1.

Soot emission is slightly below the EU4 level, whereby the fuel input for DPF regeneration is sinking. Most of the soot mass is emitted during the extra-urban

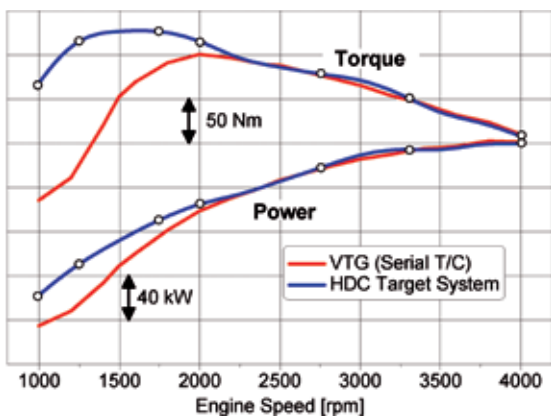


Figure 8: Full load – HDC system vs. baseline

part with relatively high engine loads where only a partly premixed combustion is reached.

### 7.2 Full Load

Two-stage charging systems push into the Diesel passenger car market to achieve outstanding specific power, e.g. in the BMW 123D. The charging system developed for the low emission approach with HDC allows a much higher low-end torque. Figure 8. Engine torque can be doubled at 1000 rpm, for instance. This would permit superior start-up behaviour with a car. A latest generation Common Rail System (≥ 2000 bar) would improve the full load performance beyond 2000 rpm through shortened combustion duration.

### 8 Fuels

In this chapter it is shown, how far the HDC concept is suitable for the use of future fuels and which potentials arise from the fuels. Three different alternative fuels were examined: pure biodiesel (100 % RME), synthetic diesel with high cetane number and higher boiling curve and synthetic diesel with low cetane number and low boiling curve. These extreme fuels were applied consciously to check the suitability of Bosch HDC concept in a wide fuel area.

Biodiesel is mixed with the fossil diesel in consistently rising amounts and also is offered, mainly for vehicle fleet application, as pure biodiesel. Biodiesel distinguishes itself, first of all, by its higher boiling curve and its oxygen content. The synthetic diesel with high cetane number (SDH) is known for its good results with conventional combustion concepts and its possible conflict with homogeneous diesel combustion concept, caused by shortened ignition delay and therefore shortened mixture time [8]. On the other hand the synthetic diesel with low cetane number and boiling curve (SDN) stands in the reputation to be particularly suitable for homogeneous diesel combustion concepts. Figure 9 shows exemplary the combustion process of the different fuels in a steady state operation point with constant operation parameters. The combustion control unit detects these different combustion processes and changes the injection timing

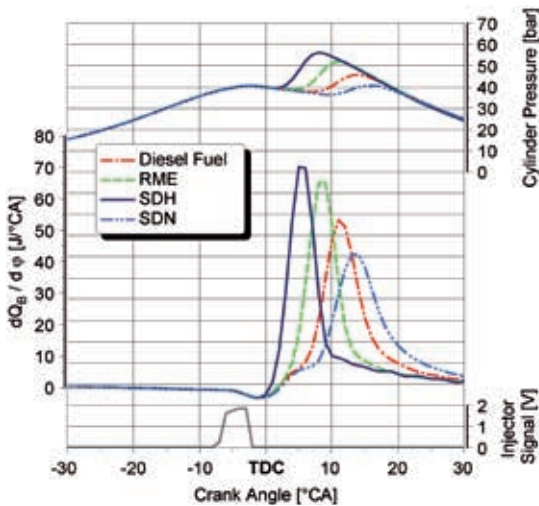


Figure 9: Combustion process of different fuels

for the fact that the combustion position is ideal again regarding the combustion noise and the emissions. This is reflected in the NEDC emissions, Figure 10.

The Bosch HDC concept reacts insensitively concerning the NO<sub>x</sub> emissions even to widely changed fuel characteristics and actually advantages can be realized at the HC/CO emissions. This also confirms the general possibility to perform a positive contribution to the emission reduction with the fuel as a design feature [9]. The examined fuels have a comparable energetic consumption with advantages for the synthetic fuels concerning CO<sub>2</sub> emissions by lower C/H ratio and for biodiesel naturally by its regenerative production.

### 9 Summary and Outlook

The well known NO<sub>x</sub> potential of homogeneous Diesel combustion can be utilised for real vehicle practise only under the following conditions:

- covering of relevant load/speed areas of the engine map
- reliable dynamic operation
- acceptable noise level
- significant reduction of HC/CO emission
- alternative fuels tolerated.

The Corporate Research of Bosch realised the above based on a EU4 four-cylinder Diesel engine with Bosch Common Rail System. To cover the complete NEDC with HDC a two-stage turbo system and a capable EGR system was prototyped. Thus high volumetric air efficiencies are possible despite the typical EGR values beyond 50 %. The engine is operated with block injection late in the compression stroke. The compression ratio CR = 15 enables a cylinder-individual control of combustion noise (dp/dα) via injection timing. EGR and boost pressure are accurately adjusted by the Bosch Model Based Air System Control ASMod. When leaving the HDC area for any reason an automatic combustion mode change will occur, including the switch-on of pilot injections.

High HC/CO emissions demand the combination of a Pre-Turbo Catalyst (PTC) and a Diesel oxidation catalyst (DOC). The PTC can be bypassed with the HP turbine bypass which is necessary anyway.

During a dynamic hot NEDC test on the engine test bed the Bosch HDC engine goes below EU6 emission limits without any drawback concerning fuel consumption. Even major differences in fuel specifications can be compensated by the combustion control unit.

### References

- [1] Flynn, P.: Diesels 2007, Promise & Problems. 7<sup>th</sup> Diesel Engine Emissions Reduction Workshop, 2001
- [2] Raatz, T.: Untersuchungen zur homogenen Dieselverbrennung. Braunschweig, Technische Universität, Dissertation, 2003
- [3] Müller, J.; Otte, R.; Weberbauer, F.: Herausforderungen bei der Entwicklung von Diesel-HCCI-Brennverfahren. Haus der Technik München, „Motorische Verbrennung“, 2007
- [4] Weberbauer, F.; Müller, J.; Otte, R.: Einsatz eines variablen Ventiltriebs zur Optimierung von Dieselbrennverfahren. Haus der Technik Essen, „Variable Ventilsteuerung“, 2007
- [5] Cook, D. J.; Pitsch, H.: Combustion and Ignition Modeling for IC Engines Report No. TF-106, Stanford University USA, 2007
- [6] Jörgl, V.; Keller, P.; Weber, O.; Müller-Haas, K.: Influence of Pre Turbo Catalyst on Diesel Engine Performance, Emissions and Fuel economy. SAE-Paper 2008-01-0071, 2008
- [7] Otte, R.; Müller, J.; Weberbauer, F.; Guggenberger, B.: Homogenous Diesel Combustion – Challenges under vehicle-conform operating conditions. IMechE London, “Internal Combustion Engines: Performance, Fuel Economy and Emissions”, 2007
- [8] Raatz, T.; Steinbach, N.; Harndorf, H.; Weberbauer, F.: Potential of synthetic diesel fuels. THIESEL Valencia, Conference on Thermo- and Fluid Dynamic Processes in Diesel Engines, 2006
- [9] Warnecke, W.; Liebig, D.; Wilbrand, K.: Fuels of the Future. Hamburg ATZ/MTZ-Konferenz Kraft- und Schmierstoffe, 2007

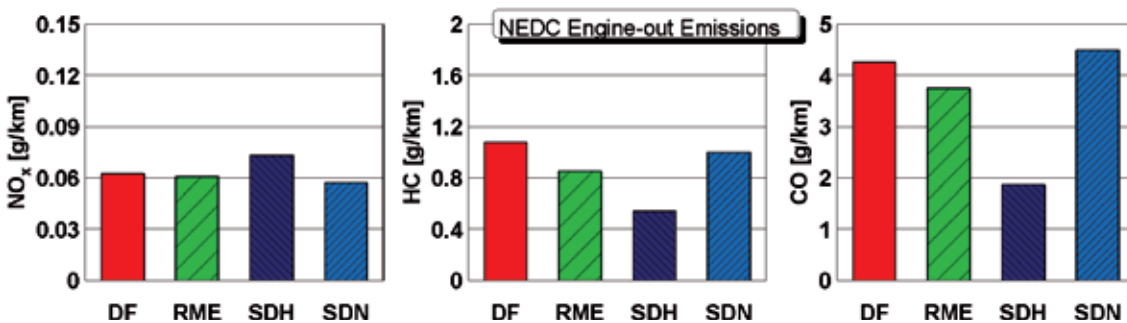
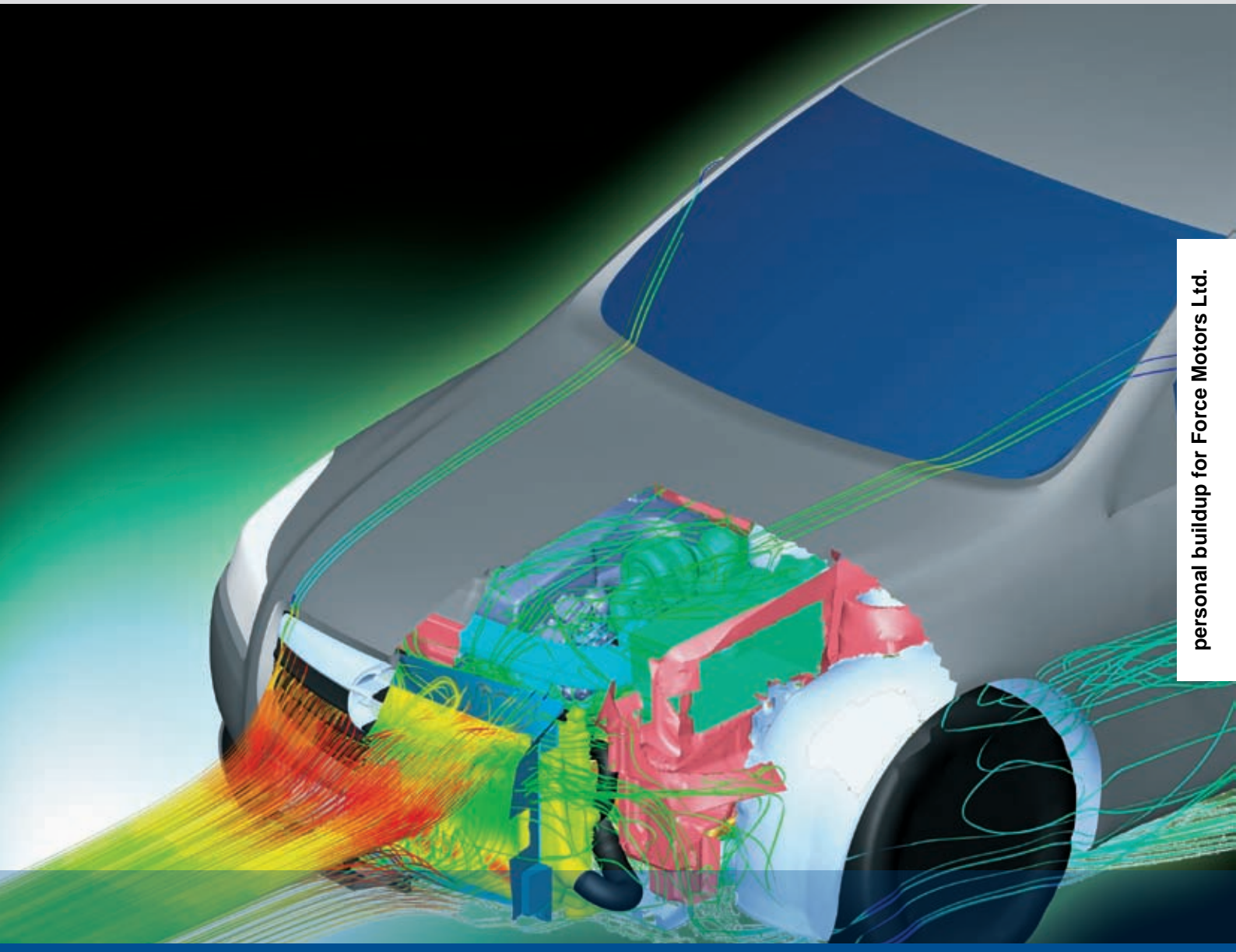


Figure 10: NEDC raw emissions with different fuels



personal buildup for Force Motors Ltd.

## Process Automation for Engine Coolant Chambers with CFD

Over the last four years, it has become possible to reduce the project processing time of a single calculation for a coolant chamber of an internal-combustion engine by 75 %. Synergetic effects in variable calculations made it possible to raise the amount of calculations per year six-fold. Tecosim uses wrapping methods, efficient meshing technologies and automatic model set-ups in its CFD simulation.

## 1 Introduction

While the development time of modern automobiles becomes shorter and shorter, the demand for quality steadily increases. Computational fluid dynamics (CFD) is a vital part of developing processes striving to reach these goals. The efficient use of numeric methods wholly depends on the amount of time needed for the single processing steps, such as geometry clean-up, grid generation and post-processing.

Using the example of the cooling of an internal-combustion engine (Powertrain Cooling [PTC]), Tecosim shows how the single steps of the simulation process are adjusted and optimised, in order to ensure increasing end-result quality with a simultaneous decrease in time demands. Efficient methods and automations are applied both in geometry clean-up, e. g., in the wrapping procedure and in grid generation, as well as in result editing, including presentation creation. In this way, the project processing time of single calculations was reduced by three-quarters over the course of the last four years. Synergetic effects in variable calculations even made it possible to increase the amount of PTC calculations per year six-fold. The following methods contributed to these progresses:

- wrapping of whole engines and engine parts
- efficient 3D meshing methods, with a modular design and hybrid grids
- automated model set-up with I/O database linking
- automated analysis procedures, including the supply of standardised alpha-numeric and graphic display
- automated creation of PowerPoint presentations for various variable comparisons.

This procedure made it possible to evaluate a coolant chamber's functionality before the prototype was built and to implement possible design corrections during an early development phase.

The efficiency of the coolant chamber is critically depending on its rates of percolation, i.e., the speed and temperatures, with which it has been admitted. These conditions are influenced by the geometry of the underhood, the engine and the underbody. Cooler grill openings and flow-guiding built-in

components (light sheet metals, retractions) have an especially big influence on cooling performance. It is not enough just to look at the immediate surroundings, that is, the underhood, to guarantee a meaningful simulation of the cooling module. Rather, it is important to look at the full vehicle, especially the front-end.

From this it follows that for PTC calculations, it is necessary to conduct a full car simulation, including external aerodynamics, detailed underhood and underbody. This requires a multiplicity of boundary condition definition. The complexity of the task, and the wish to facilitate a multiplicity of variant calculations, calls for an automation of the work steps, in order to ensure a speedy calculation, **Figure 1**.

## 2 Wrapping Procedure

A significant part of fluid flow simulation still lies in geometrical clean-up. Usually, only a small percentage of the surfaces from the complete CAD data is necessary for the CFD.

While native CAD data consists of a huge number of components, which have contact, intersect each other or are built within each other, CFD requires a closed surface enclosing just the main flow area. This surface must be available in triangulated form, for example as an STL file (surface tessellation language; description of the surface by means of triangles). Processing the geometry with CAD functionality takes several working weeks for a complete automobile. The engine is a particular challenge, due to its data volume and number of components.

Surface wrapping is a time-saving alternative as it superimposes the geometry with a Cartesian hexahedron grid, with the cells classified in and outside of the geometry. The nodes that are close to the exterior surfaces are projected into the geometry and the triangulated surfaces are generated. This procedure makes it possible to transform ancillary units, engine parts and components of the CAD system into a closed triangulated

Surface wrapping is a time-saving alternative as it superimposes the geometry with a Cartesian hexahedron grid, with the cells classified in and outside of the geometry. The nodes that are close to the exterior surfaces are projected into the geometry and the triangulated surfaces are generated. This procedure makes it possible to transform ancillary units, engine parts and components of the CAD system into a closed triangulated

## The Author



Dipl.-Ing. Matthias Heinz is department manager for CFD at Tecosim Technische Simulation GmbH in Rüsselsheim (Germany).

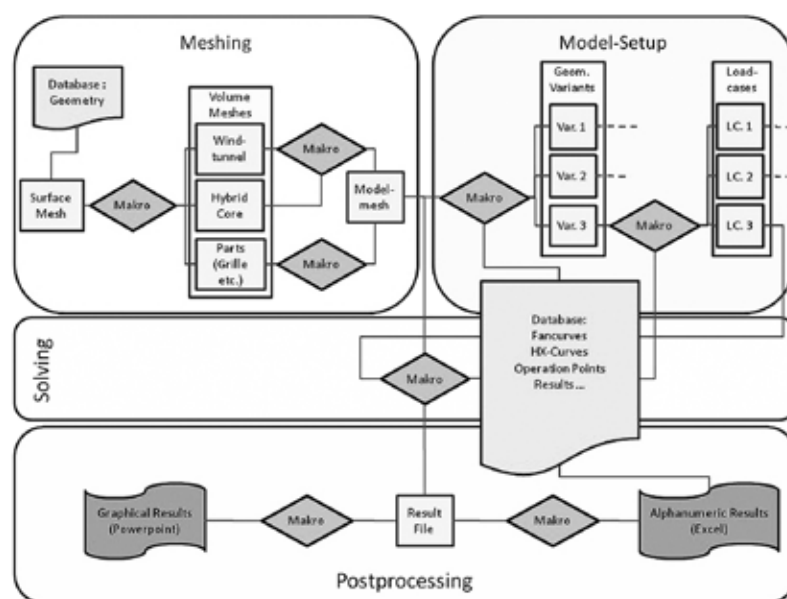
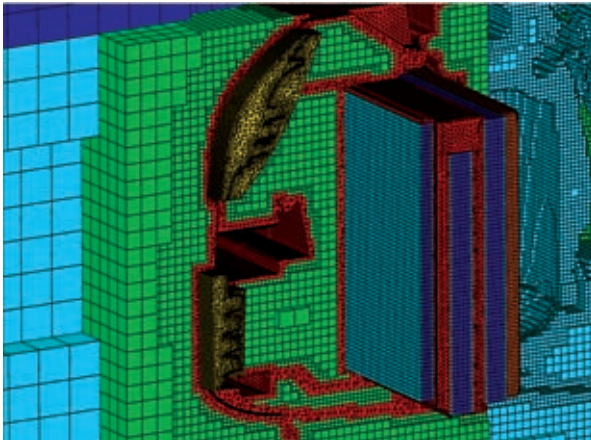


Figure 1: Automated simulation process using macros



**Figure 2:** Hybrid grid near the heat exchanger

ed surface in a single step. The advantage of this method increases in proportion to complexity, but decreases as the demand for attention to detail increases. The optimal solution is a combination of the procedures. Meanwhile it is possible, to reduce the time needed for the geometric clean-up to a few days.

### 3 Modular Design of Hybrid Grids

Since many of the models evolve from advancements in single components or component assemblies, they sometimes differ only in small details. The cooling grill design in particular is often changed and therefore has to be changed in many models. Modularising the mesh is therefore practical, in that it makes the exchange of different geometric elements as easy as possible.

The models are separated in submeshes – wind tunnel, front-end and automobile without front-end – while the front-end is also separated into different parts – coolant chamber, grill, etc. Each module is meshed separately according to a precisely defined scheme and is coupled at the boundaries after merging. The modules each form a unit with precisely defined boundaries. This means that they can be easily replaced within the model. By using a standardised procedure using macros developed exclusively by Tecosim, a high level of automation can be attained.

The meshing technology with different cell types (hybrid grid in **Figure 2**) such as hexahedrons or tetrahedrons, is adjusted to ensure a high level of preci-

sion in the targeted results, while simultaneously minimising the number of cells, providing short calculation times. In the far field, relatively coarse Cartesian hexahedron grids are used, which are refined automatically by a “classify/refine process” approximating the vehicle geometry and subsequently deleted near the solid parts of the geometry. The emerging gaps are usually filled with tetrahedron and coupled together whereas recognition of the coupling areas is mostly automatic.

### 4 Automated Model Design and Calculation

By means of a skilled design, multiple variations can be unified in one single grid by creating thin-walled components switchable. For example, air guides or splash guards can be depicted as either baffles or thin walls. The plates are infinitesimally thin, so that they are composed of surfaces, rather than cells. Depending on the definition of the boundary condition, they can be viewed either as a wall or as flow-through. Thick-walled areas can also be rendered switchable, as long as they have been meshed internally. In this way, they also can be defined as flow-through areas or as solid bodies. A shared database manages all variations. This database can hold up to several hundreds of calculations for one single automobile platform.

It is possible to create different load case models from one single geometrical variant (driving situations). Up to four different load cases are examined for

each geometric configuration, such as high-speed- or up-hill-driving, and these situations also may differ from each other according to the appropriate market (Europe, USA or Asia).

For each of these load cases, a series of boundary conditions (speed, temperature or engine performance data) needs to be changed or defined anew. The characteristic curves (fans or heat exchanger, etc.) belonging to each calculation, the driving conditions (transmission ratio, road increase, hauled load, etc.) and further conditions are also filed in the database tables and imported therefrom. The user’s effort is limited to defining the load case within the files, from which the basic conditions are automatically defined and assigned. Not only does this substantially reduce the work load, it also considerably reduces calculation errors.

The actual calculation process – the start of the calculation, the definition of the observed parameters at the appropriate points and the filing – also is documented via scripts and automated. This guarantees the consistency of the directory structure and file naming. A queuing system (software licensing administration to avoid waiting cycles during job processing) ensures the maximum possible output of calculations.

### 5 Automated Analysis

When calculating several hundred processes a year, it is not pragmatic to assign each case into a post-processing tool and analyse them individually. That is why standards were defined that determine which parameters have to be analysed for a certain point when and in which form. This guarantees the comparability of the single calculation results.

Integral and middle values are standardised, automatically created and filed in Excel tables. These values are also rewritten directly into the administering database. The compact form of the individual values makes it possible to obtain a faster overview of all input and output values. They are directly analysed within this database by comparing them to set values and documenting the discrepancies. A traffic-light indicator (green, yellow or red) shows immediately how

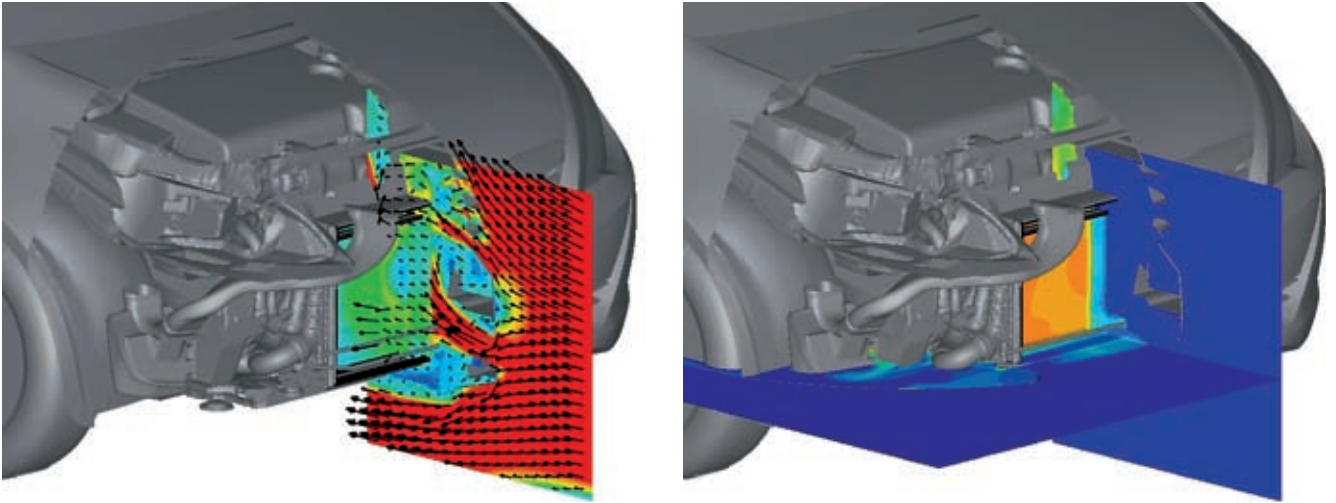


Figure 3: Automatically created analysis figure – thermal flow simulation (left) and pressure distribution (right) in the coolant chamber

closely the examined components met the requirements. By merging all data into one file, it is possible not only to evaluate the individual calculation and compare it to other variations, but also to document the developmental progress in detail and show the variation differences in the targeted parameters for each single event. An automated graphic analysis is also possible: predefined illustrations are created for each calculation. The user determines the type of illustration (geometry, speed, pressure, temperature, etc.) to be used and which variations should be compared to each other. Following the automated illustration creations, Figure 3, they are filed as presentations via PowerPoint macros. During this process, the appropriate illustrations of the to-be-compared variations are shown directly next to each other. Differences thus can be spotted easily.

### 6 Time Savings and Prospects

To use computational fluid dynamics during the developing process as efficiently as possible, it is necessary to plan the throughput times as short as possible in order to keep up with the participating disciplines. The throughput can be increased enormously by automising during most of the simulation process, Figure 4. This, however, makes a precise coordination of all steps necessary, in order to avoid moving the limitation from one processing step to the next.

Over the course of the last few years, the time savings realised via this process have already been considerable. There remains, however, some potential to rationalise the individual steps yet further. As part of the effort to speed up the single work steps, new approaches in CFD are being considered. The use of polyhe-

drons in parts of the grid could reduce the amount of necessary calculation cells and, therefore, the whole calculation time. The Immersed-Boundary Method may offer the possibility of speeding the meshing in more or less sensitive geometrical areas. The use of new methods brings a substantial verification effort in regards to precision and comparability, however. On the other hand, it gets progressively harder to change an existing process – as would be necessary with a fundamentally different meshing method – the further advanced it is.

### 7 Summary

Using the example of the CFD powertrain cooling simulation for internal-combustion engines, Tecosim was able to show how an automation is conducted, including all steps from geometry clean-up to calculation and analysis. The core of the process is the shared database of all calculations within an automobile platform, which guarantees that all data (input and output) are combined in compact form. This basis controls the entire process chain within the simulation and combines all necessary results. In this way, the project throughput time of an individual calculation is reduced by three-quarters. Synergetic effects in variable calculations make it possible to raise the amount of calculations performed per year six-fold. Complete documentation is guaranteed. ■



Figure 4: Increase in speed due to automatization of the CFD process

# Emission-based Engine Management for Heavy-Duty Applications

Continually rising demands in emission regulations throughout the service life of modern commercial-vehicle diesel engines are calling for new controlling strategies. Emission-based engine control primarily provides the means to compensate for component aging, component variance or fouling. To meet the demands for dynamic developing such concepts in ever shorter time cycles, IAV GmbH uses the modular prototype engine controller (MPEC), the new, highly flexible and powerful development environment.



## 1 Introduction

Against the backdrop of increasingly tighter emission legislation, higher power densities, shorter development times and increasingly broader model varieties, the demands being placed on heavy duty diesel engines are becoming increasingly complex all the time. In addition to intensifying the integration and distribution of overall vehicle functions and exhaust-gas aftertreatment systems, better and interlinked open and closed-loop control concepts are necessary for the combustion process. Permissible emissions are governed by strict regulations and require ever more sophisticated measures. Furthermore, future concepts will be characterized by new sensors and actuators that offer greater dynamics and accuracy or sense further variables, such as emissions.

To satisfy these demands, it is necessary to develop innovative tools in the form of software and hardware that offer the possibility to surmount today's problems. In this context, innovative and detailed solutions must be developed that are based on an understanding of the complex overall system. Developed in-house, IAV's modular prototype engine controller (MPEC) provides the facility of a development platform that can be freely parameterized on an end-to-end basis to suit the user's needs in every respect. At the same time it offers sufficient scope and flexibility as early as in the concept phase for quickly testing further-reaching detailed solutions that extend beyond familiar system boundaries. In a second step, optimization and implementation of the approaches promising the most potential for application in production can be performed. This can be done using all of the familiar calibration and dataset management tools (for example Cal-Guide). In the IAV in-house development project presented here, fundamental thermodynamic studies provided the basis for developing a closed-loop control concept for full-size commercial-vehicle engines in which the emission quantities of nitrogen oxides ( $\text{NO}_x$ ) and particulate matter (PM) are used directly as controlled variables for the control loops.

## 2 Literature Review and Preliminary IAV Studies

Emission-based engine control approaches can only be applied in production once suitable measurement technology (robustness, package, costs) is available. At this point, particular mention must be given to in-cylinder pressure,  $\text{NO}_x$ ,  $\text{NH}_3$  and, in the foreseeable future, also PM sensors. Whereas controlling fresh-air volume and EGR rate as a method for reducing emissions is frequently referred to [1], newer approaches take sensing a step closer to the point of emission formation by using "rate of heat release" controllers [2]. In this context, mention must also be given to the work by Schnorbus et al. [3] that aims to eliminate the influences of different fuel qualities by using extended "center of heat release" control.

The basic cause-effect relationships and associated parameters for meeting future emission targets are described in numerous publications [4] and are sufficiently understood. An extensive approach to reducing emissions is described in reference [5]. The aim of the concept is to bring raw  $\text{NO}_x$  emission values as well as the equivalence ratio to target levels in the closed control loop. The control variables in this case are the start of injection for influencing  $\text{NO}_x$  control and the EGR rate for influencing the equivalence ratio representing the level of sooting. Attained with a by-pass series production control unit, the results show that approaches to controlling emissions do work in principle and are able to compensate for the influences of component variance.

Unlike the publications mentioned above, the work described here focuses on the use of two "single in single out" controllers for closed-loop  $\text{NO}_x$  control that are based on the  $\text{NO}_x$  sensor value. The control variables used here are the main center of heat release on the fuel side and the position of the exhaust-gas recirculation valve on the air side. In contrast to the approaches presented above and as an alternative to the production control unit with calibration access, use was made of the fully programmable and parameterizable "full path" MPEC control unit, which

## The Authors



Dr.-Ing. Eckhard Stölting is senior manager for diesel control systems at the IAV GmbH in Gifhorn (Germany).



Dr.-Ing. Jörn Seebode is senior manager for commercial vehicle combustion systems at the IAV GmbH in Gifhorn (Germany).



Dipl.-Ing. Ralf Gratzke is head of department for diesel control systems at the IAV GmbH in Gifhorn (Germany).



Dipl.-Ing. Kai Behnk is senior vice president commercial vehicle at the IAV GmbH in Gifhorn (Germany).

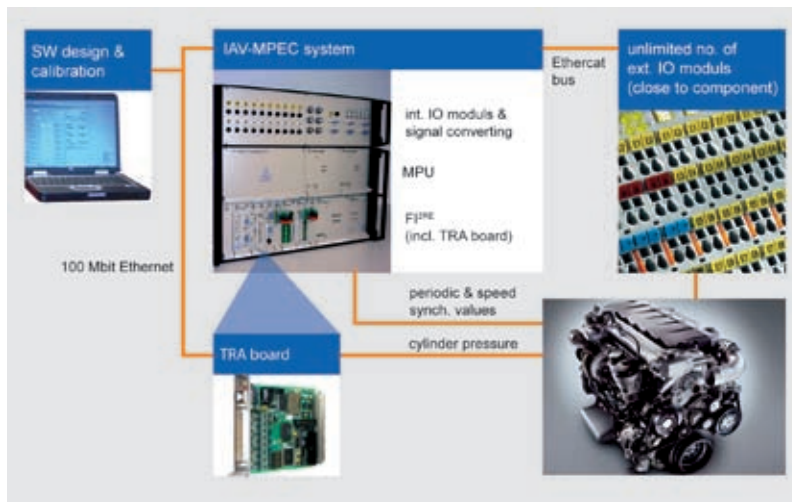


Figure 1: Setup of the modular prototype engine controller (MPEC)



Figure 2: Modular software functions of the MPEC

provided the capability of combining the control strategies freely.

Preliminary studies conducted on a single-cylinder research engine are taken as the basis for defining the most effective control variables and for obtaining a deeper understanding of the cause-effect relationships [6]. Basically, the influencing factors can be divided into fuel and air path. Fuel-path parameters are in principle better suited from the aspect of rapid control as changes can be factored in more or less in synchrony with the process. In comparison, in the air path, consideration must also be given to a response time before the target variables are reached. In addition, air-path components are in most cases heavily dependent on geometry. Maintaining the mechatronic control environment (engine management, actuators, sensors etc.) as

far as possible, the findings are transferred to a multi-cylinder engine and further optimized with regard to dynamic capability.

### 3 Engine Test-Bench Investigations

In the following test engine, modular prototype engine controller, control concept, reference measurements, emission control during steady-state engine operation, emission control during transient engine operation but also effects of aging and component variances are presented.

#### 3.1 Test Engine

An in-line six-cylinder commercial-vehicle diesel engine provides the basis for further-reaching tests. This is an engine

calibrated to meet Euro-4 legislation on the basis of external exhaust-gas recirculation. Diverging from its production configuration and in addition to the standard test bench sensors, the engine features an indication system for cylinder-pressure-based engine management and a broadband oxygen sensor in the inlet manifold for determining the concentration of oxygen. An opacimeter and a near-production  $\text{NO}_x$  sensor fitted directly downstream of the exhaust-gas turbine are also used.

#### 3.2 Modular Prototype Engine Control Unit

The modular prototype engine controller (MPEC) was developed with the aim of being as independent as possible from restrictions and platforms of component suppliers or vehicle and engine manufacturers as well as to provide maximum degrees of freedom. The system is based on state-of-the-art, industrial embedded PC technology and delivers Intel Pentium performance in the gigahertz range. Using the Windows CE operating system, MPEC is real-time capable. Any type and number of input-output (I/O) assemblies can be connected via an extremely fast Ethernet-based 100-Mbit/s field bus. In addition to digital and analog inputs and outputs, the system provides assemblies for the CAN bus, for serial RS232 communication or for the evaluation and direct connection of temperature sensors (for example thermocouples). IAV GmbH is developing special I/O block sets, for example for evaluating oxygen sensors. This avoids having to add external hardware (for example AD scanner) to the system. Use of the latest PC technology provides maximum computing capacity. At present, the entire engine control unit software is computed at 200  $\mu\text{s}$  intervals. However, total model cycle times down to as little as 100  $\mu\text{s}$  are possible.

IAV's FI<sup>2</sup>RE (flexible injection and ignition for rapid engineering) control unit integrated in the MPEC system plays a central part in the overall development environment. Above all, it takes care of actuating the injection system in synchrony with crank angle, senses the cylinder pressure signals in synchrony with the process and performs thermodynamic real-time analysis.

**Figure 1** shows the electronic test-bench set-up. The upper part of the MPEC contains all of the internal I/O modules. The embedded PC runs the Matlab/Simulink-based MPEC software which is a more advanced version of the Hocos software [7]. Using Realtime Workshop, the closed tool chain permits automatic code generation for the models produced by the user. These are compiled to suit the target system, loaded onto the hardware and executed there. The system contains custom-made Simulink block sets for all components as well as all inputs and outputs. Calibration with Inca or similar tools takes place by means of XCP through a network interface. **Figure 2** provides an overview of the software functions currently being used and the way they are distributed throughout the system.

### 3.3 Control Concept

Essentially, the controller design implemented for keeping raw emissions on target is in each case a cascaded “dual-split controller” (DSC) for controlling particulate matter and  $\text{NO}_x$ . The upper section of **Figure 3** shows the set-up for the particulate controller. The inner cascades act on rail and boost pressure. In the absence of suitable production-ready soot sensors, an opacimeter was used to measure the actual concentration of particulate matter in the exhaust gas. The “dual-split scheduler” (DSS) weights the split between the control variables of rail and boost pressure in relation to the  $\text{O}_2$  concentration in the inlet manifold and outer-cascade PM control deviation. As the test engine is fitted with a turbocharger without variabilities, it was not possible to activate the inner boost pressure control cascade for this project work.

The structure of the  $\text{NO}_x$  controller is shown in **Figure 3** bottom. Here, the  $\text{NO}_x$  emission controller forms the outer cascade that actuates the EGR valve as its first priority. The inner controller cascade’s  $\text{O}_2$  setpoint is regulated by a limiter. If a negative  $\text{NO}_x$  control deviation still continues to exist, the inner parallel “center of heat release” (COHR) cascade is additionally activated by a second DSS. This acts on a cylinder-selective basis with secondary priority. To maximize the dynamics of the rather slow  $\text{NO}_x$  sensor value and of the exhaust-gas opacity

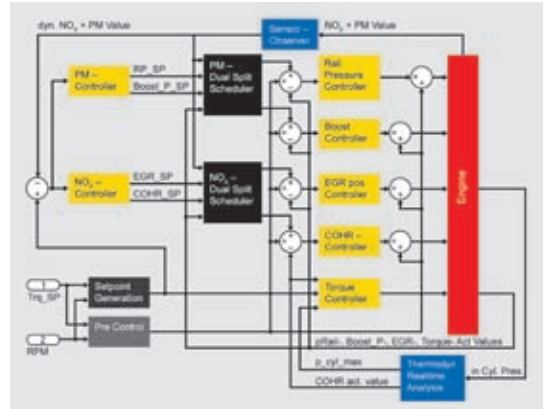


**Figure 3:** Concept outline of the raw emissions controller

value, two observers are employed that map the behavior of the measurement system being used. In the diagram, the different actual values as well as the pilot control values and setpoints are each shown on one signal arrow for the sake of simplicity.

In order to for example counteract transient effects resulting from rail pressure adjustment after a load step change, the “Advanced Closed Loop Combustion Control” system was developed that uses the given setpoint and the results of the real-time heat release rate analysis to influence the heat release rate in order to stay inside the targeted emission limits. The capability of switching over using

the DSS combined with a temporary adjustment of the injection timing prevents the soot values from overshooting.

### 3.4 Reference Measurements

To compare the system quality of the test environment used, the basic engine calibration was first brought in line with production status. Determination of the quality of the hardware and of the algorithms and functions used is only possible by clearly defining a reference. **Figure 4** exemplarily shows the results of an engine speed/load cross section. Three steady-state operating points are compared with production and MPEC engine management.

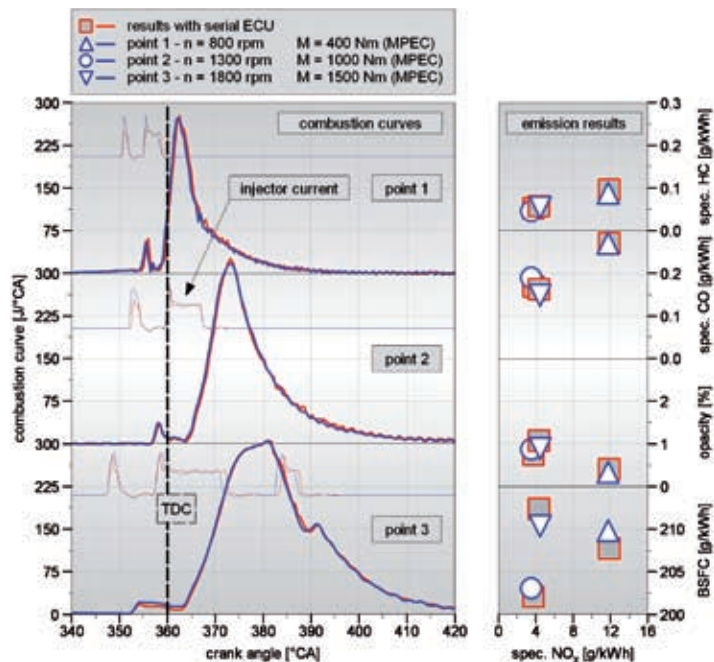


**Figure 4:** Comparison of results from series production control unit and MPEC

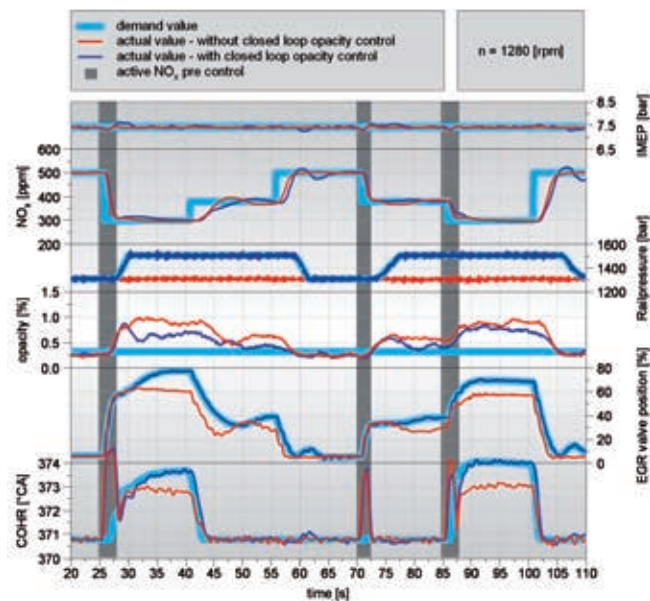


Figure 5: Emission-controlled NO<sub>x</sub> setpoint step at 1280 rpm engine speed

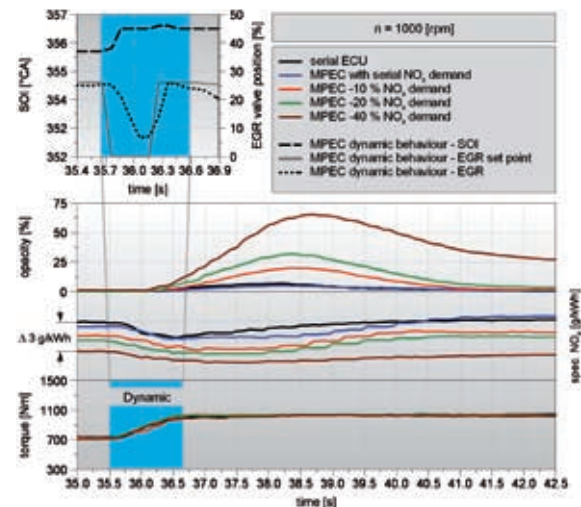


Figure 6: Transient emission behaviour

Comparability is shown to be very good, not only in terms of the cylinder pressure and resultant heat release rates but also in respect of emissions and fuel consumption. It can thus be assumed that reference measurements, although reflecting a basic dataset and displayed through the MPEC system, are identical with the results obtained using the production control unit.

### 3.5 Emission Control during Steady-State Engine Operation

To realize the closed-loop control concept in principle, various emission setpoint steps were examined at cycle-relevant operating points. Exemplarily, an operating point with IMEP = 7.5 bar and n = 1280 rpm is presented here. Figure 5 shows NO<sub>x</sub> setpoint steps at constant engine speed and accelerator-pedal position. The NO<sub>x</sub> setpoints (380, 300 and 500 ppm) correspond to the production value on the one hand and to a rise or fall of approximately 20 % in the production value on the other.

At t = 25.5 s, it is possible to see how the outer NO<sub>x</sub> controller cascade directly increases the EGR setpoint. As gas-travel-induced system delays and NO<sub>x</sub> sensor response time have a negative effect on quickly reducing NO<sub>x</sub>, it is necessary to employ pilot control at the point where the step occurs. This is done by shifting the center of heat release. By “retarding” the point of injection in this way, it is pos-

sible to make the NO<sub>x</sub> reduction gradient extremely steep. After pilot control duration expires and a defined target EGR valve position is reached, NO<sub>x</sub> emissions are additionally regulated by a significantly faster COHR controller (at t = 28 s in Figure 5). Through these measures, the setpoint can be reached after approximately 2 s according to the measurement. However, as behavior of the NO<sub>x</sub> sensors used is still less than satisfactory, it is assumed that the true control time – which is the cycle-relevant factor – is approximately one second and thus significantly shorter than measured here. After reaching the NO<sub>x</sub> setpoint, the injection point, which adversely affects fuel consumption, is advanced again.

At t = 28 s, it can be seen that the “Opac” controller counteracts the higher soot levels caused by NO<sub>x</sub> control. Increasing rail pressure to approx 1520 bar, PM emissions can be kept close to the target value while significantly reducing the NO<sub>x</sub> level. The torque controller keeps the indicated mean pressure at the setpoint of 7.5 bar. Comparing the opacity curves with and without opacity control makes it clear that this control action manages to return opacity to the setpoint. The rise in nitrogen oxide levels from higher rail pressure results in the need for the NO<sub>x</sub> controller to actuate the control variables more sharply so as to attain the same NO<sub>x</sub> values.

### 3.6 Emission Control during Transient Engine Operation

So far, it has been established that for constant operating behavior the MPEC is capable of controlling NO<sub>x</sub> and opacity quickly and precisely. This behavior must also be ensured when engine operating points or load requests quickly change. To this end, fully variable dynamics recognition was implemented in the MPEC engine management system, making it possible to activate pilot control as required. Figure 6 shows different NO<sub>x</sub> setpoint reductions. It becomes clear that when using the MPEC system and specifying production NO<sub>x</sub> values, the emission curves for production ECU and MPEC (black and blue) come very close together. This is only possible by quickly adjusting the pilot control behavior of injection start and EGR on the basis of dynamics recognition.

The graphs in Figure 6 showing gradual NO<sub>x</sub> reduction (red, green and magenta) demonstrate that the measures are well suited to meet the specified NO<sub>x</sub> values. By systematically pilot-controlling individual controller parameters, optimum control behavior is achieved at the load step. However, even through the higher rail pressure brought about by the opacity controller, it is not possible to completely avoid an increase in opacity on sharply reducing NO<sub>x</sub> with unchanged engine hardware.

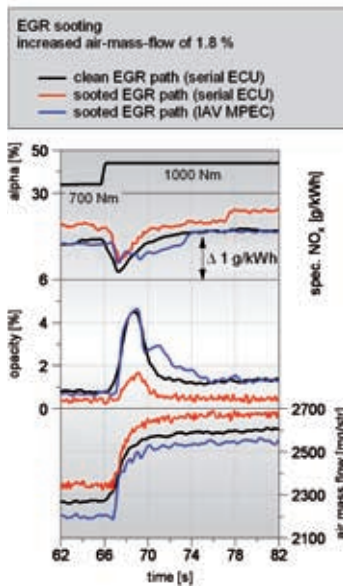


**Figure 7:** Load steps with “aged” EGR valve at 1000 rpm engine speed

### 3.7 Effects of Aging and Component Variances

One of the main motivations for developing an emission-based engine management system is to compensate for the effects of aging and component variances. In addition to the unsatisfactory accuracy of some sensors even when new, components undergo changes during their service life as a result of fouling and/or wear. For instance, the EGR system is particularly susceptible to fouling from the formation of acids or carbonization on the gas-carrying components. The adverse effect this has on emissions may, on the one hand, take the form of a change in overall flow at the same valve position or, on the other, result in deviations in position feedback as a consequence of component wear. The algorithm presented here aims to compensate for fault sources on the basis of closed-loop, result-oriented control. The following describes the simulation of faults on the EGR valve, cooler and lines as well as the effects they have. Sooting of the EGR system is simulated by imposing an offset on the EGR duty-cycle map or on the pilot control map of EGR valve positioning control. Sooting was selected that produces an air-mass increase of 1.8 %.

**Figure 7** shows the results of this measurement series with uninfluenced EGR path, with simulated EGR sooting on the

production control unit without emission control and the results obtained with the MPEC system utilizing the emission control structures implemented. Simulated sooting produces a rise in  $\text{NO}_x$  emissions of approx 1 g/kWh. This corresponds to an increase of approximately 16 %. By comparison, emission control using the MPEC can fully compensate the effect of this component restriction. As simulated EGR valve carbonization generates an increase in mass flow and thus a drop in the equivalence ratio, opacity falls by approximately 65 % in the absence of compensatory measures.

With emission control activated, setpoints were achieved on the PM and  $\text{NO}_x$  side based on the production levels. Due to the impact of temperature, pressure and hysteresis on the values measured with the  $\text{NO}_x$  sensor, a slightly lower  $\text{NO}_x$  value than was measured in production was used to achieve emission control. This becomes apparent in a slight reduction in the mass of fresh air required. With the control system activated, the setpoints are otherwise attained with a very high degree of precision both for steady-state and dynamic operation, making it possible to validate the success of applying the presented control system on air paths subject to this type of aging.

## 4 Summary and Outlook

Within this study IAV GmbH could show that it is possible to compensate fully for component-induced effects of aging and production variance within the physical limits by using existing production sensors to control emissions. In this context, the employed controller structure represents a basic state of development work which offers potentials in terms of emission reduction for use in mass production by adapting the switch-over and enabling strategies of the “dual-split schedulers” more specifically as well as by coupling the parallel control loops more intensely. Being able to select any control-variable strategy and through the availability of a fast and slow control path, directly and accurately targeted action can be taken to reduce the  $\text{NO}_x$  and PM peaks identified in the cycle.

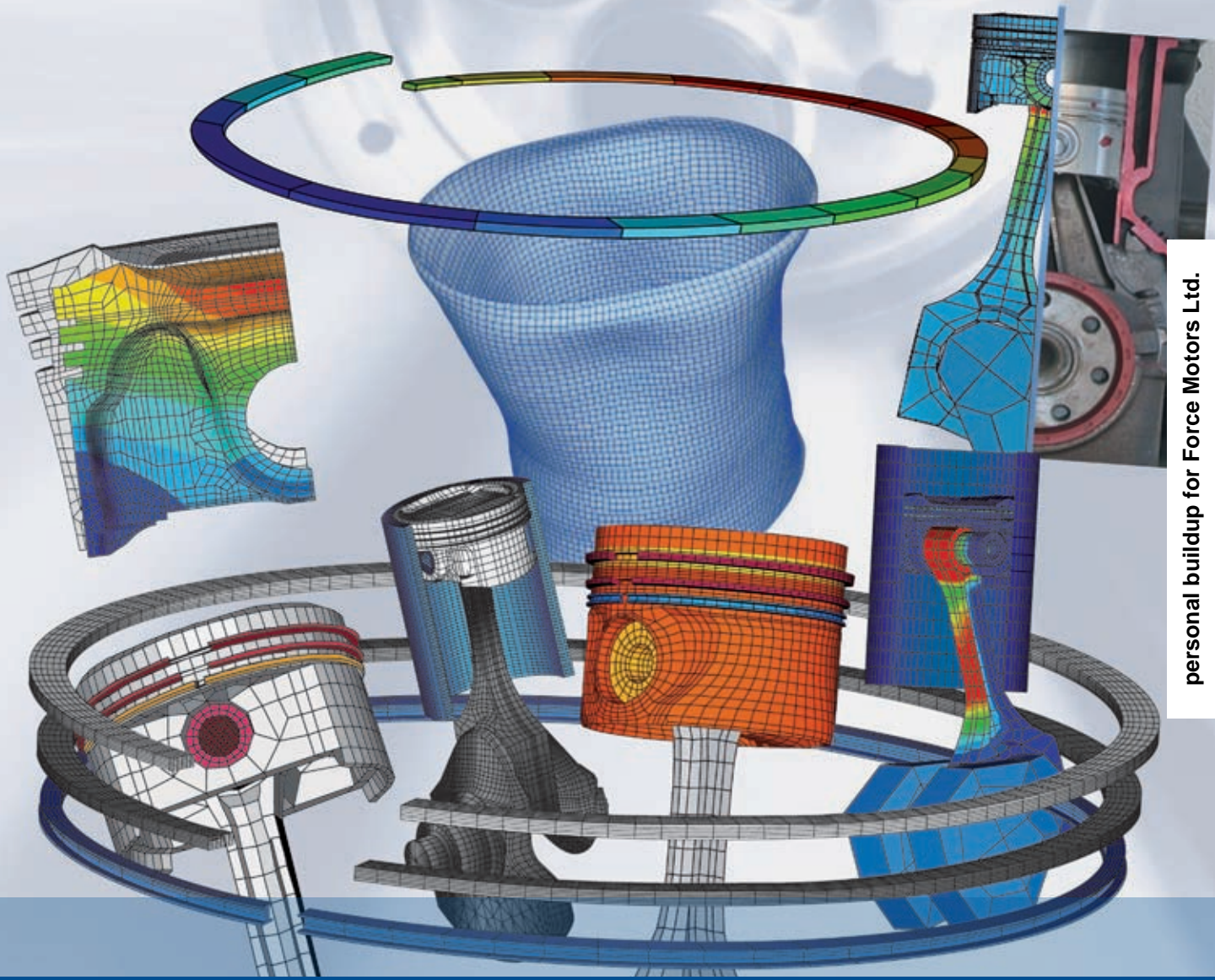
As development of production-level exhaust-gas sensors is extensively driven by OBD legislation, it must be assumed that the necessary emission sensors anticipated here will, in the near future, be found in engine concepts anyway so that emission control will merely focus on consistently utilizing the synergies of this technology.

Using the firstly available modular prototype engine controller (MPEC) development environment made available for the first time in this project, it was possible within just a few weeks to actuate an arbitrary commercial-vehicle engine from end to end and calibrate it with standard calibration software. In terms of computing power, it was possible to increase performance by orders of magnitude.

By implementing automatic I/O module configuration, the time required for integrating additional models – the number of which is already unlimited – is to be reduced in future to “plug & play” level. Extending the 100-Mbit standard so that it also covers the area between injection control unit and main computing node will furthermore make it possible to compute algorithms of greater complexity, for example also between two consecutive injection events in a cycle, and to initiate control actions to best effect.

## References

- [1] Herrmann, E.; Krüger, M.; Pischinger, S.: Regelung von Ladedruck und AGR-Rate als Mittel zur Emissionsregelung bei Nutzfahrzeugmotoren. In: MTZ 66 (2005), Nr. 10, S. 806–811
- [2] Rempel, A.; Stölting, E.; Gratzke, R.; Predelli, O.: Flexible Motorprozessregelung für neue Brennvorfahren. Tagung Autotreg, Baden-Baden 2008
- [3] Schnorbus, T.; Lamping, M.; Körfer, T.; Pischinger, S.: Weltweit unterschiedliche Kraftstoffqualitäten – Neue Anforderungen an die Verbrennungsregelung beim modernen Dieselmotor. In: MTZ 69 (2008), Nr. 4, S. 302–312
- [4] Jacob, E.: Emissionslimits zukünftiger Nfz-Motoren: Balanceakt zwischen Möglichkeit und Nutzen. 26. Internationales Wiener Motorensymposium, Wien, Österreich, 2005
- [5] Alfieri, E.; Amstutz, A.; Guzzella, L.: Emissionsgeregelte Dieselmotoren. In: MTZ 68 (2007), Nr. 11, S. 982–989
- [6] Seebode, J.; Stegemann, J.; Sommer, A.; Stölting, E.; Buschmann, G.: Höchstdruckeinspritzung und Einspritzverlaufsformung am Nfz-Einzylindermotor. 15. Aachener Kolloquium Fahrzeug- und Motorentechnik, Aachen, 2006
- [7] Däubler, L.; Gratzke, R.; Predelli, O.; Rempel, A.: Flexibles Motormanagement für innovative Brennvorfahren. In: MTZ 66 (2005), Nr. 9, S. 686–692



# Piston Ring Dynamics Simulation Based on FEA Software

Modern simulation software offers the possibility to simulate the piston ring dynamics in great detail. Therefore, a detailed understanding of the occurring mechanisms and involved physical models can be gained. At the Institute for Combustion Engines in Aachen this approach was used by coupling user subroutines with a FEA dynamic 3D model of a specified piston assembly/cylinder unit. At the institute as well as at FEV these simulation models support the development, failure analysis and optimization process.

## 1 Introduction

The piston assembly is one of the thermally and mechanically highest loaded components in modern combustion engines. Increasing ignition pressures, more efficient power use, minimized component clearances and future oriented emission legislation are going to intensify the load. Partly the numerous piston assembly requirements can lead to clashing objectives. Often the design of piston rings is based on empirical data. Modern simulation software however, offers the possibility to simulate the piston ring dynamics in great detail parallel to measurements. Therefore, a detailed understanding of the occurring mechanisms and involved physical models can be gained. At the Institute for Combustion Engines in Aachen this approach was used by coupling user subroutines with a FEA dynamic 3D model of a specified piston assembly/cylinder unit. At the institute as well as at FEV Motorentechnik GmbH these simulation models support the development, failure analysis and optimization process.

## 2 Model Description

Figure 1 shows the dynamic piston ring model. The macro-geometry, local stiffness, mass and temperature distribution is modelled by the FEA grid. This includes asymmetries due to the piston ring gap or piston design. The micro-geometry is included to a large extent in the contact interaction model formalism, implemented via the user subroutines. The essential boundary conditions are:

- the component geometry including the piston ring running surface and pretension force
- the temperature distribution and deformation of the liner surface
- the temperature distribution, deformation and skirt shape of the piston
- the gas pressure and temperature curve in the combustion chamber and crankcase
- the gas and lubricant properties
- the rotational speed of the crank shaft.

A gas model that is coupled to the FEA model generates the transient gas pressure values and blow by rates. The contact model [1, 2] that describes the interaction between the piston ring and liner surface is based on a hydrodynamic and mixed friction approach. The potential occurrence of wear is modelled as described in [3, 4]. Furthermore a simplified lubricant transport model is implemented that keeps track of the lubricant distribution on all relevant surfaces over time. The input interface consists of a parameter list that is used to initialize all subroutines prior to a simulation. All 3D components are meshed automatically based on their geometrical parameters. Because of the piston's complexity and to ensure that the asymmetric stiffness (skirt) and mass distribution behaviour are most precisely detailed the piston is only meshed with computer assistance.

## 3 Simulation

### 3.1 Piston Ring Assembly

In order to obtain a realistic stress distribution in the piston rings they are meshed in their original state, and then, via a pre-simulation step, assembled into the liner.

## The Authors



Dr.-Ing. Timo Ortjohann was deputy manager of the department dynamics and team manager base engine at FEV Motorentechnik GmbH in Aachen (Germany).



Dr.-Ir. A.P.J. Voncken is technical software engineer of the department dynamics at FEV Motorentechnik GmbH in Aachen (Germany).



Univ.-Prof. Dr.-Ing. Stefan Pischinger is director of the Institute for Internal Combustion Engines (VKA) at the RWTH Aachen (Germany).

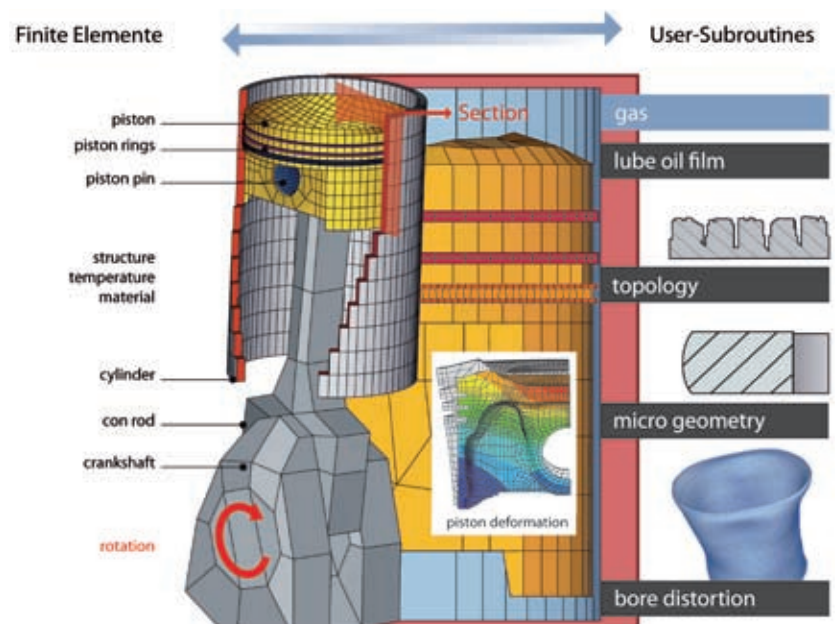


Figure 1: Set up of the piston ring dynamics simulation model

Stress distribution as a result of applying pretension ...

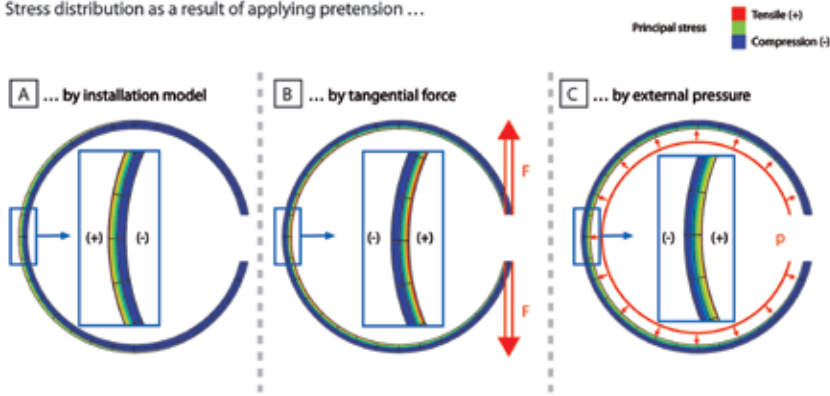


Figure 2: Comparison of piston ring pretension models

Figure 2 (A) shows the resulting stress distribution in the piston ring. As a comparison Figure 2 (B) and (C) show two often used approaches to model the pre-tension in a piston ring either via an external force, Figure 2 (B), or via an external pressure, Figure 2 (C). It becomes apparent that the pressure and tensile stress distribution reverses along the radial coordinate. The last two approaches can be used in their simplified form however they will lead to an unrealistic stress distribution in the piston ring.

3.2 Piston Assembly Dynamics

Due to the vast range of interactions that are involved in the piston ring's dynamics and the physical model depth a valida-

tion of the model is recommended wherever possible for each project. Based on the calibration of the simulation model with measurement data, simulation variants are defined, in order to investigate a problem. In the concept phase simulations are conducted for typical load cases such as: zero, part, and full load at idle, engine speed of 2000/min, engine speed at maximum power, and over-speed. All conceivable model parameters can be varied to analyze potentials. For specific problems on prototypes or series production only a selected load cases are simulated at which a failure is expected to occur. Proposed solutions can then be verified in further steps by simulation.

4 Submodels and Results

The amount and diversity of simulation output data is huge due to it's three dimensional implementation of the elastic system in the time domain and must be well structured depending on the point of focus of an investigation. All FEA model specific output data (dynamics, stresses, and contact behaviour) is available to the user via the commercial FEA post-processor software. The user subroutines support the post processing to a great extent as well, as they report essential evaluation results like blow-by, friction, wear, and lubricant distribution.

4.1 Gas Flow and Blow-by

The nodal positions of all meshed components are transmitted by the FEA solver for every time increment to the linked FEA gas flow model where they serve as input. With this information, the gas chamber volumes  $V_i(t)$  and the gas flow cross section areas  $A_x(t)$  per piston ring gap and circumferential radial clearance are calculated, Figure 3 (A). These cross section areas serve as input for the gas flow equations as described in [5]. The gas model calculates the quantities pressure  $p_i$ , temperature  $T_i$ , mass  $m_i$  and mass flow rate  $\dot{m}_{i,i+1}$  per model chamber and time increment. The gas pressures  $p_i$  are used as pressure boundary

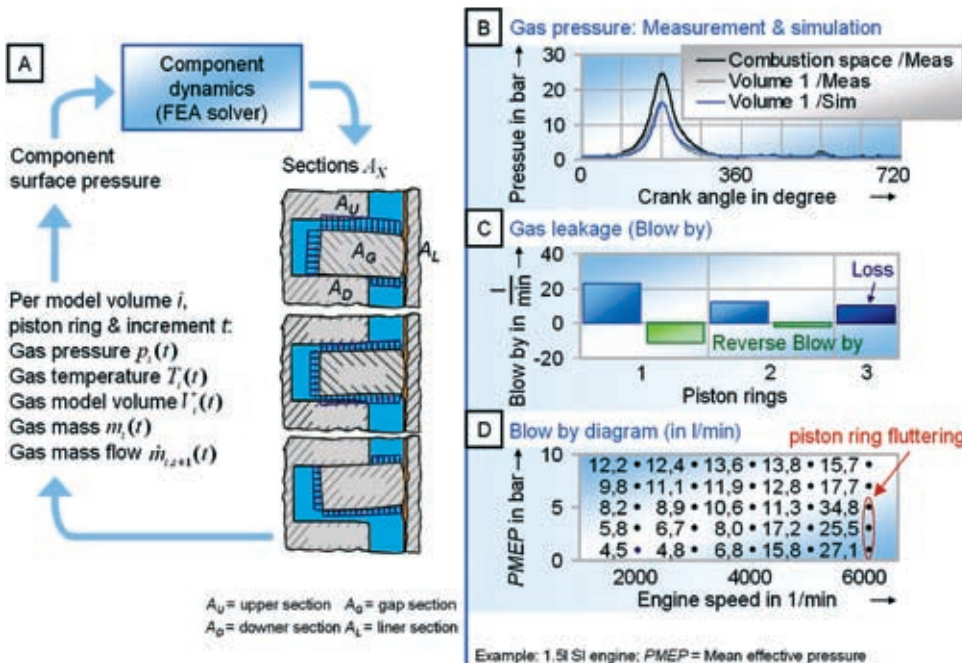


Figure 3: The coupled gas flow model with gas pressure and blow by results

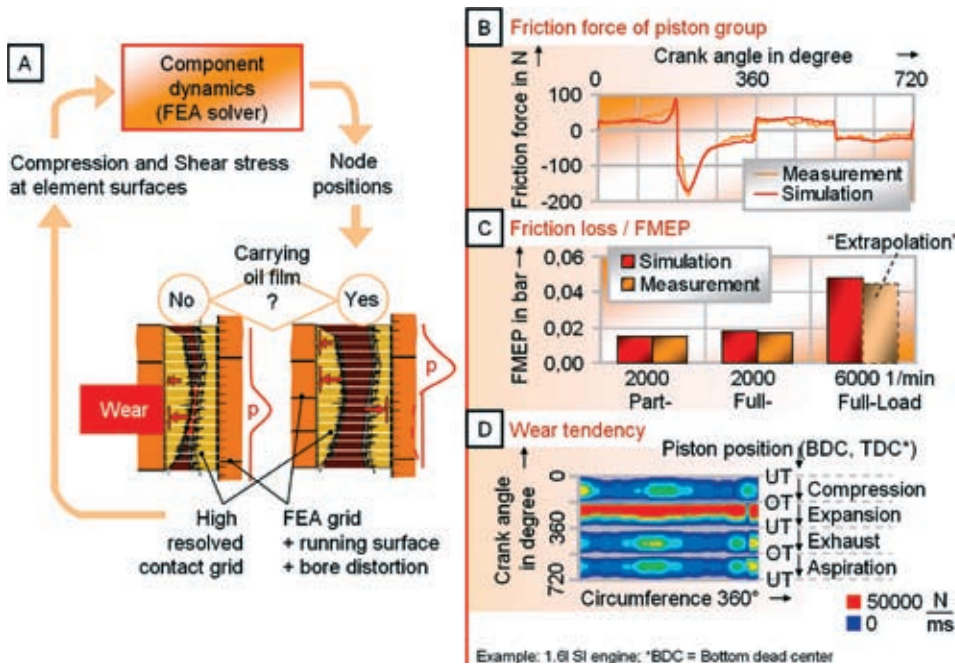


Figure 4: The coupled HD/hard contact model with friction force, friction loss and wear results

conditions on the corresponding FEM model surfaces in the next time step. The gas pressure curve in the combustion chamber and crank case serve as gas model boundary conditions.

The diagram in Figure 3 (B) shows the pressure curve in the combustion chamber (black) and between the first and second piston ring (chamber 1, blue) as a function of crank angle. The simulated pressure curve for chamber 1 matches well with the measured curve (grey) acquired from a motored 1.5 l gasoline engine as an example. Based on a measurement validated simulation model blow-by rates can be determined reliably. These are presented in the diagram in Figure 3 (C) (operating point: mean effective pressure  $p_{me} = 5$  bar, engine speed  $n = 4000$ /min) as integral values of blow-by and reverse blow-by. If these simulations are carried out for a series of operating points a so called blow-by loss-iso-diagram, as depicted in Figure 3 (D), is obtained. Conspicuous operating points can now be diagnosed, analysed (ring fluttering) and counter measures can be validated.

#### 4.2 Hydrodynamics, Friction and Wear

The input parameters for the contact model, Figure 4 (A), which allow the lubricant film geometry to be determined as a function of circumference and time

for every piston ring are the positions and velocities of the piston rings and liner surface nodes. As the meshed grid of the piston rings is too coarse for an accurate implementation of the mixed friction contact approach, the piston ring running surfaces and liner surface are applied to a significantly denser grid. Furthermore, the surface roughness for both surfaces is included by their statistical values. One result for every time step is the lubricant film's geometry which is used to check whether any asperities of the rough surfaces are in contact. If they have contact, the regime of mixed-friction is entered. Depending on the contact pressure, the hydrodynamic and metallic contact pressure are weighted over the Abbott-Firestone-curve [4] and superimposed. The summed surface pressure is returned as pressure boundary condition per time increment to the FEA solver. The potential wear of both contacting surfaces is implemented via an abrasive and adhesive wear model [3, 4]. Both these wear formalisms predict a reduction of the surface roughness peaks per time step as a function of the contact pressure, relative velocity, and surface hardness. An important result of the contact model is the friction force behaviour of the piston assembly. A comparison of simulated and measured [6] friction force is shown in Figure 4 (B). By

varying parameters the model supports the evaluation of variants regarding friction and wear behaviour. This is an advantage in concept phases, for optimisation suggestions or at high engine speeds, where measurements are either not possible or too expensive. In the diagram in Figure 4 (C), the mean effective pressure for 2000/min at part and full load are presented and compared with measurement data. Using this starting point, the values for 6000/min at full load can be rated via an extrapolation of the simulation and measurement results.

The product of local contact pressure distribution and relative contact surface velocity will be defined as wear tendency. The wear tendency of each piston ring running surface as well as the liner surface can hence be determined. This result, as shown in the diagram in Figure 4 (D), can be plotted as a function of crank angle versus liner circumference.

The diagram gives a qualitative and practical assessment on the regions on the liner surface where wear is most likely to occur. If many variants are incorporated in the analysis, potential low wear designs can be determined.

#### 4.3 Lubricant Distribution

The positions, velocities, and accelerations of all FEM-meshed nodes serve as

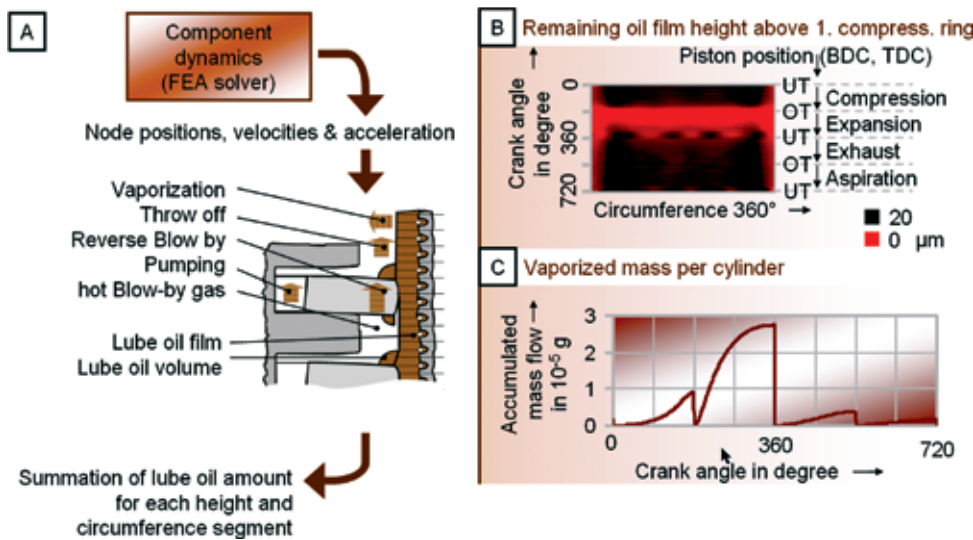


Figure 5: The coupled lubrication oil distribution model including oil film height and vaporized oil results

input for the lubricant-model. This model describes the transport of the lubricant on the liner surface due to the up- and downward scraping of the lubricant by the piston rings. For each time step, the lubricant film height on the liner surface and the lubricant volumes at piston ring top and bottom side are calculated. Figure 5 (A). These are a result from the minimal lubricant film height as im-

plemented in the hydrodynamic contact model, after the piston ring has run over the liner surface and the lubricant supply. Currently, five lubricant loss mechanisms are considered:

- the evaporation of lubricant in the combustion chamber [7]
- the loss of lubricant beyond a critical acceleration at the top side of the first piston ring

- the loss via dissolved lubricant in blow-by [8]
- the pumping of lubricant passed the first piston ring
- the coking of lubricant due to hot blow-by gases.

Figure 5 (B) shows a typical result of the lubricant film height on the liner surface after the first piston ring has run over as a function of the crank angle versus cylinder circumference. In the diagram in Figure 5 (C) the evaporated lubricant mass part as a function of crank angle is shown.

Due to its complex interactions the lubricant distribution model is very sensitive to input parameters. Momentarily it is used in practical applications for qualitative comparisons of system variants.

#### 4.4 Parameter Variation

The impact of the thermal deformation of the piston assembly components on the functional behaviour of the piston rings is in the focus of current research. For this, the 3D temperature distribution and the corresponding thermal deformation, as depicted in Figure 6 (A), is included into the model. A comparison with temperature measurements shows the accordance at five sensor positions. Based on this validated input, load cases for minimal piston assembly component clearances at higher revolution speeds can be simulated, and the impact on wear and lubrication consumption can be analysed. For example, the wear tendency index (= average value of the product of contact pressure times relative surface velocity) and the remain-

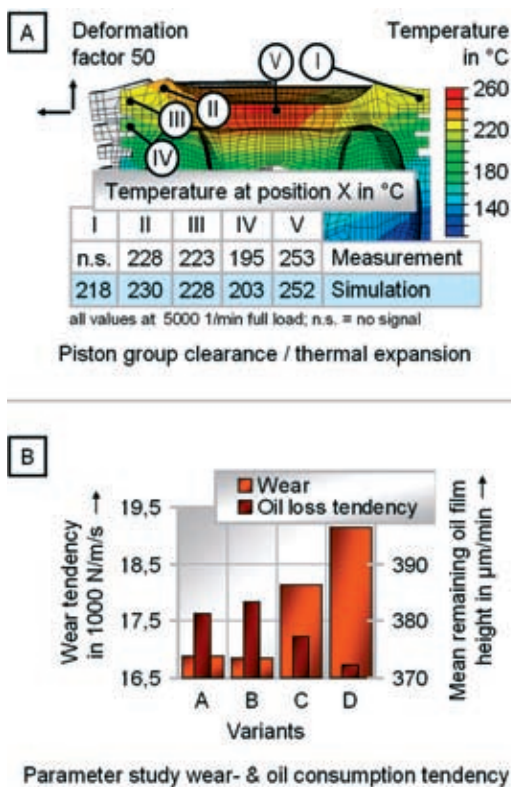


Figure 6: Parameter investigation taking into account the 3D temperature field of the piston group

ing lubricant film height on the surface above the top piston ring can be analysed for variants (A) basis, (B) without piston offset, (C) without crank offset, and (D) maximal piston ring pre-tension. The aim of such an investigation is the localisation of wear relevant model parameters and their impact on i.e. lubricant consumption.

## 5 Summary

The simulation technique offers a future oriented building block with a high degree of physical modelling depth. It allows a most realistic simulation of the three dimensional piston ring dynamics where relevant physical interactions, such as gas coupling, elasticity, non-linear contacts (EHD and solid body) and temperature influences are embedded. The simulation methodology allows a detailed study of the piston ring vertical gap position, fluttering, and rotation based on the implementation of free moving piston rings which are controlled only by gas-, HD-, and contact interactions. The long time use of measuring techniques [6, 9, 10] in research-, development-, and series-production-projects as well as the verification with supplier data supports the refinement of the model so far and in future. The knowledge gained from the simulations flow back into the measuring methodology for optimizing the mechanical signal-transfer systems and sensor technology. The application in various projects so far has shown the adaptation potential of this methodology regarding the requirements of modern developed cylinder units and in combination with various analysis techniques since its first publication in 2001 [11].

## References

- [1] Reynolds, O.: On the theory of lubrication, Phil. Trans. Royal Society 1886, Part 1, Papers on mechanical and physical subjects, Cambridge University Press 1900, 1901, 1903
- [2] Greenwood, J. A.; Tripp, J. H.: The contact of two nominally flat rough surfaces, Proceedings Institute of Mechanical Engineers Vol 185 48/71, p. 625-633, 1971
- [3] Archard, J. F.: Contact and rubbing of flat surfaces, Journal of Applied Physics, Vol 24, Nr. 8, 1953
- [4] Pint, S.; Schock, H. J.: Design and Development of a Software Module for Analysis of Three Dimensional Piston Ring Wear, SAE-Paper2000-01-0920, 2000
- [5] Eweis, M.: Reibungs- und Undichtigkeitsverluste an Kolbenringen, VDI-Forschungsheft 371, Berlin, 1935
- [6] Dohmen, J.; Hermsen, F.-G.; Barbezat, G.: Untersuchungen an plasmabeschichteten Zylinderlaufflächen. In: MTZ 2004 Nr. 3
- [7] Herbst, H. M.; Priebsch, H. H.: Simulation of Piston Ring Dynamics and Their Effect on Oil Consumption, SAE-Paper2000-01-0919, 2000
- [8] Burnett, P.J.; Bull, B.; Wetton, R. J.: Characterization of the ringpack lubricant and its environment, Part J, Proceedings Institute of Mechanical Engineers Vol 209, 1994
- [9] Koch, F.; Geiger, U.; Hermsen, F.G.: PIFFO – Piston Friction Force Measurements during Engine Operation, SAE-Paper 960306, 1996
- [10] Orlovsky, K.; Dohmen, J.; Duesmann, M.: Simulation und Messung im Kurbeltrieb, HdT Tagung, Essen, 2003
- [11] Maassen, F.; Koch F.; Schwaderlapp, M.; Ortjohann, T.; Dohmen, J.: Analytical and Empirical Methods for Optimization of Cylinder Liner Bore Distortion, International SAE Conference 2001, Detroit, SAE Paper 2001-01-0569, 2001

## IMPRINT

**MTZ** WORLDWIDE

www.MTZ-online.com

12|2008 · December 2008 · Volume 69

Springer Automotive Media | GWV Fachverlage GmbH

P.O. Box 15 46 · 65173 Wiesbaden · Germany

Abraham-Lincoln-Straße 46 · 65189 Wiesbaden · Germany

**Managing Directors** Dr. Ralf Birkelbach, Albrecht Schirmacher

**Advertising Director** Thomas Werner

**Production Director** Ingo Eichel

**Sales Director** Gabriel Göttlinger

### EDITORS-IN-CHARGE

Dr.-Ing. E. h. Richard van Basshuysen

Wolfgang Siebenpfeiffer

### EDITORIAL STAFF

#### Editor-in-Chief

Johannes Winterhagen (win)

Phone +49 611 7878-342 · Fax +49 611 7878-462

E-Mail: johannes.winterhagen@springer.com

#### Vice-Editor-in-Chief

Dipl.-Ing. Michael Reichenbach (rei)

Phone +49 611 7878-341 · Fax +49 611 7878-462

E-Mail: michael.reichenbach@springer.com

#### Chief-on-Duty

Kirsten Beckmann M. A. (kb)

Phone +49 611 7878-343 · Fax +49 611 7878-462

E-Mail: kirsten.beckmann@springer.com

#### Sections

Electrics, Electronics

Markus Schöttle (schoe)

Tel. +49 611 7878-257 · Fax +49 611 7878-462

E-Mail: markus.schoettle@springer.com

Engine

Dipl.-Ing. (FH) Richard Backhaus (rb)

Tel. +49 611 5045-982 · Fax +49 611 5045-983

E-Mail: richard.backhaus@rb-communications.de

Heavy Duty Techniques

Ruben Danisch (rd)

Phone +49 611 7878-393 · Fax +49 611 7878-462

E-Mail: ruben.danisch@springer.com

Online

Dipl.-Ing. (FH) Caterina Schröder (cs)

Phone +49 611 78 78-190 · Fax +49 611 7878-462

E-Mail: caterina.schroeder@springer.com

Production, Materials

Stefan Schlott (hlo)

Phone +49 8191 70845 · Fax +49 8191 66002

E-Mail: Redaktion\_Schlott@gmx.net

Service, Event Calendar

Martina Schraad

Phone +49 212 64 232 64

E-Mail: martina.schraad@springer.com

Transmission, Research

Dipl.-Ing. Michael Reichenbach (rei)

Phone +49 611 7878-341 · Fax +49 611 7878-462

E-Mail: michael.reichenbach@springer.com

#### English Language Consultant

Paul Willin (pw)

#### Permanent Contributors

Christian Bartsch (cb), Prof. Dr.-Ing. Peter Boy (bo),

Prof. Dr.-Ing. Stefan Breuer (sb), Jens Büchling (jb),

Jörg Christoffel (jc), Jürgen Grandel (gl),

Erich Hoepke (ho), Ulrich Knorra (kno),

Prof. Dr.-Ing. Fred Schäfer (fs), Roland Schedel (rs),

Bettina Seehawer (bs)

#### Address

P.O. Box 1546, 65173 Wiesbaden, Germany

E-Mail: redaktion@ATZonline.de

### MARKETING | OFFPRINTS

#### Product Management Automedia

Sabrina Brokopp

Phone +49 611 7878-192 · Fax +49 611 7878-407

E-Mail: sabrina.brokopp@springer.com

#### Offprints

Martin Leopold

Phone +49 2642 9075-96 · Fax +49 2642 9075-97

E-Mail: leopold@medien-kontor.de

### ADVERTISING | GWV MEDIA

#### Key Account Manager

Elisabeth Maßfeller

Phone +49 611 7878-399 · Fax +49 611 7878-140

E-Mail: elisabeth.massfeller@gwv-media.de

#### Ad Sales

Frank Nagel

Phone +49 611 7878-395 · Fax +49 611 7878-140

E-Mail: frank.nagel@gwv-media.de

#### Display Ad Manager

Susanne Bretschneider

Phone +49 611 7878-153 · Fax +49 611 7878-443

E-Mail: susanne.bretschneider@gwv-media.de

#### Ad Prices

Price List No. 51

### SUBSCRIPTIONS

VVA-Zeitschriftenservice, Abt. D6 F6, MTZ

P. O. Box 77 77, 33310 Gütersloh, Germany

Renate Vies

Phone +49 5241 80-1692 · Fax +49 5241 80-9620

E-Mail: SpringerAutomotive@abo-service.info

### SUBSCRIPTION CONDITIONS

The emagazine appears 11 times a year at an annual subscription rate of 269 €. Special rate for students on proof of status in the form of current registration certificate 124 €. Special rate for VDI/ÖVK/VKS members on proof of status in the form of current member certificate 208 €. Special rate for studying VDI members on proof of status in the form of current registration and member certificate 89 €. The subscription can be cancelled in written form at any time with effect from the next available issue.

### PRODUCTION | LAYOUT

Heiko Köllner

Phone +49 611 7878-177 · Fax +49 611 7878-464

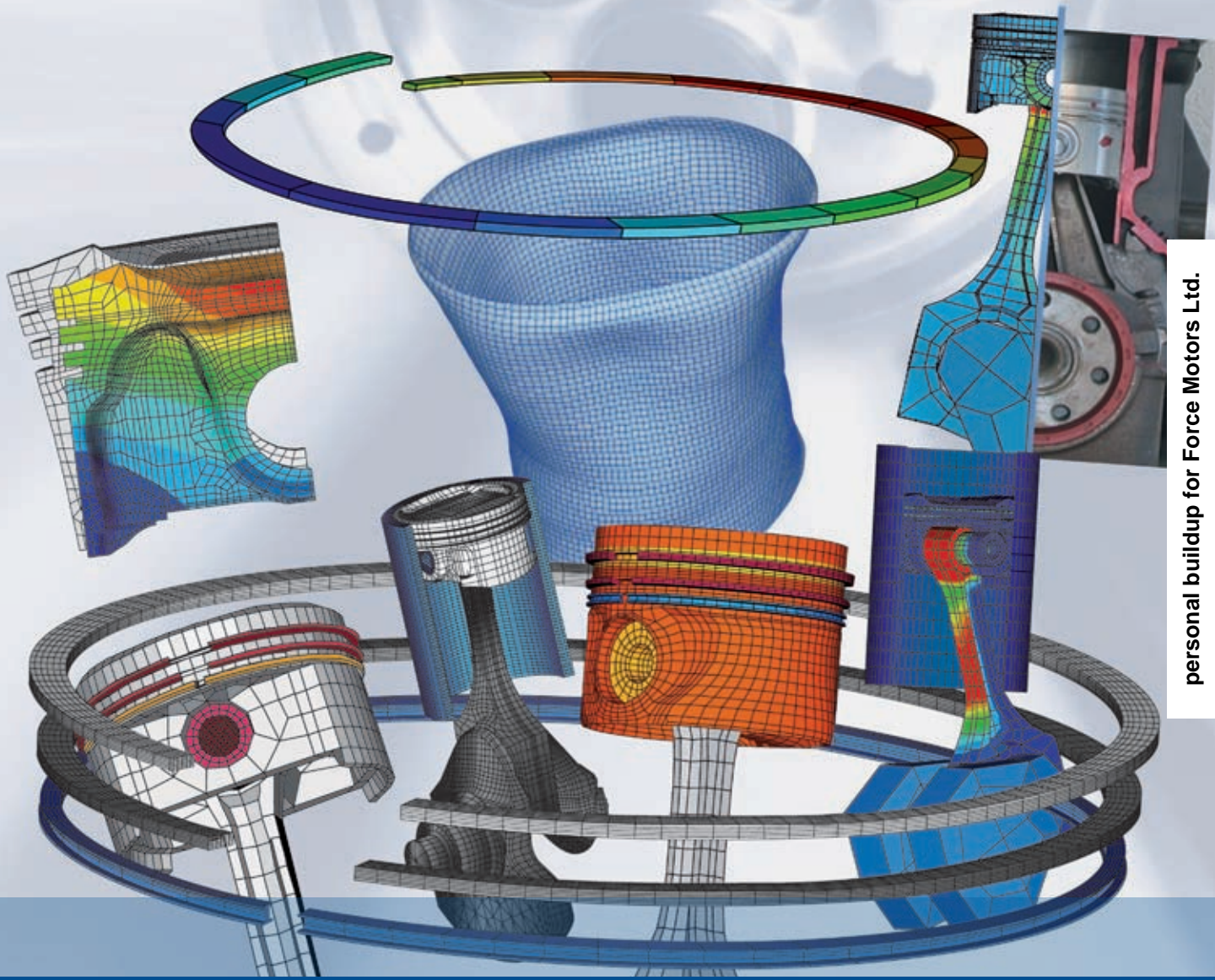
E-Mail: heiko.koellner@gwv-fachverlage.de

### HINTS FOR AUTHORS

All manuscripts should be sent directly to the editors. By submitting photographs and drawings the sender releases the publishers from claims by third parties. Only works not yet published in Germany or abroad can generally be accepted for publication. The manuscripts must not be offered for publication to other journals simultaneously. In accepting the manuscript the publisher acquires the right to produce royalty-free offprints. The journal and all articles and figures are protected by copyright. Any utilisation beyond the strict limits of the copyright law without permission of the publisher is illegal. This applies particularly to duplications, translations, microfilming and storage and processing in electronic systems.

© Springer Automotive Media | GWV Fachverlage GmbH, Wiesbaden 2008

Springer Automotive Media is part of the specialist publishing group Springer Science+Business Media.



# Piston Ring Dynamics Simulation Based on FEA Software

Modern simulation software offers the possibility to simulate the piston ring dynamics in great detail. Therefore, a detailed understanding of the occurring mechanisms and involved physical models can be gained. At the Institute for Combustion Engines in Aachen this approach was used by coupling user subroutines with a FEA dynamic 3D model of a specified piston assembly/cylinder unit. At the institute as well as at FEV these simulation models support the development, failure analysis and optimization process.

## 1 Introduction

The piston assembly is one of the thermally and mechanically highest loaded components in modern combustion engines. Increasing ignition pressures, more efficient power use, minimized component clearances and future oriented emission legislation are going to intensify the load. Partly the numerous piston assembly requirements can lead to clashing objectives. Often the design of piston rings is based on empirical data. Modern simulation software however, offers the possibility to simulate the piston ring dynamics in great detail parallel to measurements. Therefore, a detailed understanding of the occurring mechanisms and involved physical models can be gained. At the Institute for Combustion Engines in Aachen this approach was used by coupling user subroutines with a FEA dynamic 3D model of a specified piston assembly/cylinder unit. At the institute as well as at FEV Motorentechnik GmbH these simulation models support the development, failure analysis and optimization process.

## 2 Model Description

Figure 1 shows the dynamic piston ring model. The macro-geometry, local stiffness, mass and temperature distribution is modelled by the FEA grid. This includes asymmetries due to the piston ring gap or piston design. The micro-geometry is included to a large extent in the contact interaction model formalism, implemented via the user subroutines. The essential boundary conditions are:

- the component geometry including the piston ring running surface and pretension force
- the temperature distribution and deformation of the liner surface
- the temperature distribution, deformation and skirt shape of the piston
- the gas pressure and temperature curve in the combustion chamber and crankcase
- the gas and lubricant properties
- the rotational speed of the crank shaft.

A gas model that is coupled to the FEA model generates the transient gas pressure values and blow by rates. The contact model [1, 2] that describes the interaction between the piston ring and liner surface is based on a hydrodynamic and mixed friction approach. The potential occurrence of wear is modelled as described in [3, 4]. Furthermore a simplified lubricant transport model is implemented that keeps track of the lubricant distribution on all relevant surfaces over time. The input interface consists of a parameter list that is used to initialize all subroutines prior to a simulation. All 3D components are meshed automatically based on their geometrical parameters. Because of the piston's complexity and to ensure that the asymmetric stiffness (skirt) and mass distribution behaviour are most precisely detailed the piston is only meshed with computer assistance.

## 3 Simulation

### 3.1 Piston Ring Assembly

In order to obtain a realistic stress distribution in the piston rings they are meshed in their original state, and then, via a pre-simulation step, assembled into the liner.

## The Authors



Dr.-Ing. Timo Ortjohann was deputy manager of the department dynamics and team manager base engine at FEV Motorentechnik GmbH in Aachen (Germany).



Dr.-Ir. A.P.J. Voncken is technical software engineer of the department dynamics at FEV Motorentechnik GmbH in Aachen (Germany).



Univ.-Prof. Dr.-Ing. Stefan Pischinger is director of the Institute for Internal Combustion Engines (VKA) at the RWTH Aachen (Germany).

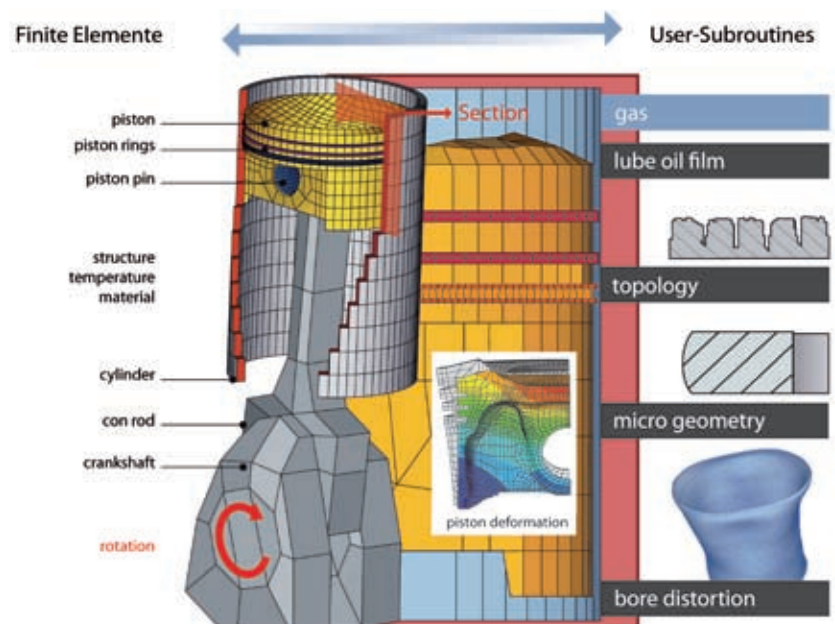


Figure 1: Set up of the piston ring dynamics simulation model

Stress distribution as a result of applying pretension ...

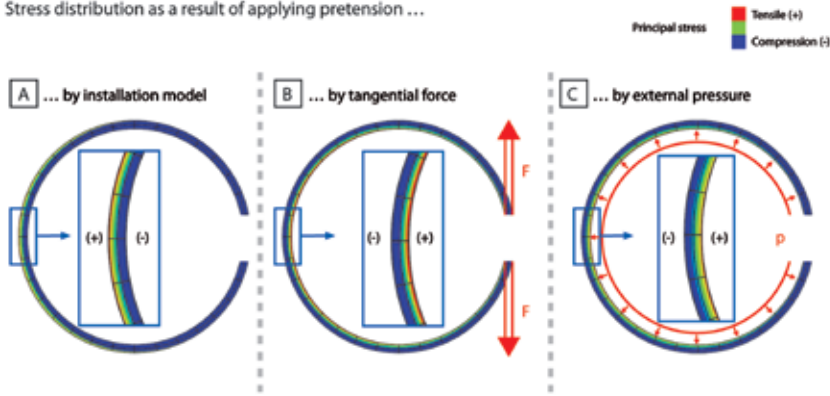


Figure 2: Comparison of piston ring pretension models

Figure 2 (A) shows the resulting stress distribution in the piston ring. As a comparison Figure 2 (B) and (C) show two often used approaches to model the pre-tension in a piston ring either via an external force, Figure 2 (B), or via an external pressure, Figure 2 (C). It becomes apparent that the pressure and tensile stress distribution reverses along the radial coordinate. The last two approaches can be used in their simplified form however they will lead to an unrealistic stress distribution in the piston ring.

3.2 Piston Assembly Dynamics

Due to the vast range of interactions that are involved in the piston ring's dynamics and the physical model depth a valida-

tion of the model is recommended wherever possible for each project. Based on the calibration of the simulation model with measurement data, simulation variants are defined, in order to investigate a problem. In the concept phase simulations are conducted for typical load cases such as: zero, part, and full load at idle, engine speed of 2000/min, engine speed at maximum power, and over-speed. All conceivable model parameters can be varied to analyze potentials. For specific problems on prototypes or series production only a selected load cases are simulated at which a failure is expected to occur. Proposed solutions can then be verified in further steps by simulation.

4 Submodels and Results

The amount and diversity of simulation output data is huge due to it's three dimensional implementation of the elastic system in the time domain and must be well structured depending on the point of focus of an investigation. All FEA model specific output data (dynamics, stresses, and contact behaviour) is available to the user via the commercial FEA post-processor software. The user subroutines support the post processing to a great extent as well, as they report essential evaluation results like blow-by, friction, wear, and lubricant distribution.

4.1 Gas Flow and Blow-by

The nodal positions of all meshed components are transmitted by the FEA solver for every time increment to the linked FEA gas flow model where they serve as input. With this information, the gas chamber volumes  $V_i(t)$  and the gas flow cross section areas  $A_x(t)$  per piston ring gap and circumferential radial clearance are calculated, Figure 3 (A). These cross section areas serve as input for the gas flow equations as described in [5]. The gas model calculates the quantities pressure  $p_i$ , temperature  $T_i$ , mass  $m_i$  and mass flow rate  $\dot{m}_{i,i+1}$  per model chamber and time increment. The gas pressures  $p_i$  are used as pressure boundary

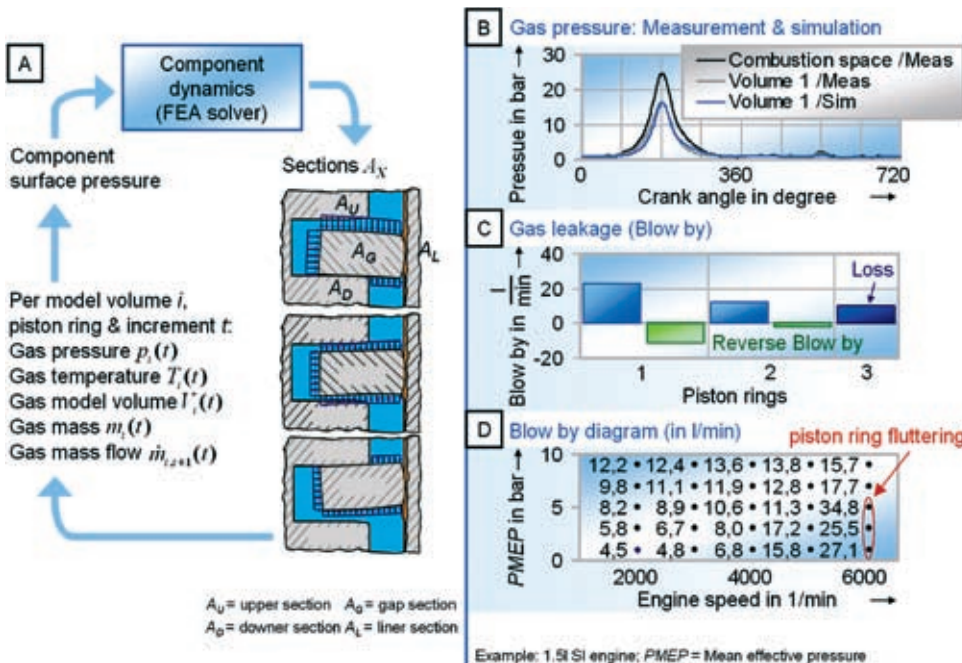


Figure 3: The coupled gas flow model with gas pressure and blow by results

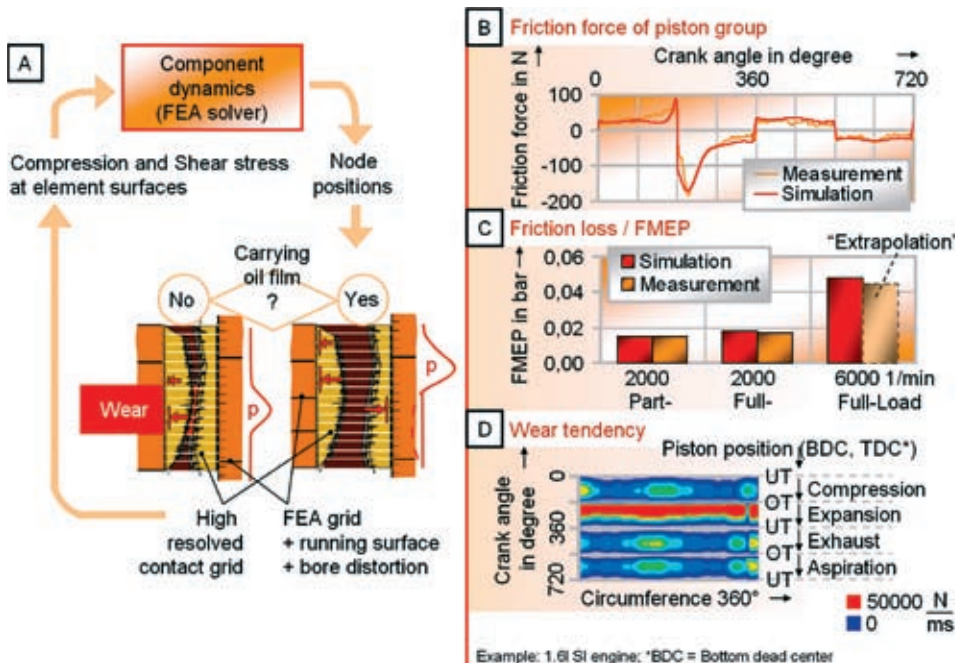


Figure 4: The coupled HD/hard contact model with friction force, friction loss and wear results

conditions on the corresponding FEM model surfaces in the next time step. The gas pressure curve in the combustion chamber and crank case serve as gas model boundary conditions.

The diagram in Figure 3 (B) shows the pressure curve in the combustion chamber (black) and between the first and second piston ring (chamber 1, blue) as a function of crank angle. The simulated pressure curve for chamber 1 matches well with the measured curve (grey) acquired from a motored 1.5 l gasoline engine as an example. Based on a measurement validated simulation model blow-by rates can be determined reliably. These are presented in the diagram in Figure 3 (C) (operating point: mean effective pressure  $p_{me} = 5$  bar, engine speed  $n = 4000$ /min) as integral values of blow-by and reverse blow-by. If these simulations are carried out for a series of operating points a so called blow-by loss-iso-diagram, as depicted in Figure 3 (D), is obtained. Conspicuous operating points can now be diagnosed, analysed (ring fluttering) and counter measures can be validated.

#### 4.2 Hydrodynamics, Friction and Wear

The input parameters for the contact model, Figure 4 (A), which allow the lubricant film geometry to be determined as a function of circumference and time

for every piston ring are the positions and velocities of the piston rings and liner surface nodes. As the meshed grid of the piston rings is too coarse for an accurate implementation of the mixed friction contact approach, the piston ring running surfaces and liner surface are applied to a significantly denser grid. Furthermore, the surface roughness for both surfaces is included by their statistical values. One result for every time step is the lubricant film's geometry which is used to check whether any asperities of the rough surfaces are in contact. If they have contact, the regime of mixed-friction is entered. Depending on the contact pressure, the hydrodynamic and metallic contact pressure are weighted over the Abbott-Firestone-curve [4] and superimposed. The summed surface pressure is returned as pressure boundary condition per time increment to the FEA solver. The potential wear of both contacting surfaces is implemented via an abrasive and adhesive wear model [3, 4]. Both these wear formalisms predict a reduction of the surface roughness peaks per time step as a function of the contact pressure, relative velocity, and surface hardness. An important result of the contact model is the friction force behaviour of the piston assembly. A comparison of simulated and measured [6] friction force is shown in Figure 4 (B). By

varying parameters the model supports the evaluation of variants regarding friction and wear behaviour. This is an advantage in concept phases, for optimisation suggestions or at high engine speeds, where measurements are either not possible or too expensive. In the diagram in Figure 4 (C), the mean effective pressure for 2000/min at part and full load are presented and compared with measurement data. Using this starting point, the values for 6000/min at full load can be rated via an extrapolation of the simulation and measurement results.

The product of local contact pressure distribution and relative contact surface velocity will be defined as wear tendency. The wear tendency of each piston ring running surface as well as the liner surface can hence be determined. This result, as shown in the diagram in Figure 4 (D), can be plotted as a function of crank angle versus liner circumference.

The diagram gives a qualitative and practical assessment on the regions on the liner surface where wear is most likely to occur. If many variants are incorporated in the analysis, potential low wear designs can be determined.

#### 4.3 Lubricant Distribution

The positions, velocities, and accelerations of all FEM-meshed nodes serve as

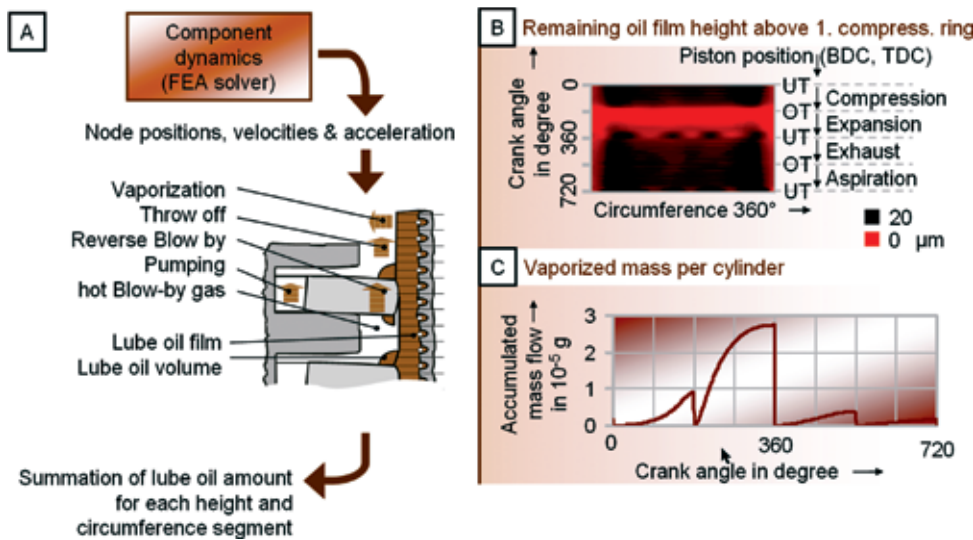


Figure 5: The coupled lubrication oil distribution model including oil film height and vaporized oil results

input for the lubricant-model. This model describes the transport of the lubricant on the liner surface due to the up- and downward scraping of the lubricant by the piston rings. For each time step, the lubricant film height on the liner surface and the lubricant volumes at piston ring top and bottom side are calculated. Figure 5 (A). These are a result from the minimal lubricant film height as im-

plemented in the hydrodynamic contact model, after the piston ring has run over the liner surface and the lubricant supply. Currently, five lubricant loss mechanisms are considered:

- the evaporation of lubricant in the combustion chamber [7]
- the loss of lubricant beyond a critical acceleration at the top side of the first piston ring

- the loss via dissolved lubricant in blow-by [8]
- the pumping of lubricant passed the first piston ring
- the coking of lubricant due to hot blow-by gases.

Figure 5 (B) shows a typical result of the lubricant film height on the liner surface after the first piston ring has run over as a function of the crank angle versus cylinder circumference. In the diagram in Figure 5 (C) the evaporated lubricant mass part as a function of crank angle is shown.

Due to its complex interactions the lubricant distribution model is very sensitive to input parameters. Momentarily it is used in practical applications for qualitative comparisons of system variants.

#### 4.4 Parameter Variation

The impact of the thermal deformation of the piston assembly components on the functional behaviour of the piston rings is in the focus of current research. For this, the 3D temperature distribution and the corresponding thermal deformation, as depicted in Figure 6 (A), is included into the model. A comparison with temperature measurements shows the accordance at five sensor positions. Based on this validated input, load cases for minimal piston assembly component clearances at higher revolution speeds can be simulated, and the impact on wear and lubrication consumption can be analysed. For example, the wear tendency index (= average value of the product of contact pressure times relative surface velocity) and the remain-

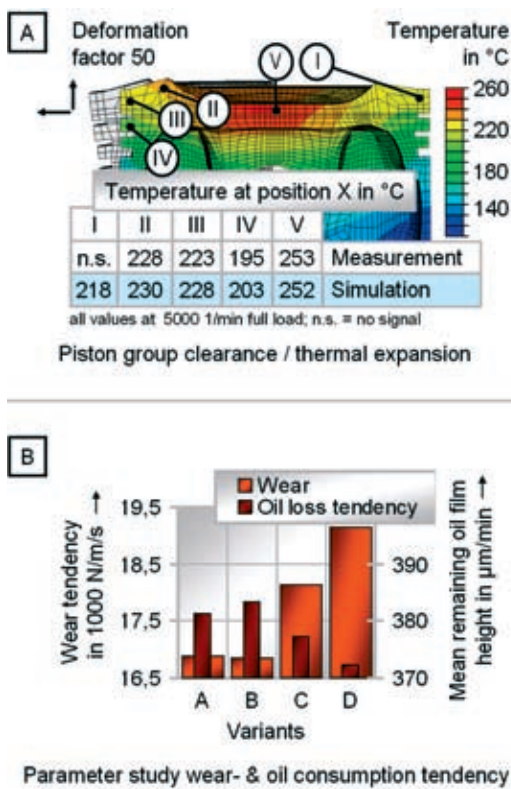


Figure 6: Parameter investigation taking into account the 3D temperature field of the piston group

ing lubricant film height on the surface above the top piston ring can be analysed for variants (A) basis, (B) without piston offset, (C) without crank offset, and (D) maximal piston ring pre-tension. The aim of such an investigation is the localisation of wear relevant model parameters and their impact on i.e. lubricant consumption.

## 5 Summary

The simulation technique offers a future oriented building block with a high degree of physical modelling depth. It allows a most realistic simulation of the three dimensional piston ring dynamics where relevant physical interactions, such as gas coupling, elasticity, non-linear contacts (EHD and solid body) and temperature influences are embedded. The simulation methodology allows a detailed study of the piston ring vertical gap position, fluttering, and rotation based on the implementation of free moving piston rings which are controlled only by gas-, HD-, and contact interactions. The long time use of measuring techniques [6, 9, 10] in research-, development-, and series-production-projects as well as the verification with supplier data supports the refinement of the model so far and in future. The knowledge gained from the simulations flow back into the measuring methodology for optimizing the mechanical signal-transfer systems and sensor technology. The application in various projects so far has shown the adaptation potential of this methodology regarding the requirements of modern developed cylinder units and in combination with various analysis techniques since its first publication in 2001 [11].

## References

- [1] Reynolds, O.: On the theory of lubrication, Phil. Trans. Royal Society 1886, Part 1, Papers on mechanical and physical subjects, Cambridge University Press 1900, 1901, 1903
- [2] Greenwood, J. A.; Tripp, J. H.: The contact of two nominally flat rough surfaces, Proceedings Institute of Mechanical Engineers Vol 185 48/71, p. 625-633, 1971
- [3] Archard, J. F.: Contact and rubbing of flat surfaces, Journal of Applied Physics, Vol 24, Nr. 8, 1953
- [4] Pint, S.; Schock, H. J.: Design and Development of a Software Module for Analysis of Three Dimensional Piston Ring Wear, SAE-Paper2000-01-0920, 2000
- [5] Eweis, M.: Reibungs- und Undichtigkeitsverluste an Kolbenringen, VDI-Forschungsheft 371, Berlin, 1935
- [6] Dohmen, J.; Hermsen, F.-G.; Barbezat, G.: Untersuchungen an plasmabeschichteten Zylinderlaufflächen. In: MTZ 2004 Nr. 3
- [7] Herbst, H. M.; Priebsch, H. H.: Simulation of Piston Ring Dynamics and Their Effect on Oil Consumption, SAE-Paper2000-01-0919, 2000
- [8] Burnett, P.J.; Bull, B.; Wetton, R. J.: Characterization of the ringpack lubricant and its environment, Part J, Proceedings Institute of Mechanical Engineers Vol 209, 1994
- [9] Koch, F.; Geiger, U.; Hermsen, F.G.: PIFFO – Piston Friction Force Measurements during Engine Operation, SAE-Paper 960306, 1996
- [10] Orlovsky, K.; Dohmen, J.; Duesmann, M.: Simulation und Messung im Kurbeltrieb, HdT Tagung, Essen, 2003
- [11] Maassen, F.; Koch F.; Schwaderlapp, M.; Ortjohann, T.; Dohmen, J.: Analytical and Empirical Methods for Optimization of Cylinder Liner Bore Distortion, International SAE Conference 2001, Detroit, SAE Paper 2001-01-0569, 2001

## IMPRINT

**MTZ** WORLDWIDE

www.MTZ-online.com

12|2008 · December 2008 · Volume 69

Springer Automotive Media | GWV Fachverlage GmbH

P.O. Box 15 46 · 65173 Wiesbaden · Germany

Abraham-Lincoln-Straße 46 · 65189 Wiesbaden · Germany

**Managing Directors** Dr. Ralf Birkelbach, Albrecht Schirmacher

**Advertising Director** Thomas Werner

**Production Director** Ingo Eichel

**Sales Director** Gabriel Göttlinger

### EDITORS-IN-CHARGE

Dr.-Ing. E. h. Richard van Basshuysen

Wolfgang Siebenpfeiffer

### EDITORIAL STAFF

#### Editor-in-Chief

Johannes Winterhagen (win)

Phone +49 611 7878-342 · Fax +49 611 7878-462

E-Mail: johannes.winterhagen@springer.com

#### Vice-Editor-in-Chief

Dipl.-Ing. Michael Reichenbach (rei)

Phone +49 611 7878-341 · Fax +49 611 7878-462

E-Mail: michael.reichenbach@springer.com

#### Chief-on-Duty

Kirsten Beckmann M. A. (kb)

Phone +49 611 7878-343 · Fax +49 611 7878-462

E-Mail: kirsten.beckmann@springer.com

#### Sections

Electrics, Electronics

Markus Schöttle (schoe)

Tel. +49 611 7878-257 · Fax +49 611 7878-462

E-Mail: markus.schoettle@springer.com

#### Engine

Dipl.-Ing. (FH) Richard Backhaus (rb)

Tel. +49 611 5045-982 · Fax +49 611 5045-983

E-Mail: richard.backhaus@rb-communications.de

#### Heavy Duty Techniques

Ruben Danisch (rd)

Phone +49 611 7878-393 · Fax +49 611 7878-462

E-Mail: ruben.danisch@springer.com

#### Online

Dipl.-Ing. (FH) Caterina Schröder (cs)

Phone +49 611 78 78-190 · Fax +49 611 7878-462

E-Mail: caterina.schroeder@springer.com

#### Production, Materials

Stefan Schlott (hlo)

Phone +49 8191 70845 · Fax +49 8191 66002

E-Mail: Redaktion\_Schlott@gmx.net

#### Service, Event Calendar

Martina Schraad

Phone +49 212 64 232 64

E-Mail: martina.schraad@springer.com

#### Transmission, Research

Dipl.-Ing. Michael Reichenbach (rei)

Phone +49 611 7878-341 · Fax +49 611 7878-462

E-Mail: michael.reichenbach@springer.com

#### English Language Consultant

Paul Willin (pw)

#### Permanent Contributors

Christian Bartsch (cb), Prof. Dr.-Ing. Peter Boy (bo),

Prof. Dr.-Ing. Stefan Breuer (sb), Jens Büchling (jb),

Jörg Christoffel (jc), Jürgen Grandel (gl),

Erich Hoepke (ho), Ulrich Knorra (kno),

Prof. Dr.-Ing. Fred Schäfer (fs), Roland Schedel (rs),

Bettina Seehawer (bs)

#### Address

P.O. Box 1546, 65173 Wiesbaden, Germany

E-Mail: redaktion@ATZonline.de

### MARKETING | OFFPRINTS

#### Product Management Automedia

Sabrina Brokopp

Phone +49 611 7878-192 · Fax +49 611 7878-407

E-Mail: sabrina.brokopp@springer.com

#### Offprints

Martin Leopold

Phone +49 2642 9075-96 · Fax +49 2642 9075-97

E-Mail: leopold@medien-kontor.de

### ADVERTISING | GWV MEDIA

#### Key Account Manager

Elisabeth Maßfeller

Phone +49 611 7878-399 · Fax +49 611 7878-140

E-Mail: elisabeth.massfeller@gwv-media.de

#### Ad Sales

Frank Nagel

Phone +49 611 7878-395 · Fax +49 611 7878-140

E-Mail: frank.nagel@gwv-media.de

#### Display Ad Manager

Susanne Bretschneider

Phone +49 611 7878-153 · Fax +49 611 7878-443

E-Mail: susanne.bretschneider@gwv-media.de

#### Ad Prices

Price List No. 51

### SUBSCRIPTIONS

VVA-Zeitschriftenservice, Abt. D6 F6, MTZ

P. O. Box 77 77, 33310 Gütersloh, Germany

Renate Vies

Phone +49 5241 80-1692 · Fax +49 5241 80-9620

E-Mail: SpringerAutomotive@abo-service.info

### SUBSCRIPTION CONDITIONS

The emagazine appears 11 times a year at an annual subscription rate of 269 €. Special rate for students on proof of status in the form of current registration certificate 124 €. Special rate for VDI/ÖVK/VKS members on proof of status in the form of current member certificate 208 €. Special rate for studying VDI members on proof of status in the form of current registration and member certificate 89 €. The subscription can be cancelled in written form at any time with effect from the next available issue.

### PRODUCTION | LAYOUT

Heiko Köllner

Phone +49 611 7878-177 · Fax +49 611 7878-464

E-Mail: heiko.koellner@gwv-fachverlage.de

### HINTS FOR AUTHORS

All manuscripts should be sent directly to the editors. By submitting photographs and drawings the sender releases the publishers from claims by third parties. Only works not yet published in Germany or abroad can generally be accepted for publication. The manuscripts must not be offered for publication to other journals simultaneously. In accepting the manuscript the publisher acquires the right to produce royalty-free offprints. The journal and all articles and figures are protected by copyright. Any utilisation beyond the strict limits of the copyright law without permission of the publisher is illegal. This applies particularly to duplications, translations, microfilming and storage and processing in electronic systems.

© Springer Automotive Media | GWV Fachverlage GmbH, Wiesbaden 2008

Springer Automotive Media is part of the specialist publishing group Springer Science+Business Media.



# The New BMW V8 Gasoline Engine with Twin Turbo

## Part 2 – Functional Characteristics

BMW's new twin turbo V8 gasoline engine is yet another milestone in the "Efficient Dynamics" approach, which is now being implemented in the luxury class as well. It stems from the powertrain development vision of "Sheer Driving Pleasure through Efficient Dynamics". The configuration of second-generation spray-guided direct injection and piezoelectric injectors in a central arrangement, twin turbochargers and the innovative arrangement of the two turbochargers and engine-mounted catalytic converters in the engine V constitutes a unique, ground-breaking combination. This engine celebrated its première in the new X6 in the spring of this year and will also provide the motive power for the newly presented fifth generation of the BMW 7 Series. While the first article in MTZ 11/2008 gave a detailed description of the basic engine, this second part outlines the engine's functional characteristics.

## 1 Introduction

The current underlying conditions facing the automotive industry are marked by a number of challenges, **Figure 1**:

- The recent massive increases in the price of oil are leading to increasingly vehement discussions about cars and fuel consumption. The general legal framework in every market is being tightened up accordingly, by means of fleet consumption rulings, CO<sub>2</sub> taxes, city tolls or registration restrictions, for example.
- The statutory requirements relating to the emission limits are also being tightened up, particularly in the USA (SULEV legislation, ZEV mandate).
- Customers still want to enjoy "Sheer Driving Pleasure", however, and only buy vehicles with the necessary dynamic performance.

BMW's approach to resolving these, in some respects, contradictory requirements goes by the name of "Efficient Dynamics". Innovative engine concepts offer the only means of achieving the objective of combining a high level of driving pleasure with environmentally compatible, low consumption. Apart from the actual idea behind them, innovative engine concepts also require the entrepreneurial courage to reconsider and challenge well-worn, familiar channels

of thought. This is the only way to achieve the development efficiency required to industrialise new solutions. The new V8 gasoline engine with its turbocharger arrangement and the associated functional advantages for the customer is a living example of such pioneering ideas.

## 2 Objectives

The requirements specification for development of the new engine centred on the following requirements.

- a noticeable improvement in engine performance with the emphasis on a full-bodied torque characteristic to ensure the superior ease required for use in a luxury-class vehicle
- outstanding throttle response
- reduced fuel consumption with further consumption cutting potential within the framework of engineering revision stages
- convincing V8 engine sound
- the ability to use all grades of fuel available worldwide
- compliance with all currently applicable emission standards (EU5, ULEV II).

Various different engine concepts were examined in closer detail and compared with one another during the initial phase in order to comply with these specification requirements. A decision

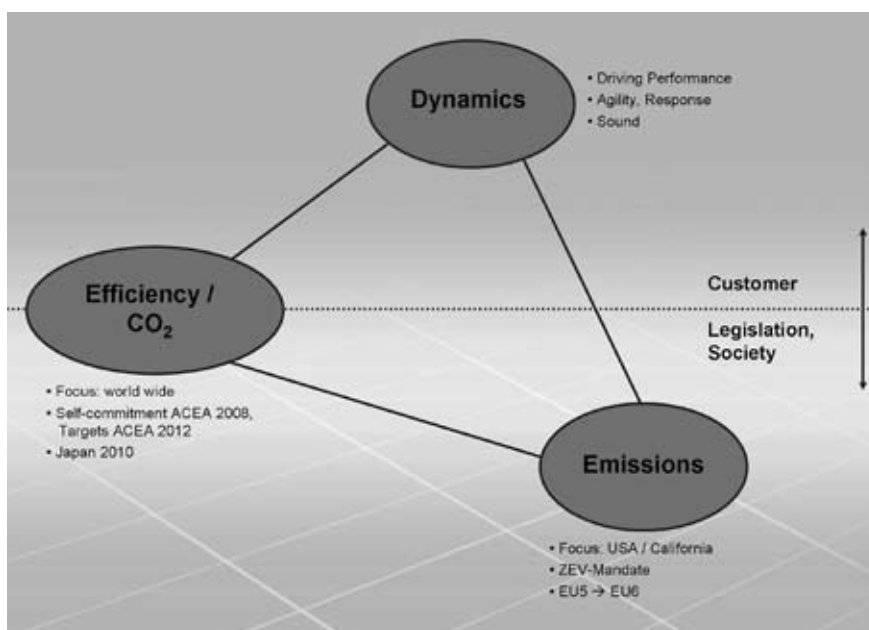


**Figure 1:** Customer expectations and statutory requirements

## The Authors



Dipl.-Ing. Christian Bock is General Manager Functions V Engines within the BMW Group in Munich (Germany).



Dipl.-Ing. Klaus Hirschfelder is General Manager V Engines Projects within the BMW Group in Munich (Germany).



Dr.-Ing. Bernd Ofner is Manager Function Development Gasoline Engines within the BMW Group in Munich (Germany).



Dr.-Ing. Christian Schwarz is General Manager Development Thermodynamics within the BMW Group in Munich (Germany).



Figure 2: View of the engine

was finally made in favour of a turbocharged V8 engine with a 90° cylinder bank angle, second-generation high-precision direct fuel injection and 4.4 l displacement.

### 3 Technical Highlights of the New V8 Engine

BMW's new V8 "Twin Turbo" engine, **Figure 2**, is the latest member of a new family of turbocharged gasoline engines, which was launched very successfully in 2006 with the 3.0-l, six-cylinder "Twin Turbo" engine. This engine received an excellent reception with outstanding feedback from the market and has won numerous prizes including the "2008 Engine of the Year Award". The engine boasts properties usually sported by naturally aspirated engines with much higher displacement, particularly in terms of throttle response. The yardstick for the anticipated performance of the new V8 engine was therefore set very high.

The V8 engine has been designed for use all over the world. It must therefore guarantee safe, reliable operation with all grades of fuel available worldwide. Because of this, a homogeneous DI combustion concept is used, which complies with all global emission requirements,

thanks to an exhaust gas aftertreatment system with preliminary and main catalytic converters mounted on the engine. The engine complies with the requirements of EU5 and ULEV II emission levels at the launch of series production.

For the first time in automotive history, a V-type engine has been designed with the intake valves on the outside and the exhaust valves in the V space of the engine block. This innovative engine con-

cept enables a very compact arrangement of the two turbochargers within the "hot V". The catalytic converter system, with preliminary and main catalytic converters, is also positioned inside the V-space, immediately behind the turbochargers. After passing through the catalytic converters, the exhaust gases are routed between the engine and splashboard to the underbody by the exhaust system.

In its central fitting location, the "High Precision Injection" (HPI) spray-guided direct fuel injection system with piezoelectric injectors is the heart of the engine. Already known for its use in the six and four-cylinder engines, this fuel injection system was adapted to the changed geometric conditions of the eight-cylinder engine with its larger bore. This system, with its outstanding mixture control, very short switching times and the possibility of introducing multiple injections of fuel, offers ideal prerequisites for optimum development of performance and efficient heating of the catalytic converters. Each bank of cylinders is equipped with a high-pressure injection pump that delivers rail pressures of up to 200 bar to the injection system, driven by the exhaust camshafts.

The Digital Motor Electronics (DME) system used to control the engine is a further development of the familiar engine control unit used with the six-cylinder engine.



Figure 3: Combustion chamber design

The important key data of the DME system are:

- Infineon TriCore TC1796 processor, 150 MHz
- 2 MB external flash memory
- integrated FlexRay controller
- dual PCB arrangement with press-fit contact technology
- 184 pins.

The high-performance output stages required to control the eight piezoelectric injectors and the ignition output stages are integrated into the DME. A fan-cooled or water-cooled variant of the control unit is used to dissipate heat according to the vehicle model.

## 4 Engine Design

### 4.1 Combustion Concept

As far as the combustion concept is concerned, attention was given to ensuring a consistent derivative of the turbocharged and stratified charge six-cylinder engines that went into series production in 2006 and 2007. This essentially applies to the central arrangement of spark plug and injector in the combustion chamber and the geometric positioning of the two components relative to one another in the cylinder head, **Figure 3**.

The 89 mm bore set for the V-type engines had to be taken into consideration, as well as the resulting combustion chamber geometry for the high compression ratio of 10.0 required for efficiency. As far as charge motion and flow rate were concerned, appropriate CFD optimisations were carried out to adapt the port geometry in such a way as to achieve approximately the same values as for a turbocharged six-cylinder engine.

Application of the “High Precision Injection” concept, that is the outward-opening piezoelectric injector in conjunction with 200 bar injection pressure, established the foundation for making full use of the excellent catalytic converter heating function of the system with triple injection and, in doing so, to significantly reduce the precious metal loading of the exhaust gas aftertreatment system. This not only offers a means of considerably increasing the enthalpy flow of the exhaust gases compared with a manifold injection system, but also enables a drastic reduction of such exhaust

gas emissions as HC thanks to the use of a triple injection system. Furthermore, the “High Precision Injection” system contributes towards a massive improvement in mixture control in combination with the necessary charge motion, and the highly flexible timing capacity of the multiple injection function ensures a noticeable reduction in the amount of fuel sprayed onto the wall of the cylinder. This also results in a very low exhaust gas emission level at all operating points.

**Figure 4** shows the specific fuel consumption of the V8 engine by comparison with that of the V12 engine at a speed of 2000 rpm. It is evident that the specific consumption values for the new engine are substantially lower while meeting the same torque requirement. A solid foundation has therefore been laid for good consumption behaviour in the vehicle.

### 4.2 Gas-exchange Cycle/Turbocharger System

As described above, the hot and cold sides have been rotated in the gas-exchange cycle concept for the engine. This opens up new degrees of freedom in the package on the outside of the engine. As attention is focussed on the design of the exhaust manifold and turbocharger of a turbocharged engine and the intake manifold is of secondary importance in the gas-exchange cycle, the pioneering car engine construction, which the only one of its kind in the world, offers a

means of realising a very compact air routing concept. Designed as a standard component as far as the even distribution of cylinders and back pressure are concerned, and subject to the boundary conditions of the different steering linkage arrangements for different vehicle packages, the intake manifold was optimised by means of CFD. The engine-mounted indirect charge-air coolers with high cooling capacity make a further contribution towards reducing the pressure losses in the air intake duct and towards the compact design of the engine.

With the turbochargers situated in the V-space of the engine block and the close-coupled catalytic converters, the design of the exhaust side is also very compact, offering distinct advantages in terms of back-pressure behaviour and emissions. The system is capable of meeting even the most stringent emission requirements without the need for an underfloor catalytic converter. The cast manifold combines ideal low-loss flow routing with optimum heat dissipation – in spite of being positioned between the cylinder heads. The manifold, designed as a 4-to-2 junction, combines with timing that has been tuned to the firing order to produce an optimum gas-exchange cycle for a V8 engine. The turbochargers are monoscroll turbines, which have been designed in interaction with the gas-exchange cycle boundary conditions to achieve a compromise between excellent

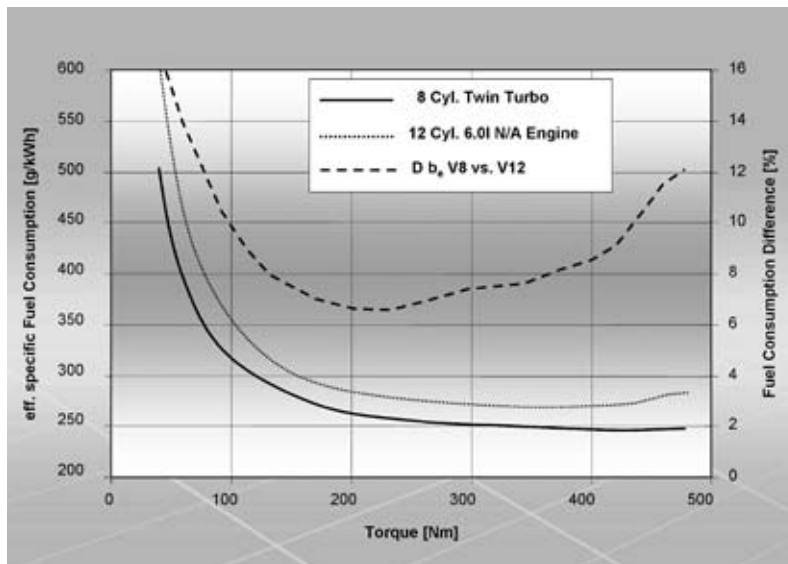


Figure 4: Specific fuel consumption at 2000 rpm

torque at low speed (600 Nm from 1750 rpm to 4500 rpm) and high, extendable output potential (300 kW from 5500 to 6400 rpm). **Figure 5** shows the full-load curves compared with those of the predecessor V8 and V12 engines. The design of the new V8 engine is specifically oriented to the concept of transient torque build-up from low engine speeds.

### 4.3 Emission Concept

The compact arrangement of the exhaust system for the innovative engine concept, with very short distances between exhaust valves, turbochargers and catalytic converters, creates ideal prerequisites for an efficient emission concept. The spray-guided DI combustion concept enables robust stratified catalytic converter heating with triple injection and extremely retarded ignition angles, allowing the catalytic converter to heat up very quickly.

During the development phase, a number of different injection strategies were devised and compared with one another in terms of numerous target values, such as rate of temperature rise, evaporative emissions, particle formation or running smoothness, **Figure 6**. A combination of a double injection during the intake stroke and a brief ignition injection just before the ignition point proved to be the ideal compromise. The catalytic converter system is supplemented by an enhanced primary oxygen sensor, which enables lambda-controlled engine operation after a very brief warm-up period. This means that the engine is capable of meeting current and future emission limits without a complicated secondary air system, in spite of the heat sink of the turbocharger.

Another advantage of the chosen engine concept is the way in which the main exhaust system components have been integrated into the basic engine. This brings the engine very close to the design ideal of the modular system; it can be adapted to various vehicle concepts, such as saloons or sport activity vehicles (SAVs) with a high level of application efficiency.

### 4.4 Engine Functions

A lot of the functions and a great deal of the software in the engine control system (DME) were developed by BMW. The sup-

plier integrates the BMW components into the overall software on the basis of a tried-and-trusted software sharing process, **Figure 7**. The scope of the work performed by BMW includes those functions, which are capable of influencing the way in which the driver experiences the engine, and functions, which cannot be provided on the basis of the supplier's industrial system modules because of BMW specific engineering requirements. This means, for example, that all of the actuator setpoint values for the new eight-cylinder engine, such as throttle angle, vari-

able camshaft control (Vanos), wastegate duty cycle, injection volume and timing, ignition point and other setpoint assignments – for fuel pressure and ancillary equipment, for example – are derived from BMW functions.

A special challenge facing the developers of the new eight-cylinder engine was to control the separate engine banks on the intake and exhaust sides and in the fuel system with just a single control unit. Many functions had to be divided up and calculated twice because of this. These particularly included open-loop

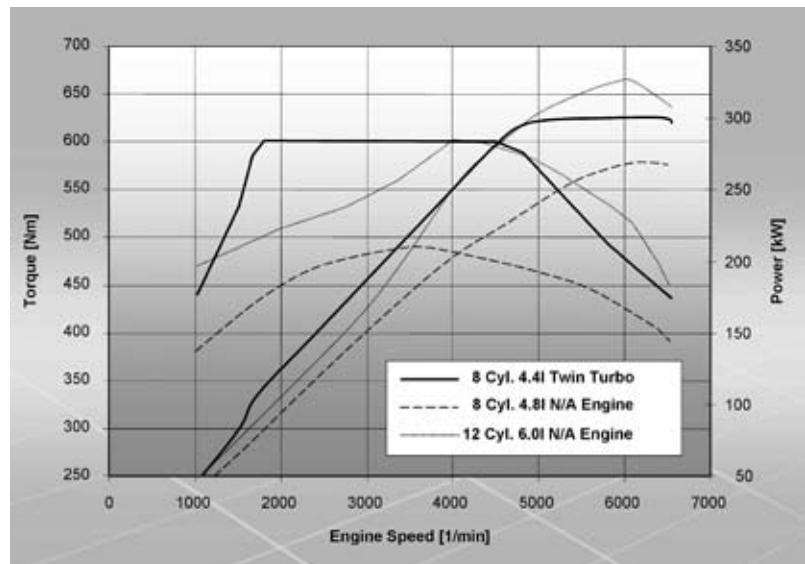


**Figure 5:** Full-load curve by comparison with the predecessor engines

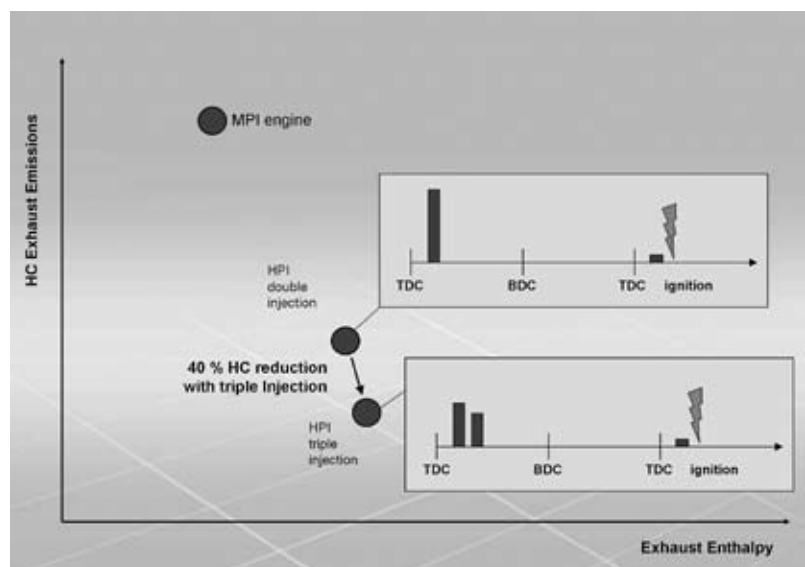


**Figure 6:** Catalytic converter heating strategies

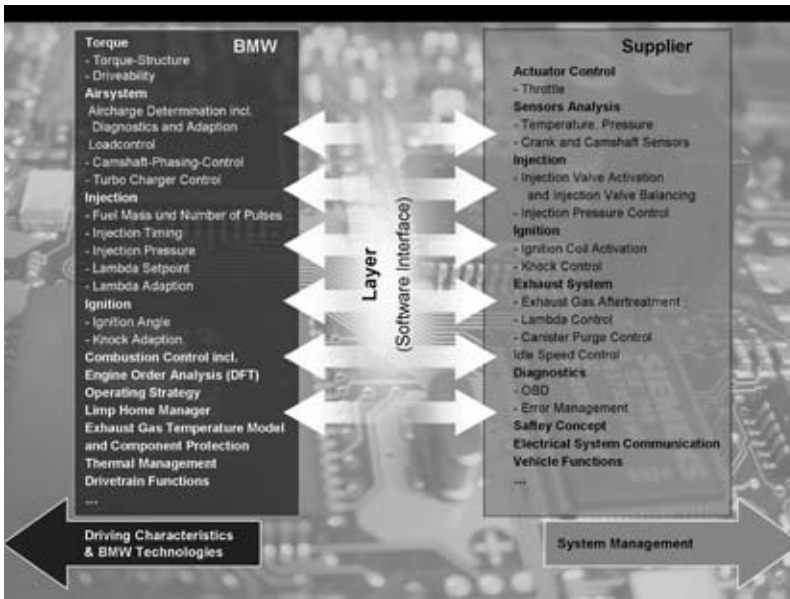


Figure 7: Functions

control of the air circuit (charge and intake manifold pressure control), closed-loop control of the fuel circuit (fuel pressure control and injection timing) and the ignition circuit. In spite of being independent of one another in the calculation, the banks had to be equalised with respect to running smoothness, output and emissions. By combining the most powerful processor available on the market with resource-optimised application of the functional and software modules, the developers were able to operate the engine with just a single DME, thereby reducing the costs and the amount of installation space required.

The positions of the oxygen sensors downstream of the turbochargers, the “4-to-2-to-1” design of the exhaust manifold and the specific firing order of the V8 engine are such as to preclude the possibility of cylinder-individual lambda control by means of a signal from the oxygen sensor because the various exhaust gas packages cannot be divided. A completely new cylinder-individual equalisation method was developed in order to meet the stringent requirements of the legislation on exhaust gas emissions and comply with future OBD requirements. This method is based on the specific lambda characteristic, that is reducing the indicated engine torque by leaning the mixture. The individual cylinders in an exhaust bank are leaned,

one after another at partial load – in a manner that cannot be perceived by the driver – until such time as a change in running smoothness takes place, defined by means of load and engine speed. The overall lambda value is maintained at a constant level, during selective leaning as well, by proportionately enriching the remaining cylinders. The leaning factor for each cylinder is determined when the change in running smoothness occurs. Cylinder-individual adaptations are calculated from the deviation of the leaning factor from the mean value for an exhaust bank.

The modular functions for specification of injection mode with appropriate division of the quantity and the timing of the injection pulse constitute another new development. Individual injection strategies with up to three injection pulses per working cycle and cylinder can be configured for the various operating states of the engine, such as start-up, warm-up, catalytic converter heating or normal running. At the same time, the injection modes with up to two pulses linked to the ignition angle offer considerable potential with respect to emission optimisation, Figure 6.

In an attempt to master the globally increasing variability of fuel properties to a better extent, BMW’s function modules use efficient adaptation functions on the basis of neural networks. These adapt the tolerances in the air-mass flow according to engine speed and load, as well as lambda deviations and the knock resistance of the fuel.

A function was developed, which offers a means of eliminating uneven distribution of cylinder charge in order to ensure optimum smooth running of the engine. Such uneven distribution may be caused by tolerances in the air circuit or by initiating tank ventilation on just one cylinder bank. Using the two closed-loop intake manifold control systems, the function utilises the mutual independence of the actuators for the two cylinder banks to achieve adaptation of the cylinder charge for both banks and equalise the cylinder bank torque values. The run-

Table: Comparing the characteristics of the V8 engine with predecessor engines

Engine	Unit	V8 Twin Turbo Spray Guided, High Precision Injection (central)	V8 N/A Valvetronic	V12 N/A Valvetronic DI, Swirl Injektor (side mounted)
Displacement	[l]	4,395	4,799	5,972
Compression Ratio	[-]	10,0	10,5	11,3
Power (at rpm)	[kW]	300 (5500 – 6400)	270 (6300)	327 (6000)
Specific Power	[kW/l]	68,3	56,3	54,8
Torque (at rpm)	[Nm]	600 (1750 – 4500)	490 (3400)	600 (3950)
Specific Consumption (best)	[g/kWh]	238	241	245

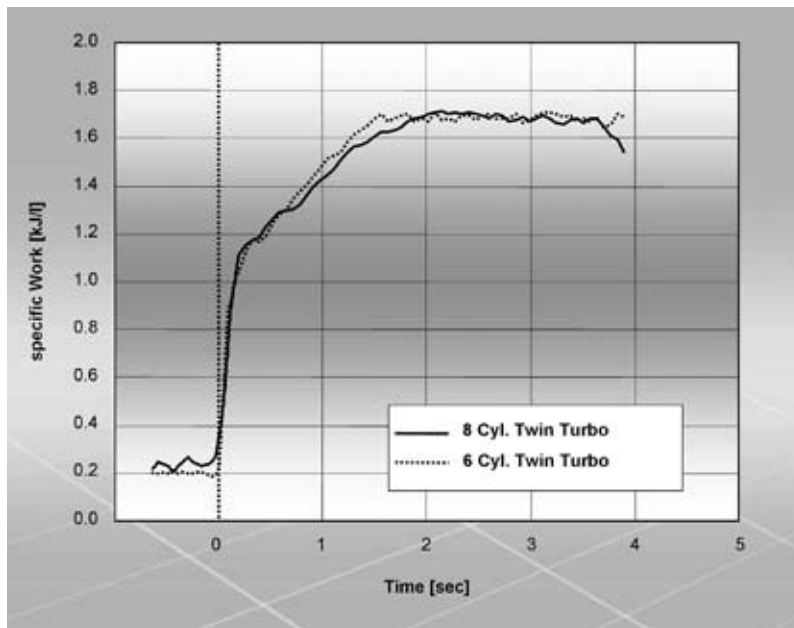


Figure 8: Throttle response

ning smoothness of the engine is classified in terms of engine order with the help of a discrete Fourier transformation calculated in real time. Based on this, a combustion control system is used for selective intervention on individual cylinders to reduce engine excitation.

5 Functional Results

The Table shows the key data and a brief summary of the functional results achieved for the new V8 engine and compares these with the results obtained for predecessor engines. The table not only contains the data for the immediately preceding V8 engine, but also the 6-l twelve-cylinder engine, which has more comparable performance values.

5.1 Power and Torque

The engine has a very broad useful engine speed band. The 600 Nm maximum torque is already achieved at 1750 rpm and remains constantly available up to 4500 rpm. This high level of low-end torque and the wide nominal torque plateau guarantee superior ease and constitute the basis for shift-relieved calibration of the automatic transmission. The maximum output of 300 kW is reached between 5500 and 6400 rpm and the cut-off speed is reached at 6800 rpm.

5.2 Throttle Response

Special priority was given to the throttle response during the development process. The six-cylinder “Twin Turbo” engine that has been praised so highly in many test reports served as the internal benchmark for this. During a standard acceleration process with a constant speed of 1500 rpm and a sudden load variation of  $w_e = 0.2 \text{ kJ/l}$  to full load, values exceeding 25 Nm/l/s are reached

during the build-up of torque, Figure 8. This puts the V8 engine very close to the six-cylinder benchmark and its transient response also gives the impression of a naturally aspirated engine with higher displacement. The maximum exhaust temperature for this design amounts to 950 °C.

Apart from the classical concept described here, the compact arrangement of the turbochargers in the engine V also offers a means of realising other innovative charging concepts to increase engine performance.

5.3 Driving Performance/ Fuel Consumption

The chart showing consumption as a function of driving performance in Figure 9 compares the new BMW 7 Series with the predecessor vehicles. It is clearly evident that the new V8 engine is not only a replacement for its direct predecessor, the 750i with its 4.8-l V8 engine, but actually succeeds the 760i with its 6-l V12 engine. Although the new BMW 750i achieves slightly better driving performance than the preceding BMW 760i when accelerating from a standstill up to 100 km/h, its consumption values are much lower.

The practical consumption figures are also well below those of the old BMW 760i. Based on the pleasing throttle response and the high level of low-end

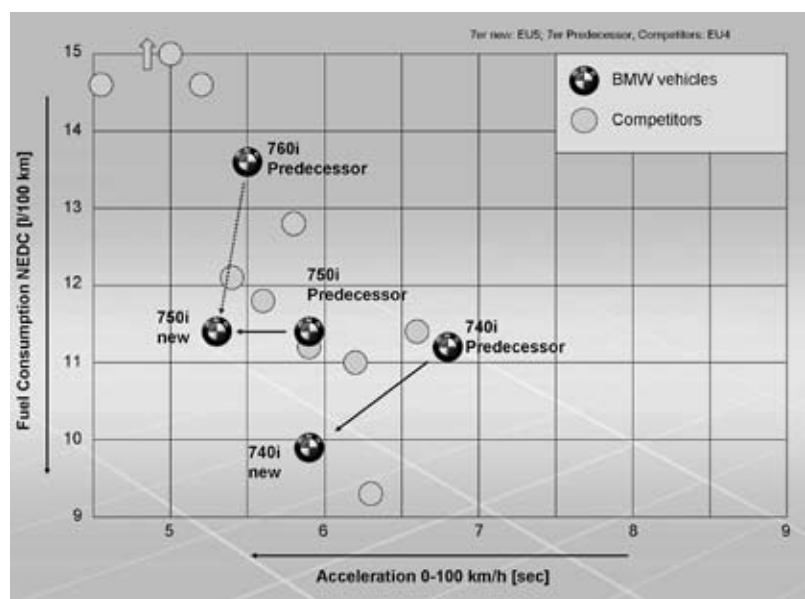


Figure 9: Comparing driving performance / consumption with predecessor vehicles

torque, the developers were able to design the six-speed automatic transmission for much fewer shifting operations and torque orientation. This accentuates the character of effortless, superior locomotion and very favourable consumption values can be achieved at the same time. The new V8 engine is therefore carrying BMW's "Efficient Dynamics" approach over into the luxury class.

### 5.4 Engine Sound

While developing the powertrain acoustics, particular attention was given to achieving a typical V8 sound, which is clearly audible both inside and outside the vehicle. It goes without saying that these considerations were based on compliance with all globally applicable regulations and standards relating to external noise. The sound engineering objectives were to achieve a high level of comfort when travelling at a constant speed and, depending on the model of vehicle, distinctive noise development at higher load. When designing the intake and exhaust routes, special attention was given to bringing out the typical n.5<sup>th</sup> engine orders produced by the design-specific firing order of the V8 engine, while keeping the pressure losses as low as possible.

### 5.5 Calibration Methods

Continuously growing requirements are leading to increasingly complex engine

concepts. The aim of steadily further reducing fuel consumption, in particular, is giving rise to such complicated technical solutions as lean burn combustion or down-sizing concepts with turbocharged engines.

Another driving factor for growing complexity is the increasing functional internetworking of systems within the vehicle. The numerous control units communicate with one another via increasingly powerful bus systems in order to provide appropriate functions that are relevant to the customer. The level of complexity of the electronic engine management systems continues to grow accordingly. One characteristic index is the number of labels to be applied.

The engine management system for BMW's new eight-cylinder has now reached the astoundingly high number of more than 12 000 calibration labels (characteristic values, characteristic curves and engine characteristics maps). The pertinent programme documentation covers more than 12 000 pages.

The calibration specialists are now facing the challenge of keeping abreast of these developments. An unthinkable task without suitable powerful calibration tools to provide intensive support for the calibration process.

The following objectives and challenges emerge for the application methods, **Figure 10**:

- mastering the growing complexity
- a highly efficient calibration process
- ensuring that data is of a high quality standard.

Apart from these tool optimisation objectives, which are of rather more operational nature, there is also a chance of making a contribution towards product differentiation. It will not be possible to implement future engine concepts with even higher calibration requirements if we do not have correspondingly powerful tools. Suitable calibration methods can also play an important role in defining the precise nature of certain product characteristics, however, by objectifying and exactly describing such driving characteristics as throttle response, for example. This offers a means of clearly carving out driving characteristics that are typically BMW and making a contribution towards distinguishing BMW from the competition.

## 6 Conclusion

The new V8 "Twin Turbo" engine with "High Precision Injection" and the innovative arrangement of both turbochargers in the V-space of the engine block combines superior driving performance with favourable consumption to produce a new benchmark in the segment. The engine therefore constitutes an important building block for the "BMW Efficient Dynamics" strategy in the luxury class.

The new engine demonstrates its performance capability convincingly in the new vehicle. This engine celebrated its première in the new Sports Activity Coupé X6 in the spring of this year and will be fitted in the newly presented fifth generation of the BMW 7 Series as the ultimate engine option. Initial press reports are correspondingly positive. Particular attention is drawn to the superior ease with which the engine builds up power, which is unusually spontaneous for a turbocharged engine. This means that a ground-breaking engine concept is now available for the luxury class, which will be used in other vehicle derivatives as well. Furthermore, the engine also offers considerable development potential for compliance with future requirements. ■

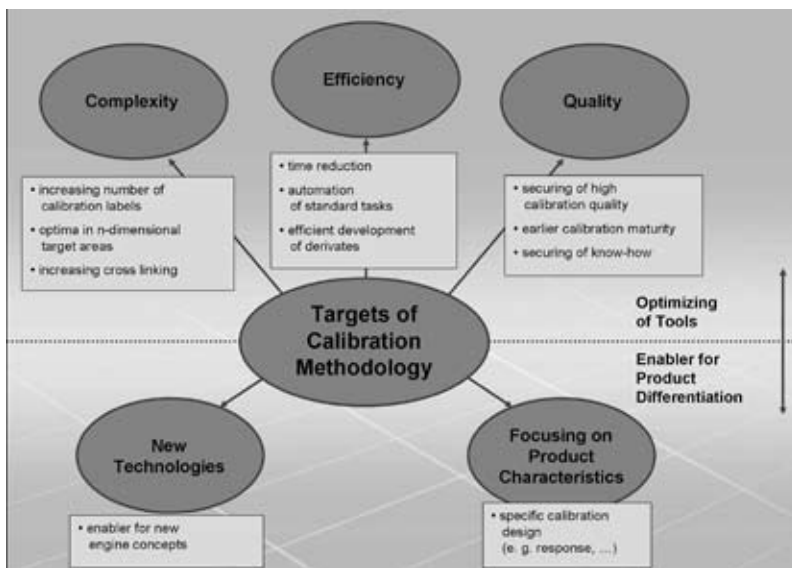


**Figure 10:** Calibration method objectives

## Peer Review ATZ|MTZ

## Peer Review Process for Research Articles in ATZ and MTZ

## Steering Committee

<b>Prof. Dr.-Ing. Stefan Gies</b>	RWTH Aachen	Institut für Kraftfahrwesen Aachen
<b>Prof. Dipl.-Des. Wolfgang Kraus</b>	HAW Hamburg	Department Fahrzeugtechnik und Flugzeugbau
<b>Prof. Dr.-Ing. Ferit Küçükay</b>	Technische Universität Braunschweig	Institut für Fahrzeugtechnik
<b>Prof. Dr.-Ing. Stefan Pischinger</b>	RWTH Aachen	Lehrstuhl für Verbrennungskraftmaschinen
<b>Prof. Dr.-Ing. Hans-Christian Reuss</b>	Universität Stuttgart	Institut für Verbrennungsmotoren und Kraftfahrwesen
<b>Prof. Dr.-Ing. Ulrich Spicher</b>	Universität Karlsruhe	Institut für Kolbenmaschinen
<b>Prof. Dr.-Ing. Hans Zellbeck</b>	Technische Universität Dresden	Lehrstuhl für Verbrennungsmotoren

## Advisory Board

<b>Prof. Dr.-Ing. Klaus Augsburg</b>	<b>Prof. Dr.-Ing. Martin Meywerk</b>
<b>Prof. Dr.-Ing. Bernard Bäker</b>	<b>Prof. Dr.-Ing. Werner Mischke</b>
<b>Dr.-Ing. Christoph Bollig</b>	<b>Prof. Dr.-Ing. Klaus D. Müller-Glaser</b>
<b>Prof. Dr. sc. techn. Konstantinos Boulouchos</b>	<b>Dr. techn. Reinhard Mundl</b>
<b>Prof. Dr.-Ing. Ralph Bruder</b>	<b>Dipl.-Ing. Sascha Ott</b>
<b>Dr. Gerhard Bruner</b>	<b>Dr.-Ing. Lothar Patberg</b>
<b>Prof. Dr. rer. nat. habil. Olaf Deutschmann</b>	<b>Prof. Dr.-Ing. Peter Pelz</b>
<b>Dr. techn. Arno Eichberger</b>	<b>Prof. Dr. techn. Ernst Pucher</b>
<b>Prof. Dr. techn. Helmut Eichlseder</b>	<b>Dr. Jochen Rauh</b>
<b>Dr.-Ing. Gerald Eifler</b>	<b>Prof. Dr.-Ing. Konrad Reif</b>
<b>Prof. Dr.-Ing. Wolfgang Eifler</b>	<b>Dr.-Ing. Sven Schaub</b>
<b>Prof. Dr. rer. nat. Frank Gauterin</b>	<b>Prof. Dr. rer.-nat. Christof Schulz</b>
<b>Prof. Dr. techn. Bernhard Geringer</b>	<b>Prof. Dr. rer. nat. Andy Schür</b>
<b>Prof. Dr.-Ing. Uwe Grebe (enquired)</b>	<b>Prof. Dr.-Ing. Ulrich Seiffert</b>
<b>Prof. Dr.-Ing. Horst Harndorf</b>	<b>Prof. Dr.-Ing. Hermann J. Stadtfeld</b>
<b>Prof. Dr. techn. Wolfgang Hirschberg</b>	<b>Prof. Dr. techn. Hermann Steffan</b>
<b>Univ.-Doz. Dr. techn. Peter Hofmann</b>	<b>Dr.-Ing. Wolfgang Steiger</b>
<b>Prof. Dr.-Ing. Günter Hohenberg</b>	<b>Prof. Dr.-Ing. Peter Steinberg</b>
<b>Prof. Dr.-Ing. Bernd-Robert Höhn</b>	<b>Prof. Dr.-Ing. Christoph Stiller</b>
<b>Prof. Dr. rer. nat. Peter Holstein</b>	<b>Dr.-Ing. Peter Stommel</b>
<b>Prof. Dr.-Ing. habil. Werner Hufenbach</b>	<b>Prof. Dr.-Ing. Wolfgang Thiemann</b>
<b>Prof. Dr.-Ing. Roland Kasper</b>	<b>Prof. Dr.-Ing. Helmut Tschöke</b>
<b>Prof. Dr.-Ing. Tran Quoc Khanh</b>	<b>Dr.-Ing. Pim van der Jagt</b>
<b>Dr. Philip Köhn</b>	<b>Prof. Dr.-Ing. Georg Wachtmeister</b>
<b>Prof. Dr.-Ing. Ulrich Konigorski</b>	<b>Prof. Dr.-Ing. Henning Wallentowitz</b>
<b>Dr. Oliver Kröcher</b>	<b>Prof. Dr.-Ing. Jochen Wiedemann</b>
<b>Dr. Christian Krüger</b>	<b>Prof. Dr. techn. Andreas Wimmer</b>
<b>Univ.-Ass. Dr. techn. Thomas Lauer</b>	<b>Prof. Dr. rer. nat. Hermann Winner</b>
<b>Dr. Malte Lewerenz</b>	<b>Prof. Dr. med. habil. Hartmut Witte</b>
<b>Dr.-Ing. Markus Lienkamp</b>	<b>Dr. rer. nat. Bodo Wolf</b>
<b>Prof. Dr. rer. nat. habil. Ulrich Maas</b>	

Seal of Approval – this seal is awarded to articles in ATZ/MTZ that have successfully completed the peer review process

Scientific articles in ATZ Automobiltechnische Zeitschrift and MTZ Motortechnische Zeitschrift are subject to a proofing method, the so-called peer review process. Articles accepted by the editors are reviewed by experts from research and industry before publication. For the reader, the peer review process further enhances the quality of ATZ and MTZ as leading scientific journals in the field of vehicle and engine technology on a national and international level. For authors, it provides a scientifically recognised publication platform.

Therefore, since the second quarter of 2008, ATZ and MTZ have the status of refereed publications. The German association "WKM Wissenschaftliche Gesellschaft für Kraftfahrzeug- und Motorentechnik" supports the magazines in the introduction and execution of the peer review process. The WKM has also applied to the German Research Foundation (DFG) for the magazines to be included in the "Impact Factor" (IF) list.

In the ATZ/MTZ Peer Review Process, once the editorial staff has received an article, it is reviewed by two experts from the Advisory Board. If these experts do not reach a unanimous agreement, a member of the Steering Committee acts as an arbitrator. Following the experts' recommended corrections and subsequent editing by the author, the article is accepted. *rei*

### MTZ Peer Review

The Seal of Approval for scientific articles in MTZ.

Reviewed by experts from research and industry.

Received .....  
Reviewed .....  
Accepted .....





personal buildup for Force Motors Ltd.

# New Technologies for Emerging Markets

## Strategies for European Automotive Companies to meet Customers' Needs

- Market entry in new countries
- Low cost cars
- Active and passive safety
- Eco-friendly production
- Co-operation with local companies
- Get-together on the eve of the conference

Conference made by:

## ATZ MTZ

**\_\_\_ Yes, I would like to know more!**

Please send me more detailed information about the conference  
"New Technologies for Emerging Markets 2008" via e-mail.

first name	family name
company	sector
department	position
street	
postcode/city	
telephone	fax
e-mail	

vieweg technology forum  
Abraham-Lincoln-Straße 46  
65189 Wiesbaden | Germany  
Telephone +49(0)611. 7878-131  
[www.viewegtechnologyforum.de](http://www.viewegtechnologyforum.de)

**FAX +49(0)611. 7878-452**

# Rotation of a Piston Pin in the Small Connecting Rod Eye During Engine Operation



personal buildup for Force Motors Ltd.

A constant increase of powerful combustion engines has led to higher loads on the crankshaft drive and piston pin. To ensure a robust design the effective forces and movements at the piston pin have to be known. At the Technische Universität München, Chair of Internal Combustion Engines, a research project looked into the piston pins movement during engine operation. The main goal was to determine the rotary movements of the piston pin by measurement at a 4-l gas SI engine as a function of the engine load and speed and to clarify the mechanisms that cause the rotary movement of the piston pin especially in the small connecting rod eye.

## 1 Introduction and Goal

The maximum combustion chamber pressure has steadily increased as a result of the ever-increasing specific power output of engines. The resulting temperature and pressure loads on the components of the combustion chamber have correspondingly increased. The pressure is transferred by the piston to the piston pin and then to the connecting rod. The piston-side and connecting rod-side bearings of the piston pin are subject to major stress. In order to robustly design these bearings, both the arising forces and related movements must be known. Radial movements arise within the bearing play, and axial movements arise in the piston as a function of the axial fixation of the piston pin.

In addition, the piston pin may execute a circumferential movement in relation to the small connecting rod eye or piston. Very little is presently known about the circumferential movement of

the piston pin. The mechanisms that can cause the rotary movement also have not been clarified. It was therefore the goal of a research project [1, 2] to determine the rotary movement of the piston pin of a single cylinder, 4-l gas SI engine as a function of the engine load and speed. Therefore the relative movement between the small connecting rod eye and piston pin was measured.

## 2 Used Measuring Technique and Geometry

Two challenges had to be addressed in order to experimentally determine the piston pin movement. The signals of the moved connecting rod must be transmitted outward, and the tribological behaviour within the connecting rod bearing may not be changed by the sensors. To minimize the measuring systems influence on the piston pin's circumferential

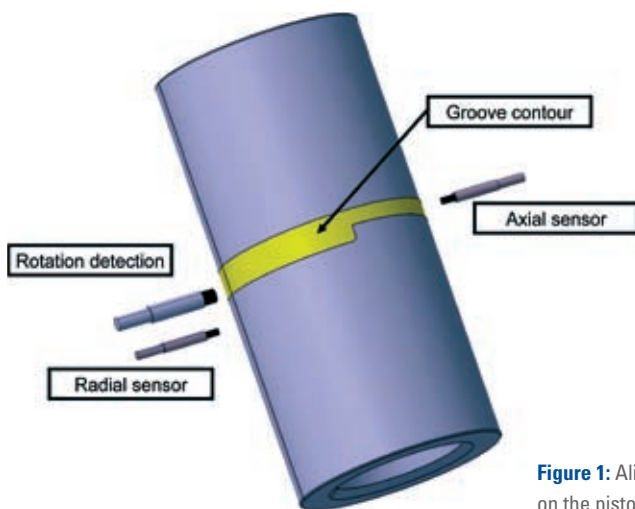


Figure 1: Alignment of the sensors on the piston pin

## The Authors



Prof. Dr.-Ing. Georg Wachtmeister has the chair of Internal Combustion Engines (LVK) at the TU München (Germany).



Dipl.-Ing. Andreas Hubert is research assistant to the chair of Internal Combustion Engines (LVK) at the TU München (Germany).

### MTZ Peer Review

The Seal of Approval for scientific articles in MTZ.

Reviewed by experts from research and industry.

Received ..... August 13, 2008

Reviewed ..... August 27, 2008

Accepted ..... September 26, 2008



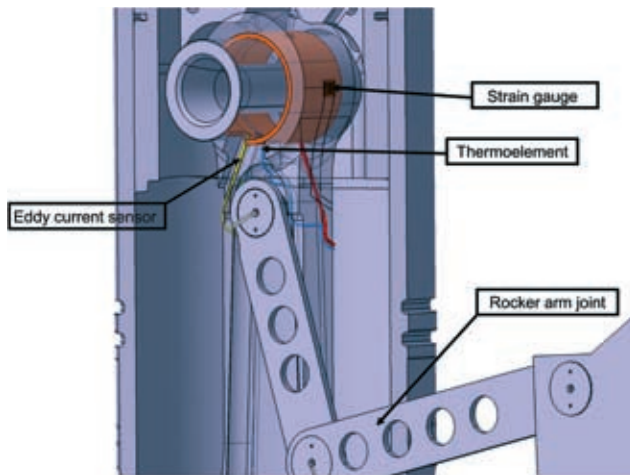


**Figure 2:** Measuring system in and on the connecting rod and rocker arm joint

movement, an eddy-current-based contact-less measuring system adapted to the single cylinder connecting rod was used to detect the movement. A change in impedance in the sensor coil caused by an electrically conductive object moved within a magnetic field generates an electric signal that indicates the distance or position of this object relative to the sensor. Three eddy current sensors, **Figure 1**, were installed in the small connecting rod eye to measure rotation and the axial and radial movement of the piston pin. In addition, two strain gauges were affixed in the small eye to detect the elastic deformation of the small connecting rod eye as well as a temperature measuring site on the friction bearing.

When the rotation sensor is correctly aligned, a conical narrowing groove in the piston pin will cause the impedance to change in the sensor coil by the change in amount of material as a function of the peripheral movement of the piston pin. To prevent the groove from changing the tribological behaviour, it was filled with an aluminum/bronze alloy by means of plasma spraying. To the eddy current sensor, aluminum bronze is a neutral material that functions as an air gap.

### 3 Engine Modifications to Adapt the Measuring Technique

The entire measuring system was incorporated in and on the connecting rod, **Figure 2**. Holes were created in the small connecting rod eye to hold the position

sensors. The diameters of the sensors were as small as possible to minimize the influence on the lubrication gap. The unavoidable residual gap was minimized by installing the sensors flush, and the sensitivity of the sensors was optimally exploited. It can be assumed that this residual gap had no negative influence on the results measured. To obtain information on the temperature in the small connecting rod eye, a thermoelement was directly mounted on the back of the friction bearing. To detect the expansion

of the small connecting rod eye, strain gauges were fixed on the side of the small connecting rod eye.

To transmit large amounts of data and minimize susceptibility to interference, coaxial cables were used as the signal carriers. A special rocker arm joint was constructed to run the cable from the moved connecting rod out of the engine. The rocker arm joint is mounted at the top of the connecting rod shaft and to the crankcase, and consists of three parts (two arms, one housing attachment, see also **Figure 2**).

### 4 Description and Evaluation of the Measurements

Loads with average pressures ranging from 4 to 20 bar were measured at three engine speeds (1000 rpm, 1250 rpm, 1500 rpm), and maximum combustion chamber pressures of 150 bar were reached. A total of 70 individual 2-min measurements were recorded. When first viewing the measuring results, one can see that the piston pin rotates comparatively slowly and an oscillation about the lengthwise axis is superimposed on the rotation. **Figure 3** shows in the top dia-

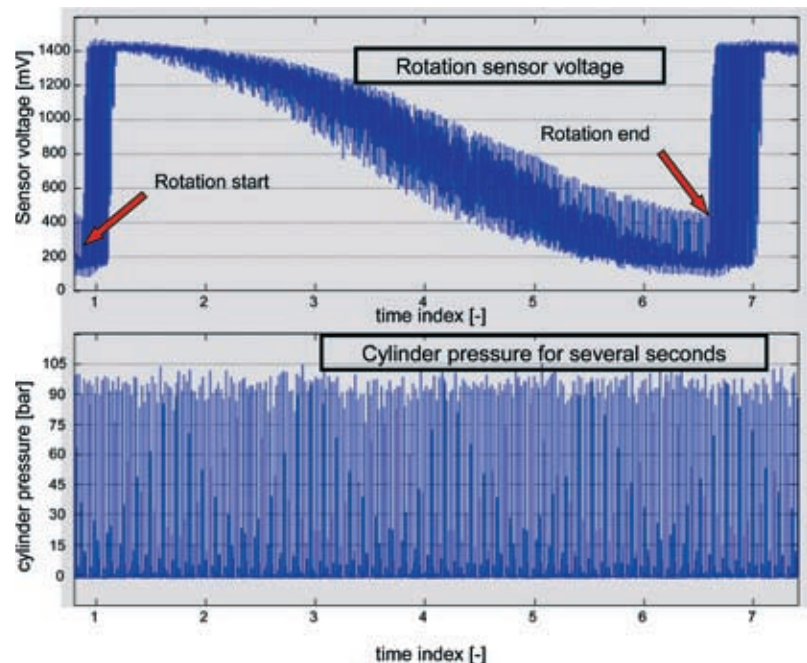


**Figure 3:** Measurement of a complete the piston pin rotation at 1000 rpm with superimposed oscillation at approximately 90 bar peak pressure (top) and measurement of the cylinder pressure (bottom)

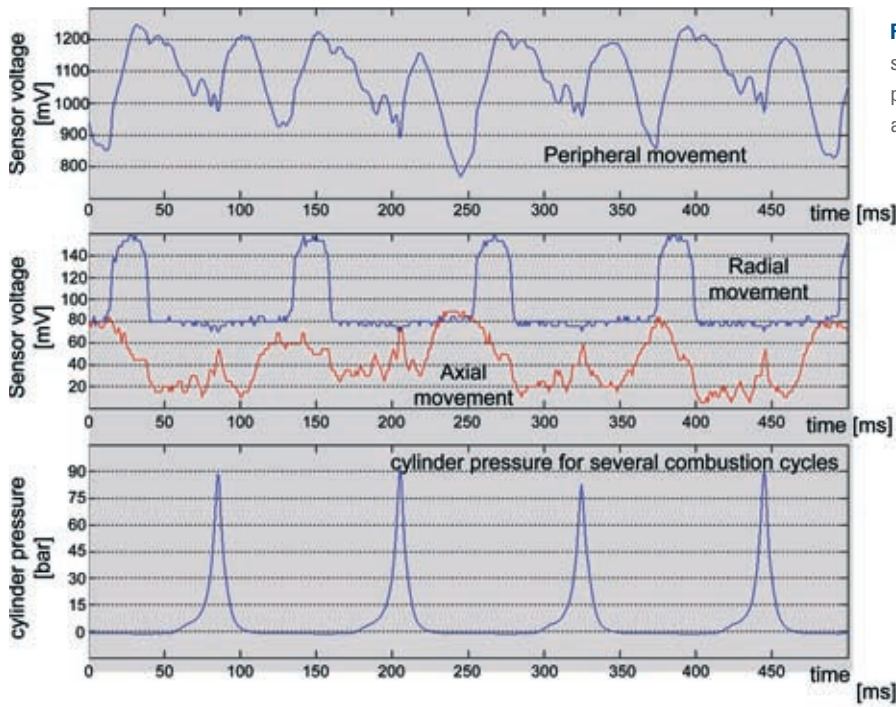


**Figure 4:** Curves of the eddy current sensors (two on top) and the cylinder pressure sensor (bottom) (measurement at 1000 rpm speed)

gram the curve from the time index of 1 to 7, which corresponds to a complete rotation. In the bottom diagram of Figure 3 the cylinder pressure curve for a complete rotation is presented.

**Figure 4** shows measurements of the eddy current sensors and the cylinder pressure sensor. A (comparatively small) axial movement (red curve in the middle diagram of Figure 4) occurs as well as a radial movement of the piston pin, and

the latter only arises during the charge cycle phase (blue curve in the middle diagram of Figure 4).

If one evaluates the measurements taken at steady-state operating points of the length of a complete piston pin rotation as a function of the engine speed and engine load, one gets the load influence of maximum cylinder pressure on the rotation duration of the piston pin in **Figure 5**.

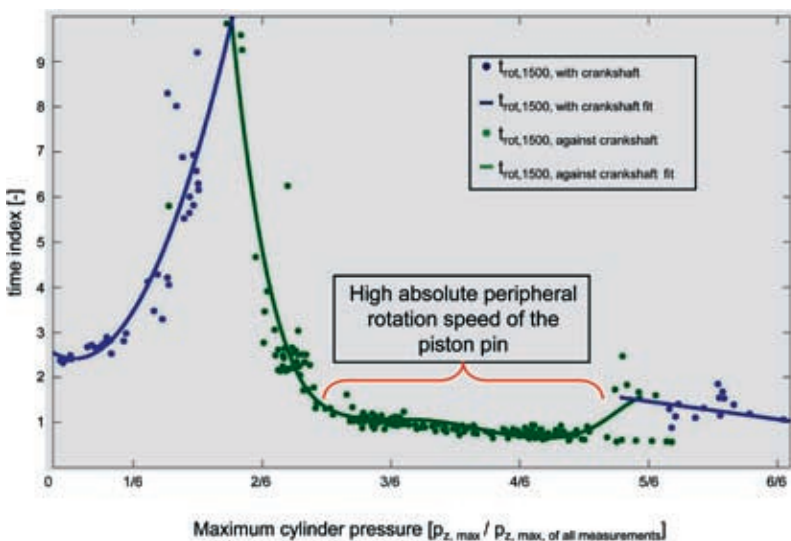


**Figure 5:** Maximum cylinder pressure influence on the piston pin rotation duration at 1500 rpm speed

The different rotation times for a total rotation lie within the second range, and two peaks can be identified at low and high load. Up to an engine load of approximately 30 % (first peak in Figure 5) the speed of the piston pin rotation declines. Then the piston pin rotates faster in peripheral direction up to the second peak (at an engine load of approximately 80 %). The maximal measured piston pin rotational speed was in the dimension of about 5 m/s.

When the signals from the measurements at 30 % load are examined more closely, one finds both a peripheral movement of the piston pin in the direction of crankshaft rotation and a rotation opposite that of the crankshaft, **Figure 6**.

Here one is able to detect a full rotation of the piston pin with the crankshaft (time index 0 until 1.3). With the ensuing engine load rise from 35 % up to 60 % (from time index 2 on), the rotation direction changes. The pin rotates now against the crankshaft (Figure 6).

The same phenomenon occurs at the second peak at approximately 80 % load.

There are apparently operating points, at which the piston pin's direction of rotation changes. This is the case with all three investigated engine speeds however the speed changes along the cylinder maximum pressure axis.

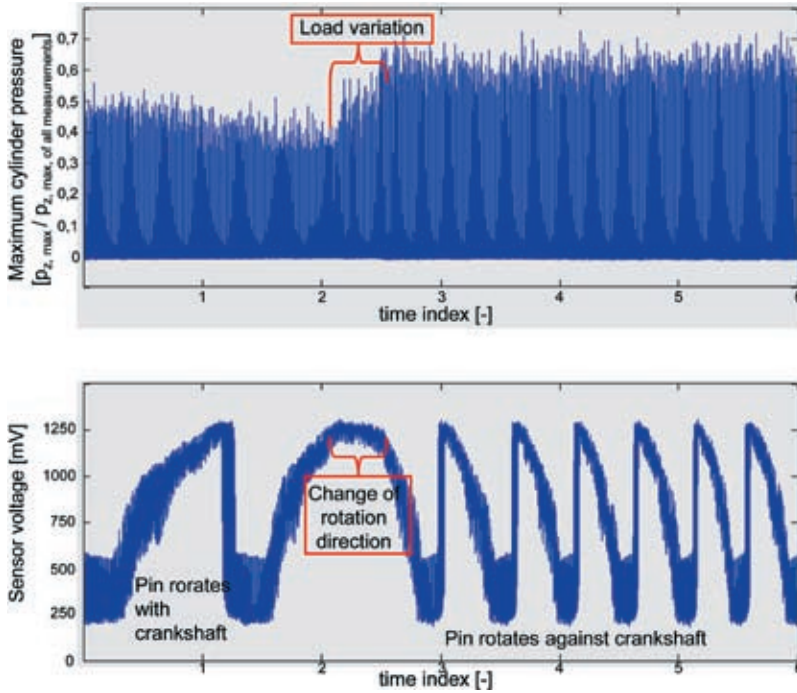


Figure 6: Influence of the engine load on the direction of piston pin rotation at 1500 rpm speed – curve of cylinder pressure (top) and curve of voltage (bottom)

This behaviour is also confirmed by measurements of non-steady-state engine operation in which operating ranges are intentionally reached that are representative of a change in the direc-

tion of rotation. The engine load was varied several times to confirm the reproducibility of the phenomenon of rotational direction change (example in Figure 6).

If the curves are examined in detail over a few working cycles, for example at a combustion chamber pressure of approximately 60 bar and engine speed of 1000 rpm, one can obtain more information on the peripheral movements of the piston pin, Figure 7.

In the top diagram of Figure 7, the signal of the peripheral movement sensor is plotted over time. One can see the continuous rotation of the piston pin from the changing voltage of the sensor signal ( $\Delta U$  in Figure 7). Since the sensor for measuring the pin rotation moves with the connecting rod, the connecting rod swing movement is included in the sensor signal. The measured oscillation is therefore generated by the swing connecting rod, and the piston pin also oscillates (stimulated by the connecting rod slewing movement).

This is seen in the middle diagram of Figure 7 where the cylinder pressure characteristic (magenta), the connecting rod swing angle speed (green) and the absolute piston pin rotational speed (red) are plotted over time. It can be clearly seen that the piston pin definitely rotates. It accelerates and stalls within certain ranges of the working cycle. The piston pin rotation is generated by the different speeds and directions in

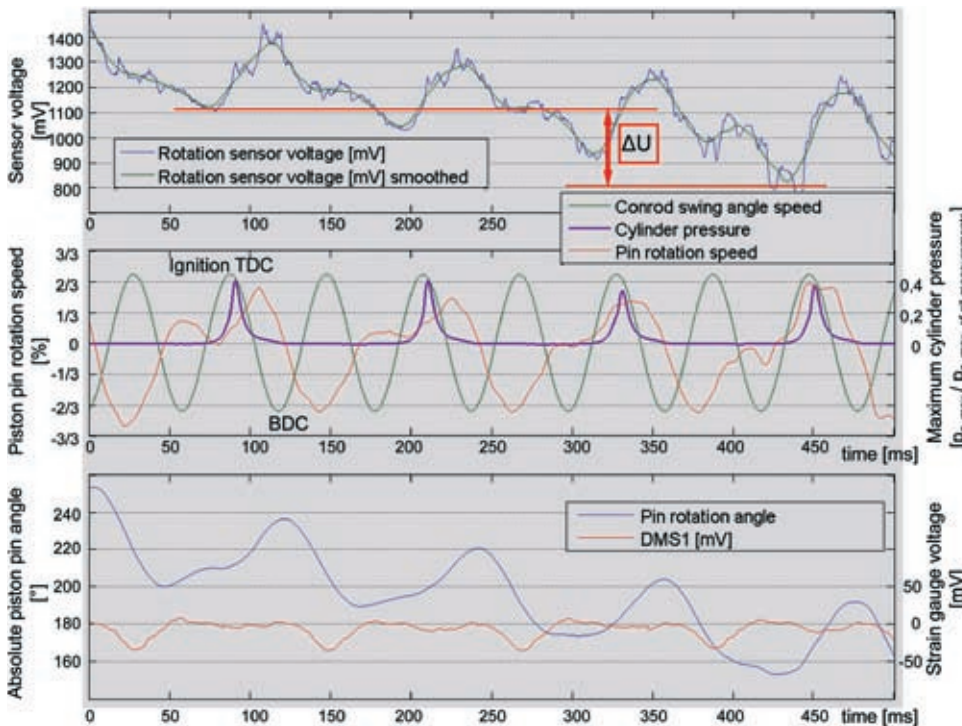
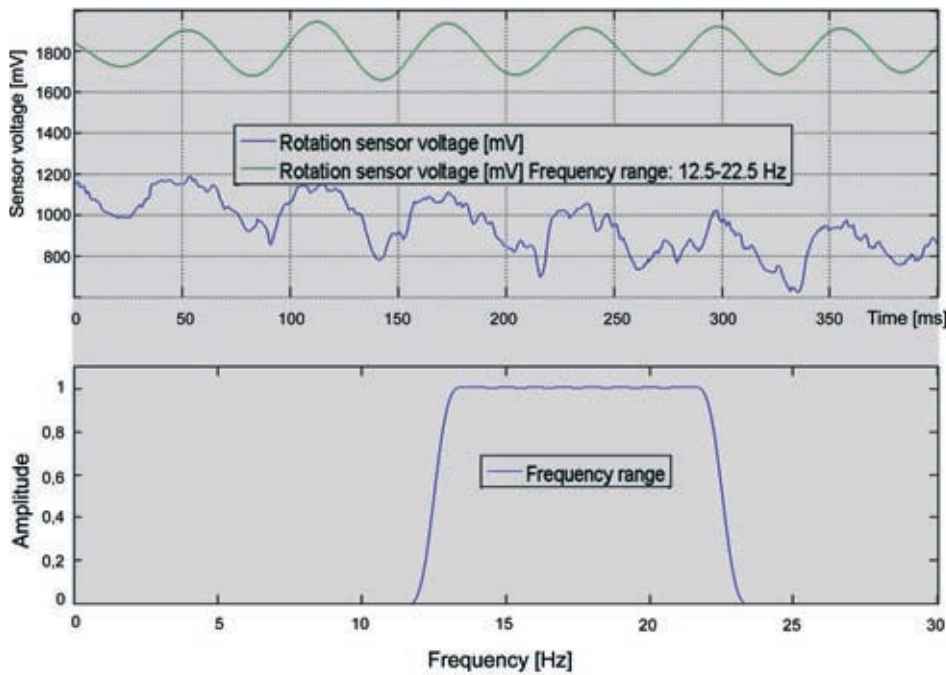


Figure 7: Excerpt of a measurement at approximately 60 bar peak pressure at 1000 rpm engine speed



**Figure 8:** Rotation sensor voltage (including offset – green) near the frequency of 1000 rpm engine speed, frequency range of the band-pass filter 12.5 to 22.5 Hz

the charge cycle and high-pressure phase.

The absolute rotational angle of the piston pin during measurement is shown in the bottom diagram of Figure 7. In addition, a DMS characteristic is plotted over time. A significant deformation of the small connecting rod eye can be seen in the charge cycle phase.

By filtering the rotation sensor signal (blue) **Figure 8** shows, that the oscillation of the piston pin is caused by the connecting rod swing movement (which has a frequency of 16,66 Hz at an engine speed of 1000 rpm). The upper diagram of Figure 8 shows the filtered rotation sensor signal (green) in the frequency band of 12.5 to 22.5 Hz. It is exclusively an oscillation whereas one can see the running rotation of the piston pin by surveying the falling blue curve progression (unfiltered rotation sensor signal).

## 5 Summary

By measuring the peripheral movement of the piston pin in the small connecting rod eye, the piston pin movement and its nature were demonstrated by the Chair of Internal Combustion Engines at the Technische Universität München (Germany). The oscillation of

the piston pin is stimulated by the swing movement of the connecting rod. The continuous rotation of the piston pin arises from the different pin speeds and directions in the charge cycle and high-pressure phase. The engine speed and load influence the rotation of the piston pin.

The piston pin moves in both axial and radial directions. However, it only moved in radial direction in the connecting rod eye during the charge cycle phase. Additional investigations of this topic can provide even more detailed information which will enable the optimization of connecting rod bearing design and production.

## References

- [1] Hubert A.: Experimentelle Ermittlung der Drehung eines Kolbenbolzens im kleinen Pleuelauge während des Motorbetriebs. [Experimental Measurement of the Rotation of the Piston Pin in the Small Conrod Eye During Engine Operation.], Lehrstuhl für Verbrennungskraftmaschinen [Chair of Internal Combustion Engines] (LVK), TU München, Germany, 2007
- [2] Fröber S.: Auswertung von Messungen der Bewegung eines Kolbenbolzens im kleinen Pleuelauge während des Motorbetriebs. [Evaluation of Measurements of the Movement of the Piston Pin in the Small Conrod Eye During Engine Operation.], Lehrstuhl für Verbrennungskraftmaschinen [Chair of Internal Combustion Engines] (LVK), TU München, Germany, 2008

- [3] Blumenthal, H.: Tribologische Beurteilung des Verschleißverhaltens der Kolbenbolzenlagerung unter Berücksichtigung der Kolbenbolzenbewegung, [Evaluation of the Abrasion Behaviour of the Piston Pin Bearing by Considering the Pin Movement], Vortrag, Tribologie-Fachtagung, Göttingen, 2005